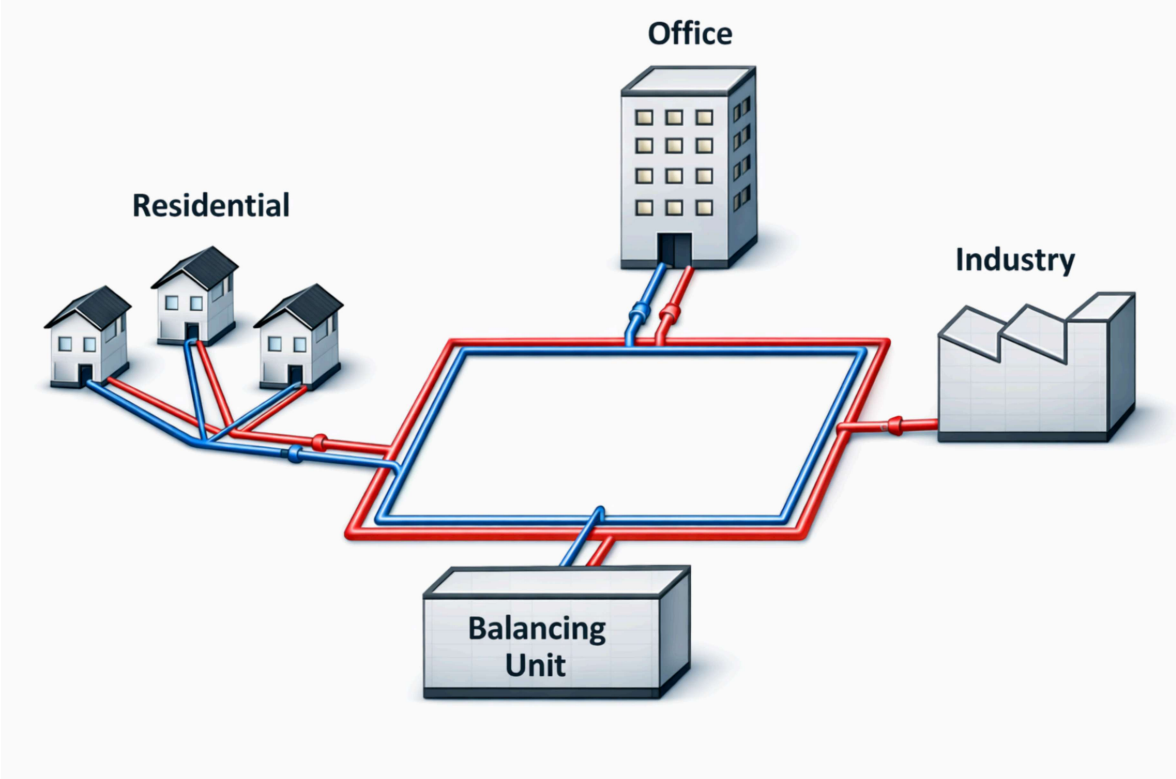

Optimizing Urban Energy Flows

Theoretical Insights into Energy Sharing Between Buildings

Master's thesis in the Master's Programme Structural Engineering and Building Technology

ANTON GUSTAFSSON

DEPARTMENT OF ARCHITECTURE AND CIVIL ENGINEERING
DIVISION OF BUILDING SERVICES ENGINEERING

CHALMERS UNIVERSITY OF TECHNOLOGY
Master's thesis ACEX30
Gothenburg, Sweden 2026

MASTER'S THESIS ACEX30

Optimizing Urban Energy Flows

Theoretical Insights into Energy Sharing Between Buildings

Master's Thesis in the Master's Programme Structural Engineering and Building Technology

ANTON GUSTAFSSON

CHALMERS
UNIVERSITY OF TECHNOLOGY

Department of Architecture and Civil Engineering
Division of Building Service Engineering
CHALMERS UNIVERSITY OF TECHNOLOGY
Gothenburg, Sweden 2026

Optimizing Urban Energy Flows
Theoretical Insights into Energy Sharing Between Buildings
Master's Thesis in the Master's Programme Structural Engineering and Building Technology

ANTON GUSTAFSSON

Supervisors:
Kristina Nilsson, GICON Installationsledning AB
Torbjörn Lindholm, Division of Building Service Engineering

Examiner:
Anders Trüschel, Division of Building Service Engineering

Examensarbete ACEX30
Institutionen för Arkitektur och Samhällsbyggnadsteknik
Chalmers Tekniska Högskola, 2026

Department of Architecture and Civil Engineering
Division of Building Service Engineering
Chalmers University of Technology
SE-412 96 Göteborg
Sweden
Telephone +46 31 772 1000

Cover:
AI enhanced picture based on a sketch for the conceptual model of a thermal source network for energy sharing consisting of residential, office, and industry buildings along with a balancing unit.
Department of Architecture and Civil Engineering
Göteborg, Sweden, 2026

Optimizing Urban Energy Flows
Theoretical Insights into Energy Sharing Between Buildings

Master's thesis in the Master's Programme Structural Engineering and Building Technology

ANTON GUSTAFSSON

Department of Architecture and Civil Engineering
Division of Building Service Engineering
Chalmers University of Technology

ABSTRACT

Space heating and cooling of buildings make up a substantial part of the total energy use globally. Apart from reducing the energy demand, improvements could be made to the energy supply of buildings. Such an improvement could be achieved by utilizing waste energy sources and connecting buildings with different energy demands. This master's thesis evaluates the performance of a thermal source network (TSN), seen as the fifth generation of district heating and cooling or as a subclass to the fourth generation. A TSN has the ability to time shift energy through balancing units such as geothermal storage, extracting energy through heat pumps and chillers at demand.

The project studied a fictional district and compared multiple variations of a TSN to a traditional district heating and cooling (DH/DC) or geothermal base case. The fictional district consisted of four buildings, both residential and commercial, and used a supermarket as a waste heat source. The heating and cooling demand for the fictional district was 1 448.2 MWh and 860.2 MWh, respectively. Resulting in an remaining heating demand of 588.0 MWh or as a 1.7:1 ratio between the heating and cooling demand. The study concluded that the DH/DC solution has the lowest investment cost but the highest operational cost and CO_2 emissions. As a result of an improved coefficient of performance (COP), the TSN was found to have a lower operational cost and CO_2 emissions than both the DH/DC solution and the geothermal solution, but at a higher investment cost. The optimized iteration of the TSN case study, using network temperatures adjusted to a geothermal storage of boreholes, was deemed to be the most realistic. Compared to the DH/DC solution, the optimized iteration resulted in an increase of 107% in investment cost, a reduction of 84% in operational cost and a reduction of 23% for CO_2 emissions. A result that also can be presented as a payback time of 2.6 years. Compared to a geothermal base case, the investment cost for the optimized iteration was 17% higher, the operational cost was 4% lower and the CO_2 emissions were reduced by 14%. Resulting in a payback time of 91.0 years, a consequence of the assumed redundancy investment of a DH/DC connection. If this connection is omitted and redundancy is achieved in another way, the TSN might result in a lower investment cost than the geothermal base case.

Key words: Thermal source networks, 5th generation district heating and cooling, heat pumps, chillers, geothermal storage, waste heat sources.

Optimering av urbana energiflöden
Teoretisk studie angående energidelning mellan byggnader

Examensarbete inom masterprogrammet Konstruktionsteknik och byggnadsteknologi

ANTON GUSTAFSSON

Institutionen för arkitektur och samhällsbyggnadsteknik
Avdelningen för installtionsteknik
Chalmers tekniska högskola

SAMMANFATTNING

Uppvärmning och kylning av byggnader utgör en betydande del av den globala energianvändningen. Förutom att minska energibehovet kan förbättringar göras i byggnaders energiförsörjning. En sådan förbättring kan åstadkommas genom att utnyttja spillenergi och koppla samman byggnader med olika energibehov. Denna masteruppsats utvärderar prestandan hos lågtempererade fjärrnät (TSN), vilket kan ses som den femte generationens fjärrvärme och fjärrkyla eller som en underklass till den fjärde generationen. Ett TSN har förmågan att tidsförskjuta energi genom olika balanseringsmetoder såsom geotermiska lager för att sedan utvinna energin via värmepumpar och kylmaskiner vid senare behov.

Projektet studerade en fiktiv stadsdel och jämförde flera variationer av ett TSN i en fallstudie med ett traditionellt fjärrvärme och fjärrkyla (DH/DC) basfall och ett geotermiskt basfall. Den fiktiva stadsdelen bestod av fyra byggnader, både bostäder och kommersiella lokaler med en livsmedelsbutik som spillvärmekälla. Uppvärmnings- och kylbehovet för den fiktiva stadsdelen var 1 448,2 MWh respektive 860,2 MWh. Vilket gav ett resterande värmebehov på 588,0 MWh eller som ett förhållande på 1,7:1 mellan värme- och kylbehov. Studien drog slutsatsen att DH/DC basfallet har den lägsta investeringskostnaden men de högsta driftkostnaderna och CO_2-utsläppen. Som ett resultat av förbättrad coefficeint of performance (COP) visade ett TSN lägre driftkostnader och CO_2-utsläpp men med högre investeringskostnader än båda basfallen. En optimerad iteration av fallstudien med systemtemperaturerna justerade efter ett borrhålslager bedömdes vara mest realistisk. Denna iteration resulterade i en ökning av investeringskostnaden med 107%, en minskning av driftkostnaden med 84% och en minskning av CO_2-utsläppen med 23%, jämfört med DH/DC basfallet. Uttryckt istället som payback-tid, resulterade det i 2,6 år. Jämfört med det geotermiska basfallet var investeringskostnaden för den optimerade iterationen 17% högre, driftkostnaden 4% lägre och CO_2-utsläppen minskade med 14%. Detta resulterar i en payback-tid på 91,0 år vilket är en konsekvens av den antagna investeringen i en fjärrvärme- och fjärrkylaanslutning för balansering och redundans. Om redundans kan uppnås utan denna anslutning kan ett TSN nå investeringskostnader lägre än det geotermiska basfallet.

Nyckelord: Lågtempererade fjärrnät, 5:e generationen fjärrvärme och fjärrkyla, värmepump, kylmaskin, geotermisk lagring, spillvärmekällor

Contents

Preface

This master's thesis concludes my studies at the master program "Structural Engineering and Building Technology" at Chalmers University of Technology. The project was done in collaboration with GICON Installationsledning AB and was carried out to deepen the knowledge of future possibilities of energy sharing between buildings.

First of all I would like to thank Göran Andersson at GICON for sharing the idea that turned into this master's thesis, your passion for the subject has been key for this project. I am also especially grateful for all the insight and help from my supervisor at GICON, Kristina Nilsson, who has been invaluable. I would also like to thank Tobias and everyone else at the office of GICON for the friendly welcome, your patience, and for all the help I have received throughout this project.

Additionally, thank you to Gustav Adolfsson at E.ON, Martin Warneryd at RISE, and Jan Johansson at the municipality of Örebro who shared their knowledge through interviews. Furthermore, the opportunity for a study visit to NIBE, where I met with Fredrik Snygg, who shared his practical experience of the heat pump and thermal source network industry was of great value for this thesis, thank you Fredrik.

Lastly, thank you also to my supervisor and examiner at Chalmers University of Technology, Torbjörn Lindholm and Anders Trüschel for all your valuable feedback, and for your confidence in this thesis.

Gothenburg, May 2026
Anton Gustafsson

Notations

The abbreviations and notations used for this master's thesis are summarized and listed alphabetically below.

Abbreviations

CEC	Citizen Energy Community
CH	Chiller
COP	Coefficient of Performance
DC	District cooling
DH	District heating
DHW	Domestic Hot Water
GHG	Greenhouse Gasses
HP	Heat Pump
IKN	Icke Koncessionspliktiga Nät (Non-concessioned network)
IUS	Industrial and Urban Symbiosis
KPI	Key Performance Indicator
REC	Renewable Energy Community
SCOP	Seasonal Coefficient of Performance
TSN	Thermal Source Network
VAT	Value Added Tax

Notations

η_C	Carnot efficiency [-]

1

Introduction

As the global climate crisis intensifies, the urgency to transition to greener, renewable and affordable solutions increases in order to lower greenhouse gas emissions (GHG). One sector where significant potential for improvement can be made is the built environment, which accounts for a substantial share of the world's energy use and carbon emissions. Such improvements are crucial for the possibility of achieving the global warming limit of 1.5°C, as set by the Paris Agreement.

1.1 Background

Maintaining a desired indoor climate is an energy-intensive process, where varying outdoor conditions lead to both energy surpluses and deficits. Different buildings or spaces require different indoor climates due to factors such as their function, equipment, or solar exposure. These surpluses and deficits can occur simultaneously or at different points in the day or year, making efficient energy sharing an attractive method of reducing energy use within the building or system.

At the building level, this may involve, for example, transferring surplus heat from a sun-exposed room to another room experiencing a heat deficit or to an energy storage system. At the system level, it can mean utilizing waste heat from factories or office buildings to heat residential dwellings in the area, potentially eliminating the need for bought heating energy through, for example, gas. At the system level, this constitutes an alternative energy resource that, on a large scale, can reduce the climate impact of the existing built environment. It is the mentioned system level which this master's thesis will highlight. Specifically, the use of low-temperature networks or so called thermal source networks (TSN). The concept of such a network can be seen in Figure 1.1 in the form of a sketch enhanced by the use of artificial intelligence (AI).

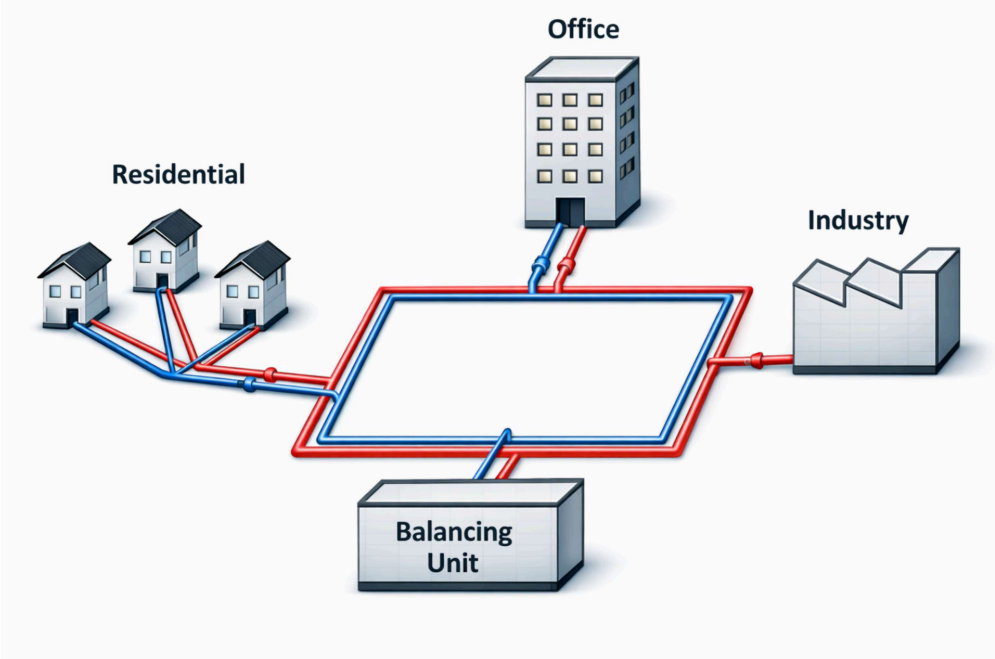

Figure 1.1: AI enhanced sketch of the concept of an energy sharing network or thermal source network, TSN.

1.2 Aim

The aim of this thesis, conducted in collaboration with GICON Installationsledning AB, is to analyze and compare the potential of current and future possibilities for alternative, shareable energy systems. For both new constructions and existing buildings on a system level, i.e., district level. Through a preliminary study of various systems, the study seeks to enhance understanding of key factors and challenges associated with different methods in the transition toward energy sharing. By comparing different approaches in a case study, where energy use, climate impact, and cost are measured and compared to a base case, the results of this work may serve as a basis for decision-makers.

1.3 Thesis questions

To achieve the outlined aim described in Section 1.2, the following thesis-specific questions were formulated and are to be investigated:

- How are laws and regulations formed in Sweden regarding energy sharing?
- What are the possible technical solutions for sharing energy between buildings through a thermal source network?
  - How do the solutions perform throughout the year and how is redundancy achieved?
- What building or tenant functions and how many are needed of each type for practicality?
- What is the performance of a solution regarding its economic and environmental aspects? How do they compare through key performance indicators to a base case?

1.4 Limitations and demarcations

The thesis demarcations are to focus on Sweden but examples of solutions from other countries are presented and discussed as well. However, no calculations are done for these. This is done to get a greater understanding of the different systems available globally but at the same time limit the scope of the calculations, thus improving the comparability for different systems.

Hydraulic aspects of the network are not taken into account. This is done to align with the thesis aim of evaluating the potential of energy reductions.

Due to the time constraint of the thesis, the performance of different buildings is gathered from completed models done by GICON.

Another demarcation of the thesis is that no design of the electrical grid is considered, however, the coverage of the additional electrical demand for the added technical systems is briefly covered through discussion. The same is done for the control strategy of the systems.

Thermal comfort and indoor air quality of the buildings are not addressed since the outlined aim focuses on energy sharing potential, and therefore the requirements of these aspects are seen as fulfilled. This is backed by the fact that real-life finished projects from GICON are used for the case study.

For the economic aspects, only a brief comparison based on investment and operational costs is made, where options for funding and the possibility for this are not covered in this thesis.

The environmental aspect is chosen to focus on kg CO_2 equivalents (CO_2 eq.), as it is the main focus of the building sector through the Swedish Klimatdeklaration. This could mean that a burden shifting for potential CO_2 eq. reductions can occur, this would need to be covered in a separate life cycle assessment which, however, is out of scope for this thesis. The calculations for the impact are limited to the operation phase, where the amount of used energy is compared.

1.5 Method

The foundation of this work is based on a study of the relevant literature, in which current and future solutions to the problem are presented and discussed. Relevant contact persons in the industry were contacted and interviewed to gain further understanding. Subsequently, several different solutions were tested in theoretical scenarios in the form of a case study to improve understanding of their potential to reduce energy use and climate impact. To also put the solutions into an economic perspective, a brief cost analysis was done to make different solutions realistically comparable. The case study was conducted by creating a fictional district where buildings with different purposes are located and different technical systems for energy sharing were inserted.

The results of the different solutions were then compared using different key performance indicators (KPI), such as

- Technical performance
  - Coefficient of performance, COP [-] / Seasonal coefficient of performance, SCOP [-]
  - Share of extracted energy [MWh]
  - Electricity use [MWh]
- Economic indicators
  - Investment cost [SEK]
  - Operating cost [SEK/year]
  - Payback time [years]
- Environmental impact
  - CO_2 emissions [kg CO_2 eq.]

Based on these KPI:s, a comparison was made between variations of a reference case (denoted as iterations) to base cases in which either all the heating and cooling demands are supplied through an external source of district heating and cooling or geothermal energy. The workflow used for the project is visualized in Figure 1.2.

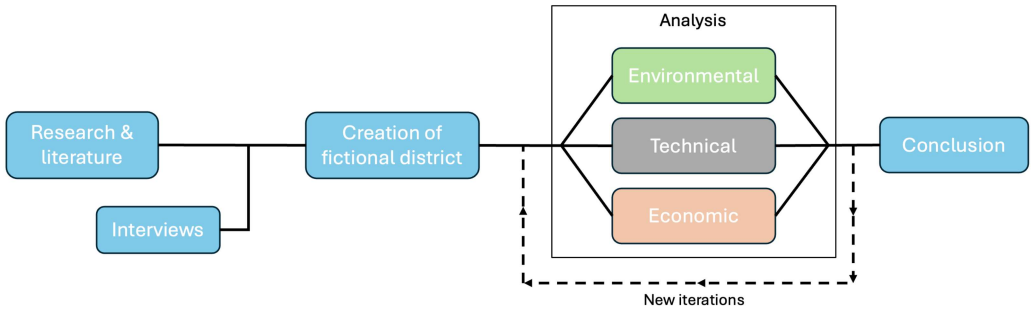

Figure 1.2: Workflow used for the project.

1.6 Use of artificial intelligence

The use of artificial intelligence has been limited to basic prompts of writing, translations, report formality, LaTeX or Excel coding, and enhancing pictures based on hand drawn sketches. Artificial intelligence has not been used for any research, calculations, or text sections.

2

Theory and examples of energy sharing

In the following chapter, relevant theory used in this thesis will be introduced. Firstly, environmental, urban, and regulative aspects will be presented, followed by different possible technical solutions. Furthermore, examples, both international and national, are presented to provide the reader with the necessary context. Lastly, the aspects of resilience for smaller grids are covered briefly.

2.1 Environmental aspects

As mentioned in the introduction of Chapter 1, the Paris Agreement set the global warming limit at 1.5^{o}C and is a legally binding international treaty adopted by 195 parties at the United Nations Climate Change Conference, COP21, in Paris, 2015. The goal of this agreement is to limit the global average temperature increase to below 2^{o}C compared to pre-industrial levels and aim towards limiting it at 1.5^{o}C. If the threshold of 1.5^{o}C is transgressed the risk of more severe and frequent impacts of climate change, such as heatwaves, rainfalls, and droughts increases (United Nations Framework Convention on Climate Change, 2015).

To align with the Paris Agreement, Sweden adopted a new climate policy framework, which includes a climate act, targets, and policy council. The framework entered into force in January of 2018 with the purpose to ensure Sweden's long-term climate strategy, a strategy that aims at Sweden having net-zero GHG emissions by the latest of 2045 (Swedish Environmental Protection Agency (Naturvårdsverket), 2025). The mentioned climate act establishes that the Swedish government shall present a climate report in its budget bill each year. Furthermore, every fourth year, a climate policy action plan should be presented on how to achieve the climate targets and supervise that the budget and climate policy goals coincide. As for the milestone targets towards the long-term goal, emissions should be reduced by 40 percent as of 2020, compared to the emissions of 1990, followed by 63 percent in 2030 and 75 percent in 2040. A separate milestone target is that domestic transport emissions excluding domestic flights should be reduced by 70 percent compared to the emissions of 2010. Supplementary targets have also been established to achieve the long-term and milestone targets (Swedish Environmental Protection Agency (Naturvårdsverket), 2025).

The Swedish building sector has also taken multiple steps towards a lowering of GHG emissions. One such step is the mandatory climate declaration for new buildings, or "Klimatdeklaration" in Swedish. The purpose of this declaration is to reduce the climate impact of new buildings during the construction phase and came into force in January 2022. The construction phase includes all stages denoted as A, that is, A1-

A3, which covers products, and A4-A5 which covers the construction of the building itself (Swedish National Board of Housing, Building and Planning (Boverket), 2024). From 2027 and beyond, Boverket proposes new threshold values and also that the entire building life cycle should be included in the climate declaration (Swedish National Board of Housing, Building and Planning (Boverket), 2023). This would put emphasis on the need to reduce emissions in the use stage in which this thesis discusses potential reduction possibilities.

A potential strategy to reduce climate impact is the application of Industrial and Urban symbiosis (IUS). RISE Research Institutes of Sweden (2024) mention in their report on behalf of the Swedish Energy Agency how an IUS creates value from residual flows of different processes, such as energy, water, and material. The report emphasizes that the key to a successful implementation of an IUS is to expand the system boundaries of an individual organization and to utilize local resource synergy flows. A well-known and frequently cited example of industrial symbiosis is Kalundborg in Denmark, which has over time expanded its scope to include urban aspects closely linked to IUS.

2.2 Regulations and directives of energy sharing

If sharing energy between buildings is to be possible, it needs laws, regulations, and directives that allow and facilitate this. REScoop.eu (European Federation of Renewable Energy Cooperatives) (2024) show how Sweden is the worst ranked country of multiple countries in Europe when it comes to facilitating and enabling a renewable energy community (REC) and a citizen energy community (CEC). CEC:s are limited to electricity but are technology-neutral while REC:s can include the energy sector, e.g. heating and cooling, but are limited to renewable energy (Swedish Energy Agency (Energimyndigheten), 2024).

Swedish Energy Agency (Energimyndigheten) (2024) mentions multiple barriers for the enabling of REC:s and CEC:s in Sweden, one being that the Swedish definitions and legal framework for these communities are not well defined. Another barrier is the Swedish Electricity Act (1997:857), or "Ellagen" in Swedish, where permits are needed for electricity distribution lines. Certain distribution lines can be exempted from the permit and are referred to as "Icke Koncessionspliktiga Nät" (Non-concessioned networks) abbreviated as IKN. The IKN Regulation declares what is needed to be exempted from the permit, and in 2022 an amendment was made to the regulation which allows for energy sharing within internal networks under certain conditions. A third barrier is to ensure that the energy user has the right to choose freely among providers.

To share electricity between buildings according to the regulations mentioned previously, the type of infrastructure is of importance. Swedish Energy Agency (Energimyndigheten) (2024) define three types of network depending on the infrastructure of each type. Complementary network, in which complementary infrastructure is built between buildings. This can be done under specific circumstances and was allowed to do so after the 2022 amendment to the IKN Regulation. This type of network allows users to avoid taxes and fees and also does not put any extra strain on the existing infrastructure. The second type of network is a private network, where the connection to the grid is "moved out", and multiple users share a private network "behind" this connection point.

A drawback of this type of network is the restriction of the user's ability to be an active consumer on the electricity market. The last type is virtual sharing, this type of network utilizes the already built infrastructure, meaning no additional infrastructure is needed and allows for more flexibility for the users. However, a drawback is that shared electricity needs to be taxed and fees taken out.

Regarding regulations for TSN:s, there is no direct equivalent to the Electricity Act or the IKN that restricts sharing. However, a TSN may fall under the Swedish District Heating Act (2008:263), or "Fjärrvärmelagen" in Swedish, if it involves selling thermal energy to a third party. Therefore, the economic model chosen for a network will determine if the District Heating Act will apply or not. The implication of the District Heating Act results in the need of, for example, contracts and pricing transparency between stakeholders for the transaction of thermal energy.

2.3 Technical solutions

This section covers the principle and to some extent the history of different possible technical solutions for the case study. Solutions such as heat pumps, district heating, and geothermal.

2.3.1 Heat pumps and chillers

Both heat pumps (HP) and chillers (CH) use the same concept of a thermodynamic cycle to generate either heat or cold. The cycle for a HP uses a refrigerant that evaporates at low pressure and temperature and condenses at high pressure and temperature. Using a compressor and an expansion valve, the refrigerant can be cycled between a liquid and a gas phase. In the liquid phase, the refrigerant is heated in the evaporator by some source, for example, outdoor or exhaust air, and then evaporates into cold gas. Then, the temperature and pressure are raised in the compressor, allowing the refrigerant to heat the target medium, for example, water or air used for space heating, in the condenser. The chiller reverses this process to instead cool the target medium (Warfvinge & Dahlblom, 2010). A sketch of the thermodynamic cycle can be seen in Figure 2.1.

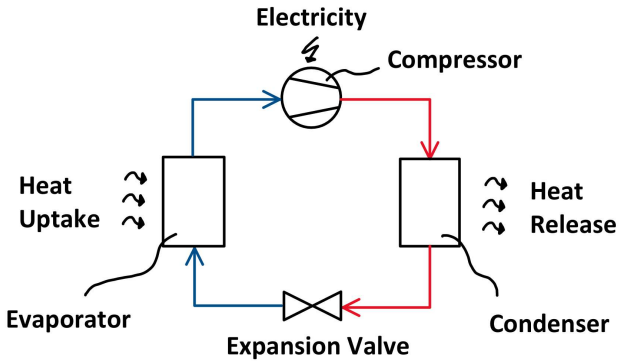

Figure 2.1: Sketch of the thermodynamic cycle of an HP and CH based on Warfvinge and Dahlblom (2010).

For a HP, the target medium would be on the heat release side and heat source on the heat uptake side in Figure 2.1. For a CH this would instead be reversed, with the target medium on the heat uptake side.

To evaluate the efficiency of a HP or CH, the term coefficient of performance (COP) can be formulated. Warfvinge and Dahlblom (2010) described the term as the ratio between the emitted heating or cooling effect divided by the input effect of the compressor. Based on this description, the ratio in Equation 2.1 can be derived.

$$COP = \frac{\dot{Q}_{emitted}}{\dot{W}_{in}} \tag{2.1}$$

For a HP, $\dot{Q}_{emitted}$ is the emitted heating effect, and for a CH, $\dot{Q}_{emitted}$ is the cooling effect. Based on Equation 2.1, the greater the COP is, the greater the efficiency. According to Warfvinge and Dahlblom (2010), a good COP for a HP is between 3 and 4. Furthermore, the ideal reversible thermodynamic cycle can be described through the Carnot COP, which utilizes the temperature of the hot and cold reservoirs. The ratio between the ideal Carnot COP and the actual COP is denoted as the Carnot efficiency. The equation for Carnot COP of a heat pump process stated by Schroeder (2021) can be seen in Equation 2.2.

$$COP_{C,HP} = \frac{T_H}{T_H - T_L} \tag{2.2}$$

In Equation 2.2, T_H represents the temperature of the hot or high reservoir in Kelvin and T_L the cold or low reservoir also in Kelvin. For a refrigeration process, Schroeder (2021) continues how the Carnot COP can be derived by Equation 2.3.

$$COP_{C,R} = \frac{T_L}{T_H - T_L} \tag{2.3}$$

An additional term to measure efficiency is the seasonal coefficient of performance (SCOP), which takes into account seasonal variations by using the average COP during the heating season. The SCOP for an older CH is around 3 while for a newer model, up to 6 (Warfvinge & Dahlblom, 2010).

Another aspect of importance in ensuring the efficiency and reliability of the heat pump is the working range of the compressor. Where the temperature of the incoming brine (the liquid "carrying" the heating or cooling energy that is to be extracted) affects the performance of the compressor and if the temperature is outside the preferred working range, the compressor risks damages. An example of a working range diagram from NIBE's heat pump F1345 can be seen in Figure 2.2.

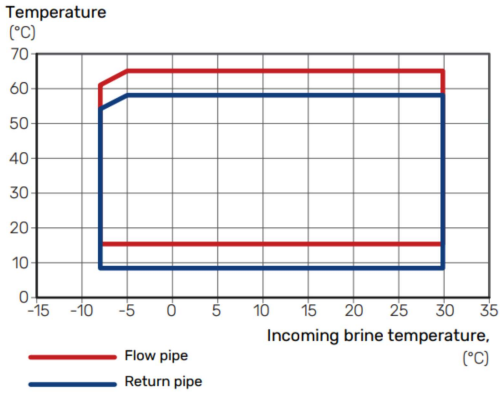

Figure 2.2: Working range for compressor operation for 30, 40, and 60 kW capacity of NIBE's heat pump F1345. The x-axis shows incoming brine temperature [^{o}C] and the y-axis shows outgoing temperature [^{o}C] (NIBE Energy Systems, 2023).

2.3.2 District heating and cooling

According to Energimyndigheten (2024) district heating (DH) is the most common type of heating for residential buildings and facilities in Sweden, providing 50%. District heating and cooling generally work in a way of using a centralized facility that distributes a primary heated or cooled medium, which then is heat exchanged in a district heating or cooling substation, with the secondary medium, the building's heating or cooling system. In this way, the primary and secondary mediums are separated, which allows different temperatures and pressures of the mediums and prevents contamination and oxygen ingress (Warfvinge & Dahlblom, 2010). Because the conditions of the mediums are often different, the separation of the primary and secondary medium is also done for safety reasons.

In a report, IEA DHC Executive Committee (2024) defines guidelines for differentiating generations of DH. The first generation is defined as using steam of any temperature. The second generation uses liquid water superheated to above 100^{o}C. The third generation lowers the temperature to between 70^{o}C and 100^{o}C, and the fourth generation is defined as using liquid water below 70^{o}C. For the fifth generation, which often refers to systems using decentralized technologies, the report suggests instead to define it as a thermal source network (TSN) and as a subclass to the fourth generation. For this thesis, the focus will be the implementation of this fifth generation or TSN.

In terms of district cooling (DC), there are four main generations, and based on Lund et al. (2014), Østergaard et al. (2022) defines the first three generations, where the first generation was introduced in the late 19th century as a pipeline refrigeration system where centralized condensers and decentralized evaporators are used with a refrigerant as distribution fluid. The second generation, introduced in the 1960s, used water as the refrigerant and was based on large compression chillers. The third generation, introduced in the 1990s, also uses water as the refrigerant, but differentiates itself by using a more diverse cold supply of absorption chillers, compression chillers with or without heat recovery, and natural cooling. Lastly, Østergaard et al. (2022) defines the fourth generation as a system using centralized or decentralized technologies to operate

in synergy with other energy sectors to meet cooling demands. Technologies such as electric heat pumps, absorption heat pumps, ambient sources, and storage facilities.

2.3.3 Geothermal energy

Petersson (2018) writes that due to the high thermal storage capacity of the ground, the temperature of the ground if undisturbed, remains relatively stable over the year, around the annual outdoor average for the area at a depth of 3 meters. For the Gothenburg area of Sweden, this temperature is approximately 8^{o}C.

Heat pumps can utilize the stable temperature of the ground as a geothermal heat source for the heating system. This can be done by using boreholes, where a refrigerant is pumped to extract heating energy from the ground and exchange it with the heating system fluid. For this process, the geological conditions must be suitable. This process also cools down the boreholes and to use them for the next heating season they must be heated again (Warfvinge & Dahlblom, 2010). Resulting in the possibility of storing energy over the seasons for a building with a balanced energy demand.

2.3.4 Solar power

Solar power is commonly used for generating electricity through solar panels, another solar power application is to directly heat a fluid. This can be done by, for example, a flat plate or an evacuated tube collector. Warfvinge and Dahlblom (2010) writes that both can be placed on the roof or on a facade where an absorber transfers the absorbed solar power to a glycol-water mixture or, in some systems, pure water. Such a solution provides a potential waste heat source that, in combination with regular solar panels providing electricity, improves the share of renewable energy use for a building.

2.4 Examples of energy sharing

The principle of sharing energy between buildings is not new and there are multiple examples of it both internationally and nationally. To create a foundation for the thesis, the work started with an extensive research period of the examples, and the following subsections will cover a few of these examples to better understand the possibilities.

2.4.1 Examples in Sweden

Firstly, national examples of energy sharing, Tamarinden in the town of Örebro, E:ON's Ectogrid in Lund, and more are presented.

Ectogrid in Lund

Medicon Village is located in the city of Lund in southern Sweden, there are 2 600 people working in this "village", and 15 commercial and residential buildings are connected through a TSN. Before this network, called Ectogrid, the "village" was supplied with district heating of 10 GWh and district cooling of 4 GWh. The vision of the network is to balance the usage at 11 GWh and reduce supplied energy by 65% (E.ON Sverige AB, 2025).

According to E.ON Sverige AB (2023) Ectogrid utilizes a more efficient temperature interval for HP:s and CH:s, which allows better efficiency and less energy losses. The

grid supplies heating and cooling in the same network through two pipes and is able to utilize waste energy which is made possible by the low temperature of 0-40^{o}C. The storage of the energy is carried out through the use of a thermal storage tank and when if not sufficient, active balancing is done by, for example, district heating or cooling, geothermal energy, or waste heat. The network is controlled by E:ON's Ectocloud, which is a digital platform using artificial intelligence, cloud-, and Internet of Things technology to control the grid in order to improve the COP of HP:s and CH:s, maximize the use of self-produced renewable electricity, and prioritize different energy sources (E.ON Sverige AB, 2024a).

Tamarinden in Örebro

Another example of the principle of energy sharing is the residential area of Tamarinden in Örebro, which consists of 10 buildings and is part of the project called "System change with locally shared energy". This project is financed by the Swedish Energy Agency and coordinated by the Research Institutes of Sweden, RISE. This four-year project investigates the possibilities of how CEC:s can reinvent the Swedish energy system (Örebro kommun, 2025). For the residential area of Tamarinden, goals have been set towards energy use. The goals include reducing energy use, using renewable sources, producing and storing energy locally, and sharing energy between buildings. For the goal of producing locally, the focus is put on solar energy, and for local storage, batteries should be utilized to better adapt to the electricity market and local production availability. Another goal is that the buildings should be "smart" through shared energy in which the buildings can share energy through a low temperature district heating network (Örebro kommun, 2023).

Geothermal coupling

Some national examples of energy sharing through geothermal solutions are Xylem in Emmaboda, Embassy of Sharing in Malmö, and Hästskon in Stockholm. These examples utilize HP:s and CH:s along with geothermal storage to shift energy demands. For Xylem in Emmaboda, the company properties have been connected with a distribution system and a geothermal storage. A total area of 110 000 m^2 consisting of factories, offices, canteens, sport halls, and data centers has been connected with 140 boreholes (NIBE Energy Systems, 2025). The Embassy of Sharing consists of 6 decentralized substations connecting a total heated space area of 61 901 m^2, regulated by geothermal storage (Abugabbara et al., 2023). Continuing, Abugabbara et al. (2023) writes that Hästskon in Stockholm is two connected city blocks, supplied through aquifer thermal energy storage. The two blocks have a total heated space area of 56 799 m^2 with 2 cold wells and 4 hot wells.

2.4.2 International examples

Energy sharing can also be seen internationally, examples of this are the benefit potential study of the city of Ulsan in Korea, E:ON's Ectogrid in Milan, the Olympic village of Whistler in Canada, and Aenergy grid of ETH Zurich campus.

Ulsan in Korea

In the article by Kim et al. (2018) the potential benefit of energy sharing is investigated in a project in Ulsan, Korea. The project focuses on the potential between different

industries or residential areas in four different scenarios. In the first scenario, waste heat from industries is utilized as energy for other industries. In the second scenario, waste heat from industries is used for one urban area located close to the industries. In the third scenario, the urban area is further expanded covering more residential buildings. For the fourth scenario, it is considered whether other regions should be connected. For the project, Kim et al. (2018) continues that there were 183 available heat sources, producing both high- and low-grade waste heat, which was conservatively assumed to be 49 321 TJ/year, 10% of the energy usage of the heat sources. In terms of heat sinks, it was assumed to be 3 146 TJ/year for industries and 15 424 TJ/year for urban regions. Which indicates the possibility of covering the heat sinks with waste sources.

Kim et al. (2018) estimates through the above-mentioned scenarios that a reduction of 243 396 tonnes per year of CO_2 emissions and 48 million US dollar per year can be made. The study also recommends that the large transition cost to an energy sharing model through district heating could be covered through an IUS private partnership business model.

Ectogrid in Milan

Milan Innovation District, MIND, located outside of Milan is a project in which the World Expo area was transformed to a center for innovation and research. The district will house an estimated population of 60 000 and connect 32 buildings with E:ON's Ectogrid (E.ON Sverige AB, 2024b) that was described in Section 2.4.1.

Whistler in Canada

A third international example of energy sharing and symbiosis is the Olympic village in Whistler, Canada. This village was built to house the Olympic athletes of the 2010 Winter Olympics in Vancouver and was later converted to a residential area of 400 units. The main energy source for the units is a district energy sharing system. The system utilizes low temperature waste energy from the sewage treatment plant through multiple heat exchangers to heat up the system fluid. When there is not sufficient energy achieved from the heat exchangers, boilers are used to reach the set temperature. From the plant a pipe network distributes the energy from which the surrounding residential building receives this energy through HP:s. The HP:s are designed to cover 60% of the peak capacity and are installed in each building along with a backup electric heater. The completed project was designed to achieve reductions of 50% and 70% in energy consumption and GHG emissions, respectively (District Energy Award Secretariat, 2011).

Aenergy grid of ETH Zurich

ETH Zürich (2020) describes how campus Hönggerberg of ETH Zürich houses 12 000 students and staff in 30 buildings that consume a total of almost 77 GWh of energy for electricity and heating yearly, where heating covers 22 GWh yearly. Up until 2010, the campus' main energy source for heating was fossil fuels, and in 2013 the Aenergy Grid started operating. In 2019, the grid supplies 14 buildings with heating and cooling and consists of three underground storages, five substations, along with hot and cold supply loops. The energy flows of the system uses the underground storages as buffers where energy can be extracted or deposited. This leads to a varying temperature of the supply loops over the year. The hot loop has a temperature varying between 8^{o}C and

22^{o}C, with the cold loop between 4^{o}C and 18^{o}C. The high point temperatures of the loops are aimed to be achieved for the beginning of the heating season, in the end of September and the low points are aimed to be achieved at the end of the heating season, May. The substations uses HP:s and exchangers to cover the needs of the connected buildings and in 2016, 81% of the energy requirement for heating and 87% for cooling were covered (ETH Zürich, 2020).

In ETH Zürich (2020) the COP of the substations are presented and can be seen in Table 2.1.

Table 2.1: COP values of heating and cooling for three of the substations in the Aenergy grid of ETH Zurich.

Substation	HPZ	HPL	HWN
COP for heating	7.5	7.7	7.8
COP for cooling	36.5	33.0	22.1

In Table 2.1 ETH Zürich (2020) defines the COP for cooling as "Direct cooling via Aenergy Grid including pumping energy" and this COP for substation HWN only includes air conditioning.

2.5 Resilience

Swedish Civil Defence and Resilience Agency (Myndigheten för samhällsskydd och beredskap) (2021) describes how the production and distribution of energy should be regarded as critical societal functions and, furthermore, should be considered as part of the total defense of Sweden. Disruption and outages risk affecting all types of functions in a municipality. Disruption and outages could include causes such as natural disasters or antagonistic threats, e.g., cyber attacks. Swedish Civil Defence and Resilience Agency (Myndigheten för samhällsskydd och beredskap) (2021) continues that in order to manage the before mentioned risk, there is a need for advance planning which could include work procedures, and contact lists. Another measure to promote resilience is island operation or microgrids which can sustain itself independently from the main grid for a set time duration and at different scales, for example, individual buildings or city districts (Swedish Civil Defence and Resilience Agency (Myndigheten för samhällsskydd och beredskap), 2021).

Decentralization of energy supply and microgrids implies lower demands on the main grid. However, Swedish Energy Agency (Energimyndigheten) et al. (2024) describes how major decentralization increases the difficulty of power balancing in the main grid. Additionally, this risks reducing the cost-effectiveness of larger centralized power plants and could further increase the difficulty of power balancing if major power plants need to be shut down.

3

Case study

In the following chapter, the method and creation of the case study will be described by text and figures supported by the theory covered in Chapter 2. Additionally, to obtain a deeper understanding and practical experience of the systems, a study visit was made to the headquarters of NIBE in Markaryd, Sweden. This study visit gave valuable insights for practical experience in HP technology and TSN:s, which helped define the case study. Interviews with other contact persons from the industry was also held, one interview with Gustav Adolfsson at E.ON regarding Ectogrid, and another with Martin Warneryd at RISE, togheter with Jan Johansson at the municipality of Örebro regarding Tamarinden. These interviews helped to expand the practical knowledge further.

The basis for this case study is to evaluate different investment options for a reference building that wants to reduce its energy use. The building will be evaluated by either connecting to the DH and DC network (1), invest in geothermal energy extracted by a HP and CH (2), or as a third option is the connection to a local energy sharing system (3). In Figure 3.1 the options for the reference building can be visualized.

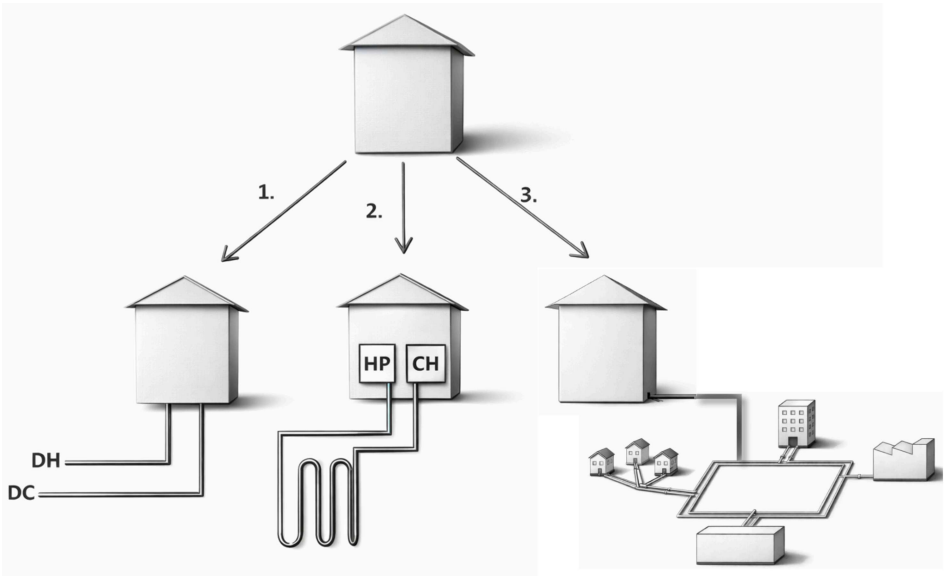

Figure 3.1: AI enhanced sketch of the potential upgrade of energy supply system showing the three possible cases, connection to district heating and cooling, boreholes, and local energy sharing network.

3.1 Interviews

As mentioned in this chapter's introduction, interviews were held with multiple people from the industry to gain practical knowledge to apply to this project. The interviewees were Gustav Adolfsson at E.ON, Martin Warneryd at RISE, and Jan Johansson at the municipality of Örebro. As more of an informal interview, Fredrik Snygg at NIBE was also met during a study visit to NIBE headquarters in Markaryd, Sweden, on the 29th of September. The study visit provided knowledge of the available HP:s and previous projects of heat recovery or energy sharing through HP:s.

3.1.1 Interview with Gustav Adolfsson at E.ON

After recommendation from Fredrik Snygg, Gustav Adolfsson at E.ON was interviewed on the 16th of October 2025 to better understand how E.ON's Ectogrid works both technically and economically. Going into this interview, multiple main questions were formed and can be seen below, translated from Swedish to English.

- How is the ownership of pipes, land, and other technical components formed?
- How is the economic model designed? Who pays for the investment, maintenance, and so on?
- How are the temperature of the network set and designed?
- How is redundancy achieved? What if a needed stakeholder wants to leave or goes bankrupt?

Gustav described how E.ON, own the whole Ectogrid, i.e. all parts of the system, so that the consumers only pay a fee for the energy they use. No investment or maintenance costs are needed for consumers specifically. To achieve the needed redundancy, consumers sign a contract with E.ON, in which E.ON will be obliged to provide the needed energy. If an important energy producer stopped providing energy, then E.ON would have the responsibility to provide another source of the energy. In, for example, the Milan project of Ectogrid there are some contracts for 99 years. If a consumer would want to leave, then this would be done according to what was set in the contract. For the system design, Gustav described how the pipes are not insulated and therefore the system temperature is wanted as close to the soil temperature as possible. The design temperature is set at 7.5^{o}C for the cold supply and a temperature difference of 10^{o}C is set between the loops, resulting in 17.5^{o}C in the hot supply. When there is a large energy supply to the network, the temperature will be allowed to increase to 25^{o}C and 35^{o}C, respectively. If the temperature increases or decreases below these setpoints, then active heating or cooling of the system will initiate to keep the setpoints. The choice of balancing differs between cases and is based on available sources in the area.

3.1.2 Interview with Martin Warneryd at RISE and Jan Johansson at the municipality of Örebro

An interview was also conducted with Martin Warneryd at RISE together with Jan Johansson at the municipality of Örebro to get an insight into their experiences and knowledge from similar energy sharing projects, especially the Tamarinden project in Örebro. Following is the main questions discussed during the interview, translated from Swedish to English.

- How has ownership of the system and its components been designed?
- What was the choice of an economic model? Who pays for costs such as maintenance or investment?
- How are redundancy and balancing solved for the system?

For these questions, Martin Warneryd and Jan Johansson described how the ownership of both the electrical network and the heating network in Tamarinden has been set up as joint facilities where everything is owned by all the property owners together. The joint facility is then operated by a joint property association as the legal form that most closely represents a CEC. However, Tamarinden has decided to restrict affiliation and withdrawals to maintain stable and secure ownership, something that a CEC requires. That the definition of CEC is not fully fulfilled could potentially lead to the project missing out on funds and support from the EU. Although the property owners affiliation and withdrawal to the joint property is restricted, they are free to optimize the building as they see fit but with the benefits of the joint facility as the priority.

The interviewees continued that as of the date of the interview, 23 October 2025, only four of the ten properties have been built due to the economic situation of Sweden's construction sector, which until the completion of the other properties have their heating supplied by traditional DH from E.ON. When the other six properties have been completed, the mentioned joint facility for heating will be implemented where E.ON according to the signed contract will supply the balancing and redundancy of the heating network. The network is set to be below 65^{o}C, and its number one priority is to balance demand and supply between properties before buying energy from an exterior grid or supplier. The project of Tamarinden is also looking into the possibilities of recovering waste heat from a nearby supermarket, which would lower the dependence of exterior balancing through primary energy. The economic model of choice for a potential deal with the supermarket is yet to be finalized, but Tamarinden is implementing an open and honest negotiation to acquire waste heat sources.

In summary of the interviews, both the interview with Gustav Adolfsson and the interview with Martin Warneryd and Jan Johansson helped motivate and shape the case study of this thesis further regarding both economic and technical aspects.

3.2 Analysis

In the following section, the tools used for analyzing the case study and the method used for this will be covered.

3.2.1 Tools for analyzing

The tools used for the analysis of the fictional district will be IDA Indoor Climate and Energy (ICE) version 5.1 developed by EQUA Simulation AB, Microsoft Excel developed by Microsoft Corporation, Earth Energy Designer (EED) version 4.3 developed by buildingphysics.com, and MATLAB R2023b developed by MathWorks.

For the energy data for different buildings, IDA ICE will be used to collect the necessary data for each building. Then, by using Excel the total results of the fictional district can

be summarized. Excel will also be used to evaluate the economic and environmental aspects of the system. Additionally, EED and MATLAB will be used for calculating the geothermal storage possibilities and, for example, how many and how deep each boreholes need to be.

3.2.2 Method of analysis

When data were collected for the case study, the chosen finished projects from GICON was loaded into IDA ICE 5.1 where an energy simulation was run for a setup period of 14 days, then a full year with the relevant output parameters. The results were then extracted from IDA ICE 5.1 and inserted into Excel for postprocessing. In Excel, a template was created in which the data for each project was stored and then the project of interest's data can be copied into a sheet which calculates KPI:s and presents graphs of these. For projects where GICON has done energy monitoring, the available data were inserted into Excel directly. The template also calculates the total demands of the whole fictional district based on the chosen composition of different buildings, allowing for multiple iterations where the composition can be varied. By creating a template for the input data calculations, consistency and fair comparability can be achieved for all the iterations of the case study.

For the environmental impact of the system, emission factors were used to calculate the impact of different energy supplies. As per the demarcation the focus emissions are that of CO_2 eq. where the unit for the emission factors were in grams of CO_2 eq. per kWh. Thereby, the demands of the system were multiplied with the respective emission factor to get the total CO_2 emissions of the system. The factor used for different energy supplies can be seen in Table 3.1. For district heating and cooling in Table 3.1, the value consists of two terms, the left for combustion and the right for transport and production for the year 2024.

Table 3.1: Emission factor [g CO_2 eq./kWh] for different energy carriers.

Energy type	Emission factor [g CO_2 eq./kWh]	Source
District heating	41 + 7 = 48	Göteborg Energi
District cooling	0 + 0 = 0	Göteborg Energi
Bought electricity	150	Göteborg Energi
Produced electricity	10.8 - 44	European Commission

The DH information was gathered from Göteborg Energi (2025c) and the DC information from Göteborg Energi (2025b). The emissions factor of 150 g CO_2 eq./kWh for bought electricity was also gathered from Göteborg Energi (Göteborg Energi, 2025a). The produced electricity in Table 3.1 acts as a comparable example and refer to the electricity produced from solar panel on a roof top. Joint Research Centre (2025) present a span of 10.8 to 44 g CO_2 eq./kWh. However, this also includes raw material extraction through to distribution and production.

3.3 Creation of the fictional district

To achieve a relevant result of the case study, it is of importance that the boundaries are set correctly and as few parameters as possible are left unknown. Firstly, the boundaries and setting of the fictional district need to be specified, and then relevant components can be added. When the fictional district and its components are set, it can be analyzed over multiple iterations which can be compared to the KPI:s described in Section 1.5.

3.3.1 Concept and system boundaries

To expand on the concept of the energy sharing system shown in the third option of Figure 3.1, one can see it in detail in Figure 3.2. The idea of the system is to utilize the available waste heat and cold of the surrounding buildings through a TSN, where waste heat or cold can be "dumped" to a hot or cold supply distribution loop in which another building can extract through the use of a HP or CH. The balancing unit regulates the temperatures of the system and circulates the TSN fluid.

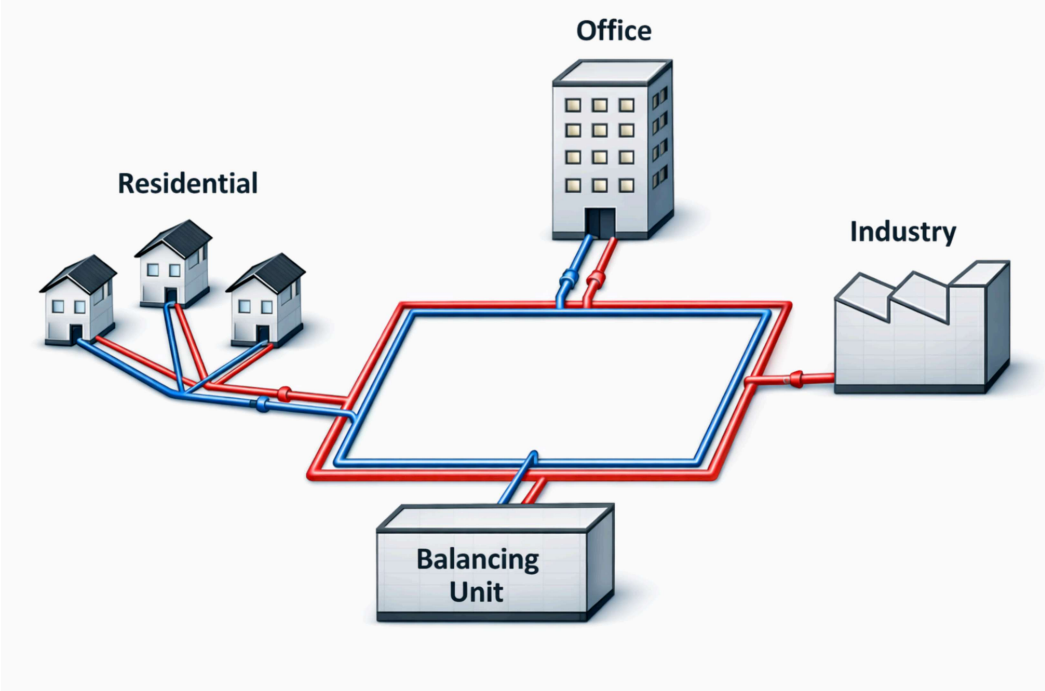

Figure 3.2: AI enhanced conceptual sketch of the energy sharing system. Blue indicates cold supply loop while red indicates the hot supply loop.

In line with Section 1.4, the case study will limit itself to Sweden and to evaluate the technical performance. Therefore, the distribution system, the balancing unit, and the connections between building's substation are the evaluated system components. The design parameters in focus for the evaluation will be the temperature of the distribution network, and the type of balancing unit for the fictional district.

An important aspect of the system is the electrical support of the added HP:s and CH:s where the choice of electrical network and the way electricity is generated matters. As mentioned in Section 2.2, there are multiple different types of networks and regulations.

For the study, it is assumed that the electric demand is covered by the electricity supplier. Subsequently, the possibilities of sharing electricity between buildings are not covered in this study, but could prove beneficial if done in further studies.

3.3.2 Included components

The included components of the case study, the building types, and technical systems, will be covered in this subsection.

For this case study, a combination of different projects from GICON will be used, the demands of the buildings are for some projects from the design phase while others are from measurements done after the building has been built. Also, the company NIBE was consulted in the choice and design of the HP:s thus allowing for even more practical information and knowledge for the thesis.

Building types

When studying a city district, multiple types of buildings can be identified, such as residential, office, industry, and leisure. These types of buildings have different demands and at different times that can be utilized. Common for all building types is that a higher temperature difference between outdoor and indoor will result in greater thermal losses. Commonly, spaces where humans reside are heated or cooled to around 20^{o}C depending on the function of the building, which means that the yearly variation of the outdoor temperature dictates these thermal losses. Therefore, the heating demand will generally be highest during winter and lower during summer. Subsequently, the cooling demand will generally be highest during sunny summer days and lower during winter days.

Residential buildings remain generally empty during the day while residents are at work. These hours are also when the solar load is at its peak. Therefore, residential buildings are rarely equipped with cooling units and instead only units for heating, such as radiators. Warfvinge and Dahlblom (2010) describes how instead of active cooling, passive actions, such as window sizing, are performed for residential buildings if the building becomes overheated. The schedule of the residents also results in high demand for domestic hot water (DHW) in the morning and evening. The daily demand varies from day to day depending on multiple factors, such as weather. Figure 3.3 shows a sketch of the general daily heating demand during the heating season, highlighting the generally higher energy demand in the mornings and evenings due to the DHW use and the lower outdoor temperatures.

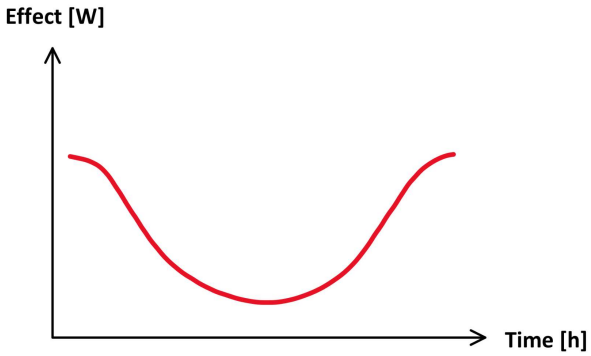

Figure 3.3: Sketch of the general daily heating demand curve during the heating season for a residential building. The x-axis shows unspecified time in hours and the y-axis shows unspecified effect in W.

By changing the interval, one would also see that the shape of an annual curve would be similar to the daily shown in Figure 3.3 where heating demand is greater in the beginning and end of the year due to seasonal weather changes.

In contrast, office buildings will generally be empty outside of work hours, i.e., in the morning, evening, and night. This implies that during peak solar load hours, the building will most often also be full of people and active office equipment, resulting in high cooling demands. Figure 3.4 shows a sketch of the general daily cooling and heating demand curve during the cooling and heating season of an office. In contrast to the residential building, the DHW use is lower for an office and the heating demand is generally dominated by the outdoor temperature.

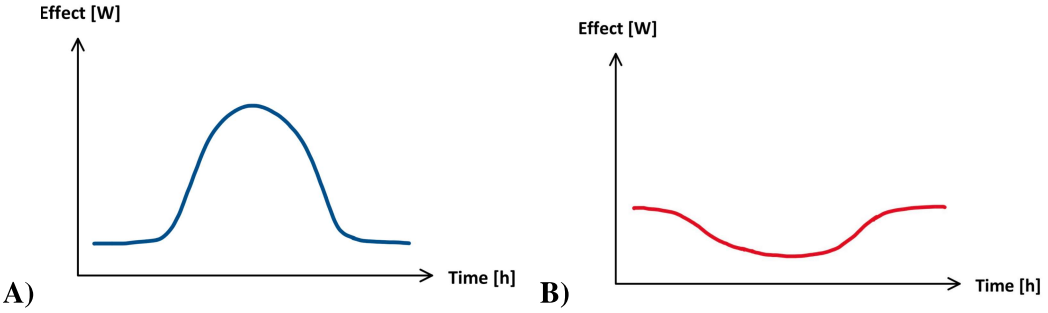

Figure 3.4: Sketch of an office building's general daily A) cooling demand curve during the cooling season and B) the heating demand curve during the heating season. The x-axis shows unspecified time in hours and the y-axis shows unspecified effect in W.

Once again, by changing the interval one would see that the shape of an annual curve would be similar to the daily shown in Figure 3.4.

Lastly, the heating and cooling demands of industrial or leisure buildings are heavily dependent on the type of activities the industry conducts. Some industries have a high heating demand, while others have a high cooling demand on top of the base demand

reliant on the building envelope and outdoor temperature. Examples of buildings relevant for an energy sharing system that have a higher cooling demand would be a data center or a supermarket. Both examples have an activity that results in waste heat that the energy sharing system could utilize. However, if the energy sharing system as a whole would have a higher cooling demand than heating demand, it could be solved by utilizing district cooling or free cooling sources such as lakes.

Chosen buildings

As mentioned previously, projects from GICON are used, where both calculations from the design stage and measurements from the operation stage will be used as data. In the following section, the data type will be noted along with a description of each chosen building.

The first building of the system is the planned building, denoted Building A, and is a residential and commercial building located in Gothenburg. The building has a total heated floor area of 28 085 m^2, split into 24 271 m^2 of commercial and 3 814 m^2 of residential. The energy carriers for the buildings are DH and DC. The yearly heating and cooling demand for Building A have been calculated in IDA ICE 5.1 and can be seen Figure in 3.5.

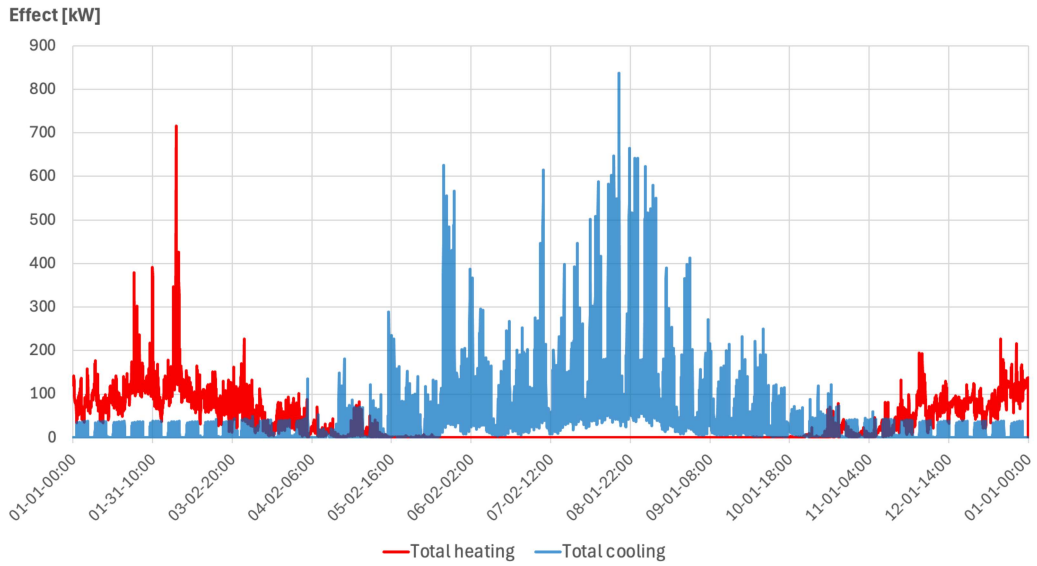

Figure 3.5: Yearly demand for heating in red and cooling in blue for Building A. The x-axis show the date of the year and the y-axis show the hourly effect in kW.

The second building of the system is a newly built residential building, denoted Building B, and is located in Gothenburg. The building has a heated floor area of 1 905 m^2 and is supplied by DH. As the building is residential, there is no cooling installed and thus, the yearly heating can be seen in Figure 3.6 have been calculated in IDA ICE 5.1.

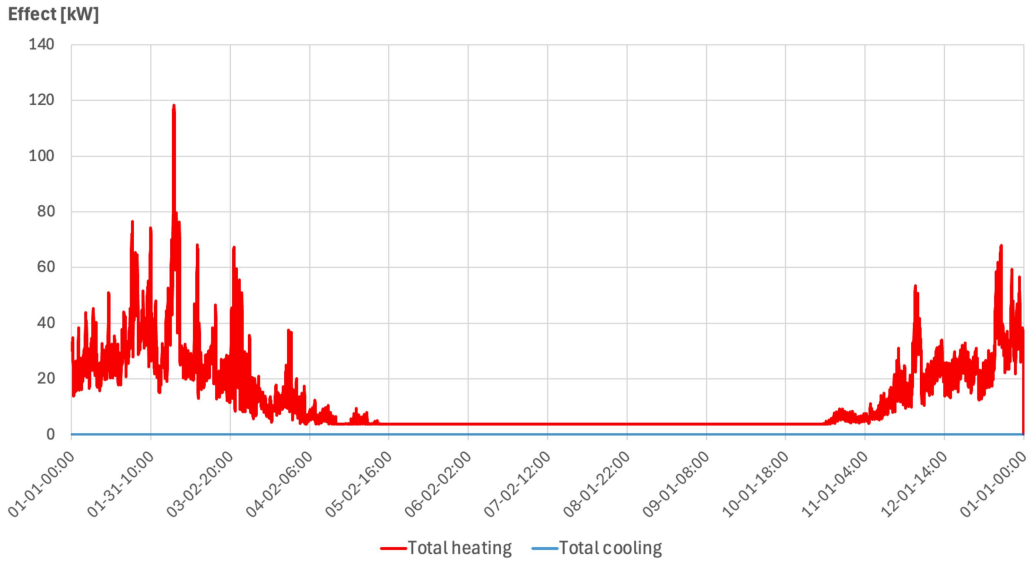

Figure 3.6: Yearly demand for heating in red and cooling in blue of Building B. The x-axis shows the date of the year and the y-axis shows the hourly effect in kW.

The third building of the system is a newly built building, denoted Building C. It is a residential building at 5 478 m^2 of heated floor area and is also located in Gothenburg. The building is supplied through DH (no cooling for a residential building), and the energy use was measured during the operation phase and can be seen in Figure 3.7

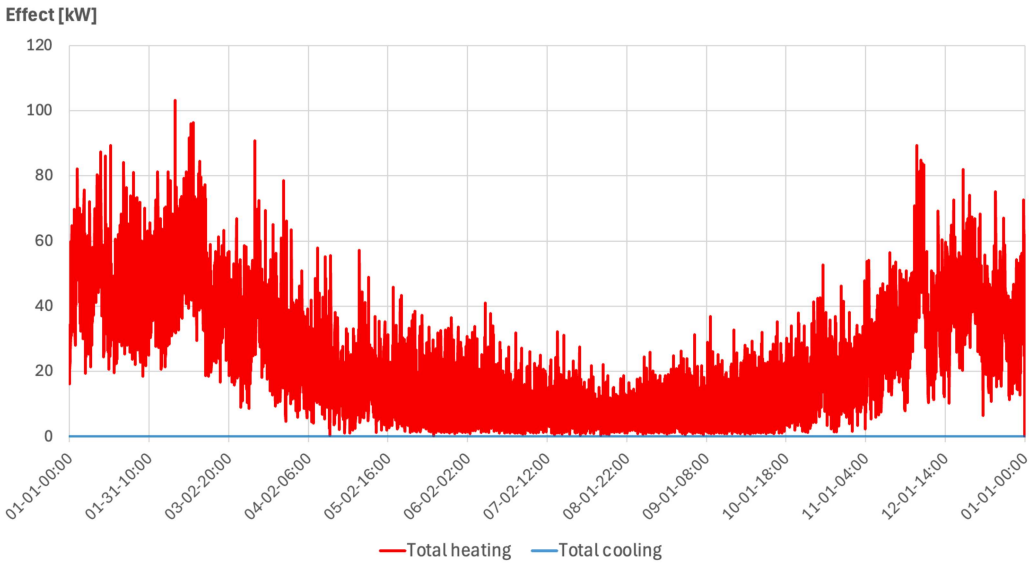

Figure 3.7: Yearly demand for heating in red and cooling in blue of Building C. The x-axis shows the date of the year and the y-axis shows the hourly effect in kW.

The fourth building of the system is denoted Building D and is a commercial building. The heated floor area is 26 912 m^2, where the data similarly to Building C have been measured during the operation phase. However, the data for Building D only covered

up until and including August. Thereafter, the data were extrapolated to cover a full year by assuming the demand of the 1st of September is equal to the 31st of June and going backwards. This building is also located in Gothenburg and the yearly heating and cooling demand can be seen in Figure 3.8

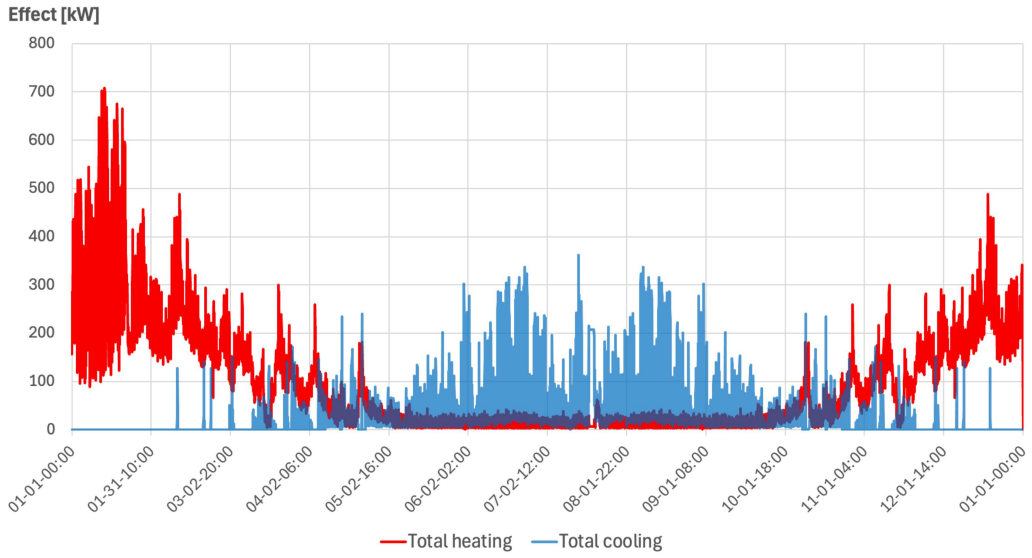

Figure 3.8: Yearly demand for heating in red and cooling in blue for Building D.The x-axis shows the date of the year and the y-axis shows the effect in kW.

Lastly, due to the high heating demand of the system, a waste heat source is needed to improve the system balance. The cooling demand of the refrigeration and freezer units of a 929 m^2 large supermarket, denoted Building SM, will be utilized for this. That is, the remaining heating and cooling demand of the building is not taken into account and only the available waste heat from refrigeration and freezer processes is considered.

Data were gathered from a contact person, Marcus Andersson, and analyzed. The available data were meters measuring the electricity effect and the heating effect that the supermarket is supplying to the building. Using the COP at a constant 2.2 (M. Andersson, personal communication, October 8, 2025), the cooling demand of the refrigeration processes could be calculated and then used for the case study. The data resulted in daily fluctuations, but were stable over longer periods of up to four months. However, it was lowered during the summer months and lead to further discussions with Marcus. It was determined that the HP performance varies with the heat recovery system of the building. The cooling demand therefore can't be calculated with the same COP when the heat recovery is dialed back. As a result of this, the cooling demand was conservatively assumed with the values for the 1st of December to the 31st of March being repeated. Resulting in a lower total cooling demand than if an assumed increase would have been set during the summer months. The final conservatively assumed yearly variation of the refrigeration and freezer cooling demand for Building SM can be seen in Figure 3.9.

Figure 3.9: Yearly variation of cooling demand from Building SM that could be utilized for waste heat. The x-axis shows the date of the year and the y-axis shows the effect in kW.

The total cooling energy available for waste heat from Building SM is 226.9 MWh and a further motivation for the choice of using a supermarket as a heat source can be motivated by the high frequency of these in cities, which makes them easily available. Gyms are also an example of a frequent cooling demand in a city. Furthermore, another potential waste heat source could be data centers as the need for these increases due to the demand for computational processes. However, the location of data centers and other industries with cooling demands are often not located in the center of a city.

The combination of the building types is of importance for the system's potential, aligning with the thesis question of how many buildings are needed for practicality. A higher heating or cooling load would require that external energy need to be used to cover the demand. The waste energy of this uncovered demand would then either need to be sold to an external consumer or be wasted. The yearly heating and cooling demand of each building and the total yearly demands of the TSN reference case for the case study can be seen in Table 3.2.

Table 3.2: Floor area [m^2], and yearly heating and cooling demand [MWh], and maximum heating and cooling effect [kW] for each building in the reference case.

Building type	Floor area [m^2]	Yearly heating demand [MWh]	Yearly cooling demand [MWh]	Max heating effect [kW]	Max cooling effect [kW]
A	28 085	304.8	353.3	715.2	836.9
B	1 905	112.1	0	118.3	0
C	5 478	200.5	0	103.2	0
D	26 912	837.0	280.0	707.6	361.7
SM	929	0	226.9	0	34.5
Total	**63 309**	**1 454.4**	**860.2**	**1 085.9**	**1 033.8**

Technical systems

The distribution system for the fictional district will be two uninsulated supply loops, one "hot" and one "cold". As a reference case, the hot supply loop's temperature will vary between 6 and 20^{o}C and the cold supply loop between 2 and 16^{o}C. Thus, motivating the choice of using uninsulated pipes as the temperature gradient to the exterior is low. The minimum values occur in the beginning of May, while the maximum values occur in the beginning of October. These values and when they occur are inspired by the Aenergy grid of ETH Zurich mentioned in Section 2.4.2. Due to the yearly mean outdoor temperature in Zurich being two degrees higher than for Gothenburg, the TSN temperature of the project's systems was lowered by two degrees. Between the maximum and minimum value of each loop, the temperature is assumed to vary linearly. The yearly temperature variation of the supply loops are visualized by the graphs in Figure 3.10

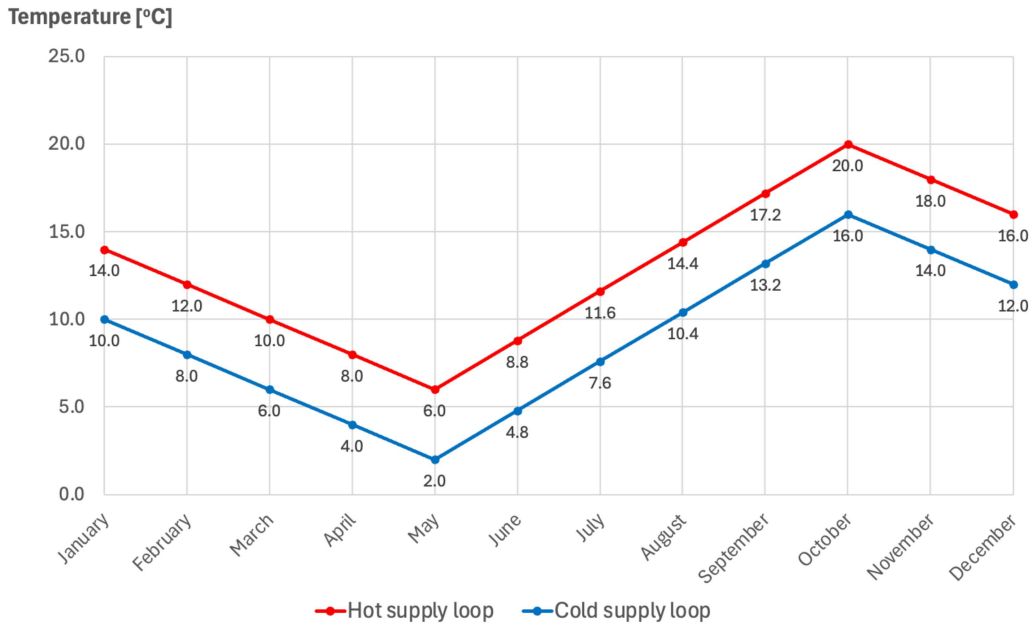

Figure 3.10: Yearly temperature [^{o}C] variation of the hot and cold supply loops for the reference case shown on the y-axis while the x-axis show the month of the year.

In Figure 3.10 the temperature varies based on the month of the year. However, to achieve this linear variation, the couplings of the buildings to the TSN are of importance. If a HP extracts energy from the hot supply, then it has to leave the remaining energy to the cold supply. Otherwise, there would be a significant decrease in the temperature over the length of the loop. Thus, the HP and CH are to be connected with the extract side on the source and the eject side to the opposite loop. The concept is visualized in a simplified sketch in Figure 3.11.

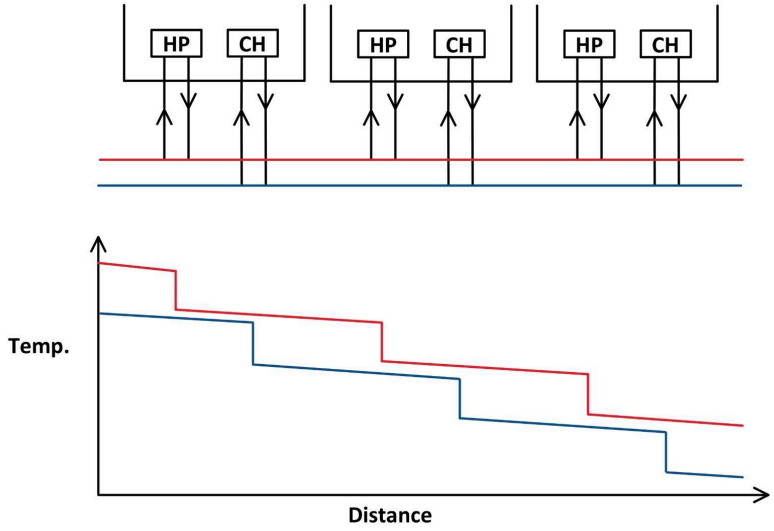

Figure 3.11: Simplified sketch of the temperature variation depending on the distance for HP:s and CH:s connected to its respective loop. The decline of the graph represents the heat losses over time.

As seen in Figure 3.11 the temperature drops for each connection as the temperature has been lowered in the energy transfer. In Figure 3.12 the HP:s and CH:s have been connected in a cross connection where the HP's return is connected to the CH's supply and vice versa. Furthermore, it is assumed that the temperature difference between the hot and cold supply loop is equal to that of the temperature change over the HP or CH.

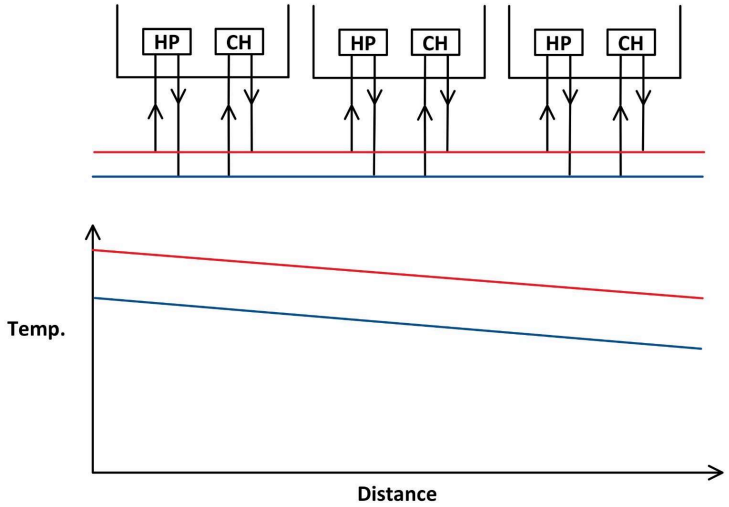

Figure 3.12: Simplified sketch of the temperature variation depending on the distance for HP:s and CH:s connected to cross-wise. The sketch assumes the temperature difference between the hot and cold loop is equal to the temperature change over the HP or CH. The decline of the graph represents the heat losses over time.

Based on the information gained from the study visit to NIBE, it was decided that in order to extract heat from the supply loop, NIBE's HP F1345 will be used. Where the temperature difference for the condenser and evaporator was assumed arbitrary at 5^{o}C and 3^{o}C respectively. Based on this, the Carnot efficiency was calculated to 60% and the calculations for this can be seen in Appendix A - Carnot efficiency. The temperature interval of the heat pump can be seen in Figure 2.2. Additionally, up to nine F1345:s have the possibility to be linked up, resulting in a maximum heating output of 540 kW.

For the COP calculations, the variation of the supply temperature in the technical systems for heating of the buildings is assumed the same for all buildings and follows a linear idealized graph based on the outdoor temperature. The temperature is set at a lower 50^{o}C to favor a heat pump configuration and can be seen in Figure 3.13.

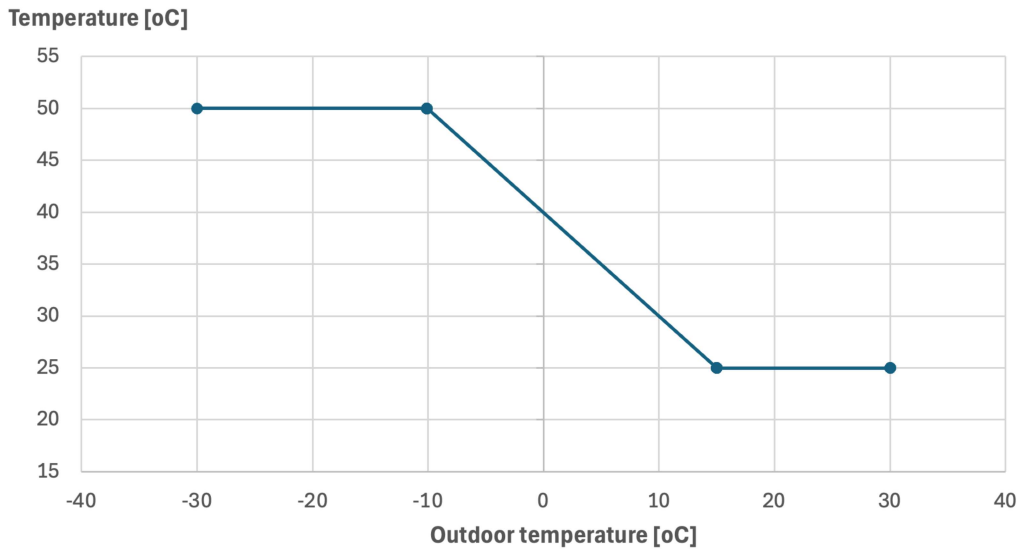

Figure 3.13: Assumed and idealized temperature variation of the heating systems in the building used for COP calculations. The x-axis shows the outdoor temperature [^{o}C] and the y-axis shows the heating system temperature [^{o}C].

In Figure 3.13 the system temperature breakpoints are set at the outdoor temperature of -10.1^{o}C, which is the dimensioning winter outdoor temperature of Gothenburg and at 15^{o}C. 15^{o}C being in the range used as common practice in the industry. Additionally, the heat pump is assumed to heat the DHW in timed intervals which give the assumed maximum temperature the heat pump works at 60^{o}C, thus affecting the COP. Based on Gothenburg's climate data, the building system's temperature demand could be calculated and can be seen in detail in Appendix B - Iteration calculations and results.

Cold will be extracted from the cold supply loop by using the HP used for heating, F1345 from NIBE in reverse. The temperature interval for the CH is the same as previously and can be seen in Figure 2.2. As for the heating purpose of F1345, the Carnot efficiency for cooling is also set at 60%. Furthermore, the calculations for the cooling COP were done by setting the building's wet cooling system's temperature to a constant 7^{o}C for supply and 12^{o}C for return. For the dry cooling systems, it is assumed

that the design temperatures are reached through shunting (wet and dry cooling refer to whether the cooling process results in condensation or not, that is, during wet cooling, the condition of the cooling fluid is below the dew point of the target fluid, and thus condensation occurs. Therefore, wet and dry cooling is suitable for different cooling purposes). Additionally, to calculate the COP for the cooling demand of Building SM, the temperatures needed for refrigerators or freezers are assumed at -5^{o}C and -30^{o}C. Based on the floor plan of the supermarket, it is assumed that 70% of the cooling demand is for the refrigerators and the remaining 30% for the freezers. To account for the distribution between the refrigeration and freezer processes of Building SM, and the comfort cooling of the remaining buildings, the final cooling COP is weighted based on the share of total cooling energy. The calculation process is described in detail in Appendix B - Iteration calculations and results.

The extraction and distribution of heat and cold is assumed to be sufficiently dimensioned in relation to hydraulic aspects, aligned with the demarcation in Section 1.4. As common practice in the industry the HP:s will be dimensioned to cover 70% of the peak power demand, denoted as capped at 70%. Using, for example, an immersion heater to cover the peak demand greatly reduces the needed size of the HP yet covering 99.6% of the heating demand for this case. This also aligns with the effect of 540 kW for the maximum amount of coupled F1345:s. For the CH:s, full capacity is used when possible as industry standard, thus the set up covers 100% of the cooling energy demand through a HP and CH respectively. However, Building A has peaks at 837 kW, which is above the maximum effect of nine F1345:s. Thus, the building is in need of an auxiliary system to cover the remaining cooling energy, or in need of time shifting strategies.

For balancing the system, a geothermal borehole system is used. The exact design, e.g., optimal fluid, insulation, and diameter, are out of the scope of this thesis, but an estimation of the amount of boreholes and the depth of these was made with EED v4.3 and MATLAB. This is covered further in Section 3.4. Furthermore, for balancing and redundancy of the system a DH and DC connection is added. This is done to ensure the operational safety if a tenant, providing valuable waste heat, moves out of the system.

3.3.3 Finalized system

Based on the system boundaries, and included components defined previously, the finalized system can be seen in Figure 3.14 and will be acting as the reference case which additional iterations will be compared to.

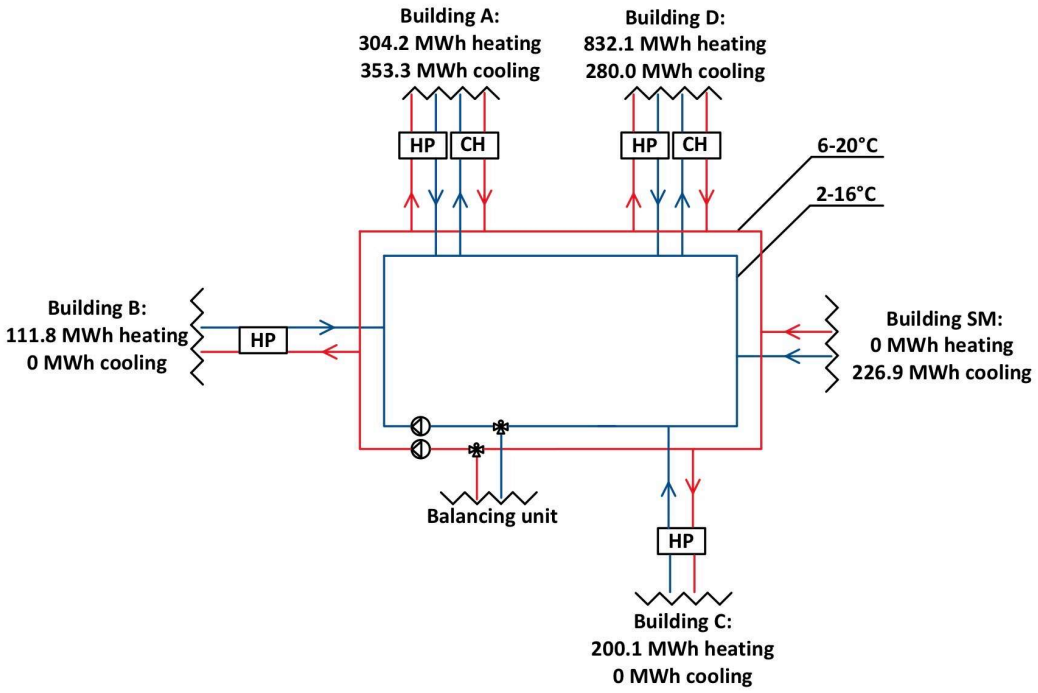

Figure 3.14: Basic schematic of the finalized system for the fictional district of the case study showing the included buildings, capped heating and cooling demand [MWh], and the temperature [^{o}C] of the supply loops.

The finalized reference case seen in Figure 3.14 consists of all buildings outlined in Section 3.3.2 for a total yearly capped (referring to the HP:s and CH:s peak effect coverage) heating demand of 1 448.2 MWh and 860.2 MWh of cooling. Resulting in a yearly surplus heating demand of 588.0 MWh. The demands for each month can be seen in Table 3.3.

Table 3.3: Capped heating and cooling demand in MWh for each month for the finalized system. A negative difference indicates a cooling demand and a positive difference a heating demand.

Month	Heating demand [MWh]	Cooling demand [MWh]	Difference [MWh]
January	365.1	23.7	341.4
February	273.5	22.0	251.4
March	153.7	31.8	121.9
April	63.9	39.2	24.7
May	24.2	93.7	-69.5
June	18.7	146.4	-127.7
July	17.6	157.8	-140.2
August	17.6	177.0	-159.4
September	20.6	70.4	-49.8
October	63.2	44.0	19.1
November	151.9	29.7	122.2
December	278.3	24.6	253.8

For the fictional district, a combined graph of the yearly variation of heating and cooling demand can be created, and Figure 3.15 shows this.

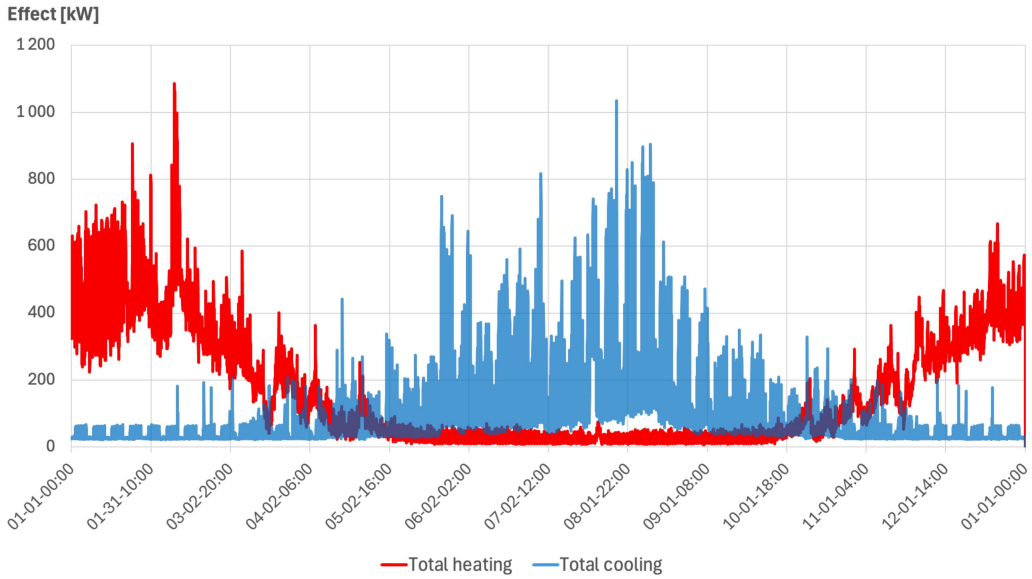

Figure 3.15: Combined demand for capped yearly heating in red and yearly cooling in blue for the finalized fictional district. The x-axis shows the date of the year and the y-axis shows the demand in kW.

Figure 3.15 clearly indicates the time shift needed through energy storage to recover the bought energy. Highlighted by the cooling demand being focused in the summer and the heating at the start, and end of the year. In Figure 3.16 the yearly variation can instead be seen in a monthly resolution without including Building SM.

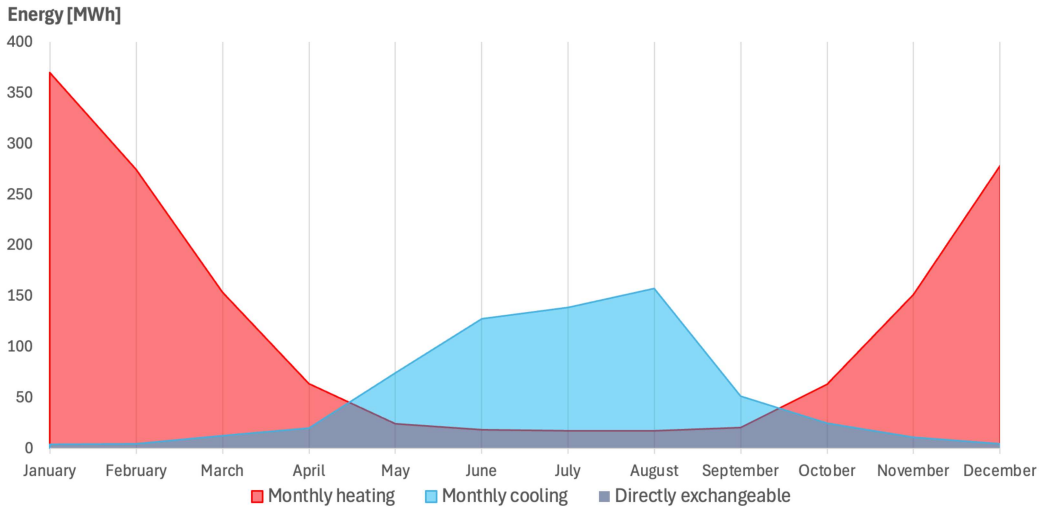

Figure 3.16: Combined monthly capped energy for heating in red, cooling in blue, and the directly exchangeable in blue-grey for the finalized fictional district **without** waste heat from Building SM. The x-axis shows the month of the year and the y-axis shows the energy demand in MWh.

Furthermore, by adding the waste heat source of Building SM, the directly exchangeable energy could be improved and can be seen in Figure 3.17 which is based directly on the values seen in Table 3.3.

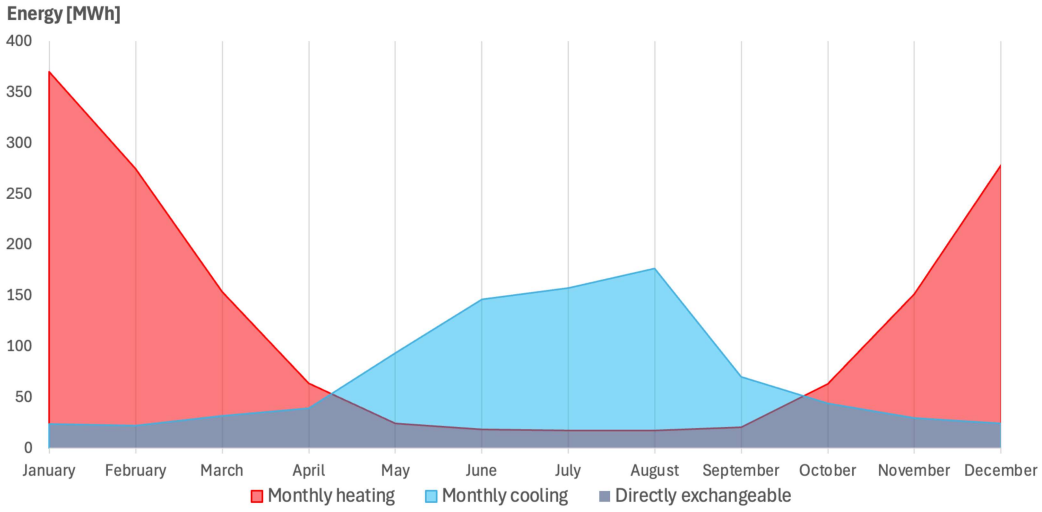

Figure 3.17: Combined monthly capped energy for heating in red, cooling in blue, and the directly exchangeable in blue-grey for the finalized fictional district **with** waste heat from Building SM. The x-axis shows the month of the year and the y-axis shows the energy demand in MWh.

By comparing Figure 3.16 and Figure 3.17, it can be seen that directly exchangeable energy is improved in the start and end of the year with the addition of the waste heat source. For the summer period, the waste heat source does not improve directly exchangeable energy because there is already a surplus cooling demand for the summer period.

To summarize the technical systems, the hot supply loop varies between 6 and 20^{o}C and the cold supply loop between 2 and 16^{o}C. The HP F1345 from NIBE with a calculated Carnot efficiency of 60% is used to extract heat and as a CH, F1345 is run in reverse with the same Carnot efficiency. To balance the system, boreholes, and district heating and cooling will be used.

3.4 Geothermal hand calculations and MATLAB

As a first measure for analyzing the finalized system, a simplified model of the ground was created in which a geothermal storage is seen as one rectangular volume and the undisturbed surrounding ground as another. The heat fluxes for the geothermal storage are seen as, between surrounding ground and storage, and between geothermal storage and the ground surface. For both volumes a simplified assumption for a homogeneous temperature across the volumes was assumed, i.e., the temperature at all spacial coordinates for a specific time step would be the same if they are in the same volume. A 2D view of this assumed and simplified ground model can be seen in Figure 3.18.

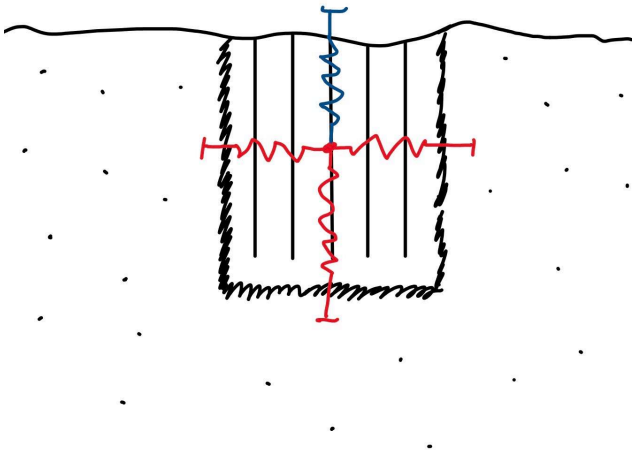

Figure 3.18: 2D schematic of the assumed ground model. The red lines denote heat flux from soil to the geothermal storage and the blue line denotes heat flux from the outdoor air to the geothermal storage.

Based on this assumed model and the differential heat equation, the temperature change in the geothermal storage volume over time was derived in Appendix C - Geothermal storage, resulting in Equation 3.1.

$$\Delta T_{geo} = (\sum_{i=1}^{5} \frac{A_i \cdot \lambda}{d_i} \cdot (T_{ground} - T_{geo}) + \frac{A_{surf.} \cdot \lambda}{d_{surf.}} \cdot (T_{out} - T_{geo}) - Q_{borehole}) \cdot \frac{dt}{C_v \cdot V} \; [^oC] \tag{3.1}$$

In Equation 3.1, A_i [m^2] is the surface area of for the rectangular sides towards the surrounding ground, d_i [m] is the distance from the geothermal storage center to the surface, λ [W/mK] is the thermal conductivity of the soil, T_{ground} [^{o}C] is the soil temperature, T_{geo} [^{o}C] is the geothermal storage temperature, $A_{surf.}$ [m^2] is the surface area towards the outdoor air, d_i [m] is the distance from the geothermal storage center to the outdoor air surface, T_{out} [^{o}C] is the outdoor temperature, $Q_{boreholes}$ [W] is the effect demand for the borehole system, dt [s] is the timestep, C_v [kWh/(m^{3}K)] is the volumetric heat capacity, and V [m^3] is the geothermal storage volume.

For Equation 3.1, a MATLAB code was created, seen in Appendix D - MATLAB code for geothermal storage, and the code takes into account three different cases. Firstly, a case where there are no surrounding heat influx, that is the temperature is only dependent on Q_{out}. For the second case, the heat influx from the surrounding ground to the geothermal storage is taken into account. For the last case, the heat influx or outflux depending on the outdoor air temperature is taken into account as well.

The resulting temperature change of the ground for the energy demand of the reference case and 100 boreholes spaced at 15 meters with a depth of 261 m each can be seen in Figure 3.19. The depth of the boreholes was derived through the maximum effect needed for the system and the maximum extraction of the boreholes at 40 W/m (Gehlin et al., 2016).

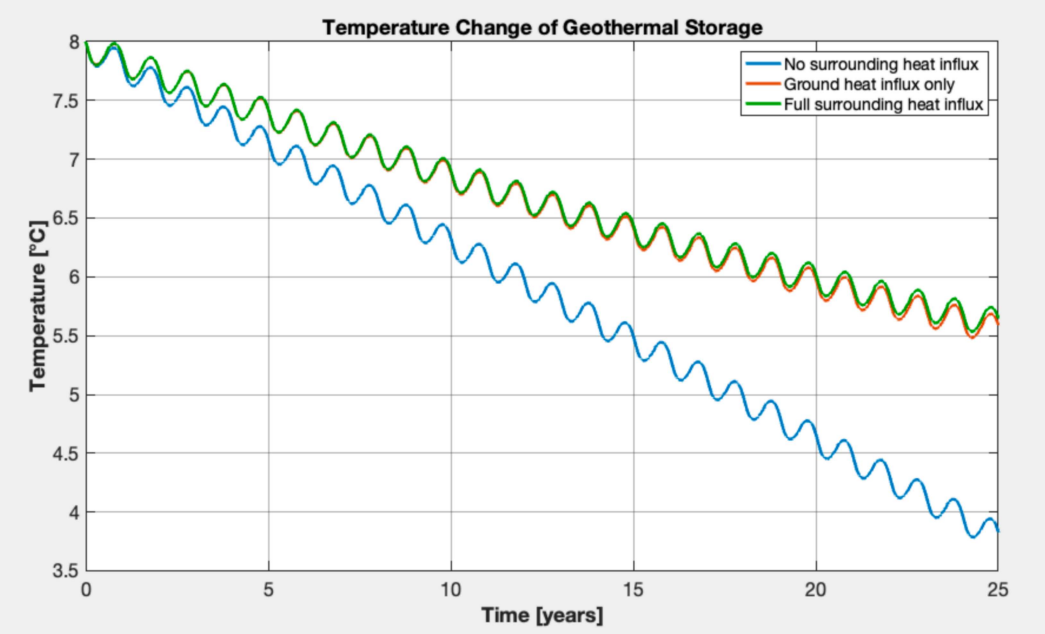

Figure 3.19: Estimated temperature change [^{o}C] of the geothermal storage over 25 years for 100 boreholes at 261 m of depth with 15 m spacing.

Figure 3.19 highlights how the cooling of the geothermal storage declines as it cools down. This aligns with the results seen in reality, validating the shape of graph. Furthermore, the gradual convergence toward a steady-state conditions confirms the feasibility of using a geothermal storage for the load of the TSN system. However, the actual average temperature of the storage can not be validated fully and in reality would most likely result between the no surrounding heat influx and the full surrounding heat flux.

4

Results

The chapter covers the results of the case study described in Chapter 3 and the thesis-specific questions defined in Chapter 1.

4.1 Laws and regulations

Regarding the first thesis question of the laws and regulations of energy sharing, it was shown, based on the study of available literature and interviews with similar projects, that the laws and regulations of Sweden for energy sharing differ from electricity sharing. The laws and regulations for sharing of electricity are stricter and more regulated, with the IKN Regulation being an obstacle for sharing along with the different network types and the financial restrictions of tax and other fees. On the other hand, for energy sharing through a TSN there is no law like the IKN Regulation which facilitates the incorporation of this. However, there is the District Heating Act (2008:263), which goes into action for transaction between a consumer and producer. This act requires transparent pricing, terms, and conditions for the parties involved in a transaction.

4.2 Current solutions

For the second thesis question regarding the possible solutions for energy sharing and as per the theory covered in Chapter 2, there are multiple TSN examples, both nationally and internationally. These examples utilize varying technologies to achieve energy sharing. A common practice is the use of geothermal storage to time shift the energy demands which are extracted through decentralized substations. Most solutions also use some sort of redundancy by a connection to, for example, DH and DC or a power plant. The examples also clearly indicate the need for different functions. By mixing residential buildings with heating demand and commercial buildings with cooling demands, an energy efficient system can be created.

4.3 Economic

An important aspect for the practicality of a TSN is the pricing and investment shares of the different consumers and producers. As covered in Section 2.2, there is the Swedish District Heating Act (2008:263) which implies that if energy is sold by a producer and bought by a consumer directly, contracts and pricing transparency are needed. For a system in total balance where all stakeholders have equal internal demand and supply to the system, this would mean that costs can be split based on the share of the total usage. However, complications arise when stakeholders only provide energy to the system but do not demand any, in which the stakeholder more than likely would want compensation for the energy it provides.

For the economic costs of a system, Table 4.1 shows the identified operational and investment types of cost for both an individual stakeholder and the TSN.

Table 4.1: Identified operational and investment costs for individual stakeholders and for a TSN.

Investment costs	
TSN:	Individual:
Pipes and pumps	HP:s and CH:s
Municipality contracts	Changes to building stock
DH DC connection	Electricity capacity
Geothermal storage	
Operationan costs	
TSN:	Individual:
Circulation	HP and CH maintenance
Top up of DH or DC	Electricity
Waste heat or cooling	
Maintenance	

The reason for having HP:s and CH:s on the individual side is for the different sizes needed for different buildings due to demand differences or available space. Another note is the individual stakeholder's potential investment cost for building stock changes. For example, there might arise a need to invest in new radiators due to a lowered system temperature in the building.

As a first potential model, the stakeholders buy and sell energy between each other directly and investment and maintenance costs are covered either equally or by the share each stakeholder use of the total demands. This model would need contracts and transparency between all stakeholders, which could lead to a complicated juridical situation due to the large amount of active contracts.

Another model would be that the stakeholder creates a joint cooperative which acts as the service provider, as seen in Tamarinden. In this model, each stakeholder could only need one contract between themselves and the cooperative, thus minimizing juridical complications and also abiding with the District Heating Act. The contract could, for example, base itself on the share of the total usage where the stakeholder pay a monthly or annual fee for both running and investment costs based on this share. The stakeholders who only supply energy will then also have a contract directly with the cooperative instead of having one per stakeholder that uses the supplied energy.

4.4 Base cases

To compare the practicality of the TSN-solution, the results of comparable base cases are of importance. For the first base case the building utilizes DH and DC from Göteborg Energi as the energy carrier, and in the second base case, geothermal storage with HP:s and CH:s are used.

Primarily, a comparison of the economics between the base cases and the TSN was created for the investment and operational costs excluding maintenance. A comparison that can be seen in Table 4.2 below.

Table 4.2: Identified investment and operational costs for the base cases and the TSN.

Type	(1) DH / DC	(2) Geothermal	(3) TSN
Types of investment costs	Connection	Drilling per borehole + drilling per meter + HP and CH	DH and DC connection + drilling per borehole + drilling per meter + HP and CH + distribution system
Types of operational costs	Energy price	Electricity	Electricity and circulation + energy for DH and DC

Thereafter, the investment and operational cost, excluding the value added tax (VAT), along with the CO_2 emissions for the first base case, DH and DC, was calculated. The results of this case can be seen in Table 4.3 and detailed explanations of the economics are covered in Appendix E - Economic analysis. The CO_2 emissions are based on the environmental factors seen in Table 3.1.

Table 4.3: Investment [SEK], operational cost for [SEK/year], and CO_2 emissions [kg CO_2 eq.] for the DH and DC base case.

Type	Investment [SEK]	Operational cost [SEK/year]	CO_2 emissions [kg CO_2 eq.]
DH	4 388 462	2 823 387	69 514
DC	3 841 194	1 254 714	0
Total	**8 229 656**	**4 078 101**	**69 514**

For the second base case, the utilized energy carrier is a ground-source heat pump, NIBE's F1345. The calculations for the second base case can be seen in Appendix F - Geothermal base case and the results can be seen in Table 4.4.

Table 4.4: Resulting investment [SEK] and operational cost [SEK/year] excluding VAT along with CO_2 emissions [kg CO_2 eq.] for the geothermal base case.

Building	Investment [SEK]	Operational cost [SEK/year]	CO_2 emissions [kg CO_2 eq.]
A	4 896 460	163 631	13 971
B	1 146 680	47 375	3 770
C	1 114 000	78 350	7 097
D	6 951 260	316 919	31 203
SM	450 000	60 011	5 937
Total	**14 558 400**	**666 285**	**61 978**

4.5 Case study - ideal scenario

The results of the case study's evaluation will be shown in the following section, covering energy replacement and emissions. For the iterations and for the reference case, it is of importance to note that the temperature set for each month is assumed to be achieved and potential energy required to heat or cool to the set temperature is not included.

The variation of the TSN temperature for each iteration in relation to the reference case is shown in detail in Appendix B - Iteration calculations and results along with further explanations of the calculation process.

4.5.1 Reference of the fictional district

For the reference case (or iteration zero), the total capped heating demand of 1448.2 MWh at 70% results in the need of 6.4 Building SM to cover the full capped heating demand in directly exchangeable energy. This implies that 1.6 of Building SM is needed per building in the reference system and by utilizing the cooling demand of the other buildings this can be lowered to 0.9 of Building SM per building. Such a value can be argued isn't likely to be the case in a real city district. Furthermore, as per the third thesis question, this highlights the importance of the heating and cooling mix of included buildings. However, a full study of how the mix affects the need for additional waste sources is needed for a complete conclusion.

The reference case's results for the electricity demand and the extracted source energy, i.e., the additional energy gained through the thermodynamic cycle, for heating and cooling energy can be seen in Table 4.5. The Carnot efficiency is set at 60% and derived as seen in Appendix A - Carnot efficiency.

Table 4.5: Resulting COP [-] and electricity demand [MWh] for each month and the total for the reference case.

Month	Heating		Cooling	
	COP [-]	Elec. [MWh]	COP [-]	Elec. [MWh]
January	5.5	66.4	12.8	1.9
February	5.1	53.5	15.1	1.5
March	5.1	30.4	18.5	1.7
April	5.1	12.6	23.8	1.6
May	5.3	4.6	33.3	2.8
June	5.9	3.2	21.3	6.9
July	6.9	2.6	15.7	10.1
August	7.7	2.3	12.4	14.3
September	7.8	2.6	10.3	6.9
October	7.9	8.0	8.8	5.0
November	6.7	22.7	9.8	3.0
December	6.0	46.3	11.1	2.2
Total electricity demand [MWh]	-	255.2	-	68.8
Extracted source energy [MWh]	-	1 193.0	-	791.5
Share of extracted energy [%]	-	82	-	92

In Table 4.5, the extracted source energy denotes the energy gained from the thermodynamic cycle. That is, adding the electricity demand and the extracted source energy results in the total energy demand. The share of extracted energy is thus the ratio of how much energy has been gained from the thermodynamic cycle compared to the total energy demand.

4.5.2 First iteration - increased temperature

For the first iteration, the temperature of the TSN was increased by 4^{o}C, i.e., the hot supply loop varies between 10^{o}C and 24^{o}C, and the cold supply loop varies between 6^{o}C and 20^{o}C. The total result of this iteration can be seen in Figure 4.6 and for each month in Appendix B - Iteration calculations and results.

Table 4.6: Electricity demand [MWh], extracted source energy [MWh], and share of extracted energy [%] for the first iteration in which the TSN temperature has been raised by 4^{o}C for both loops.

	Heating	Cooling	Total
Total electricity demand [MWh]	224.5	91.7	316.2
Extracted source energy [MWh]	1 223.7	768.6	1 992.2
Share of extracted energy [%]	84	89	86

As seen in Table 4.6, an increased TSN temperature indicates an increase in heating coverage but a decrease in cooling coverage.

4.5.3 Second iteration - Ectogrid adjusted

Based on the results of the first iteration, the TSN temperature was further increased and set similarly to the same maximum and minimum values used for Ectogrid in Lund, i.e. 35^{o}C as maximum for the hot supply loop and 8^{o}C as minimum for the cold supply loop. However, due to the maximum temperature range of the compressor, the maximum for this iteration was set at 30^{o}C and the temperature difference between the loops was still set at 4^{o}C and the total results of this iteration can be seen in Table 4.7. The results for each month can be seen in Appendix B - Iteration calculations and results.

Table 4.7: Electricity demand [MWh], extracted source energy [MWh], and share of extracted energy [%] for the second iteration. In which the maximum TSN hot supply temperature has been raised to 30^{o}C and the minimum cold supply set at 8^{o}C with 4^{o}C difference between loops.

	Heating	Cooling	Total
Total electricity demand [MWh]	192.1	112.7	304.9
Extracted source energy [MWh]	1 256.1	747.5	2 003.6
Share of extracted energy [%]	87	87	87

As seen in Table 4.7, and as expected, a further increase in the hot supply temperature results in a further increase of heating coverage and a decrease in cooling coverage.

4.5.4 Third iteration - increased temperature difference

For the third iteration, based on the results of the previous iterations, the temperature difference between the loops was changed. By comparing the reference case to iterations 1 and 2, one could see that more heating energy was replaced but less cooling energy. Therefore, the maximum and minimum temperatures of the reference case were altered, where the hot supply loop was kept between 15^{o}C and 25^{o}C, and the cold loop was set lower at 5^{o}C and 15^{o}C. Thus, keeping 10^{o}C between the loops, a temperature difference that Ectogrid in Lund also uses. The total results of the third iteration can be seen in Table 4.8 and for each month in Appendix B - Iteration calculations and results.

Table 4.8: Electricity demand [MWh], extracted source energy [MWh], and share of extracted energy [%] for the third iteration. For the iteration, the temperature difference between the loops is increased from 4^{o}C to 10^{o}C. The hot supply loops varies between 15 and 25^{o}C and the cold supply loop between 5 and 15^{o}C.

	Heating	Cooling	Total
Total electricity demand [MWh]	226.3	93.1	319.4
Extracted source energy [MWh]	1 221.9	767.1	1 989.0
Share of extracted energy [%]	84	89	86

An increase in temperature between supply loops and an overall temperature increase indicates, as shown in Table 4.8, that the heating coverage is increased and the cooling coverage decreased. However, the cooling coverage does not reach the same coverage as for the reference case of 92%.

4.5.5 Fourth iteration - extended heating season

For the fourth iteration, the heating season was extended in which the maximum TSN temperature occurs in September instead of October and the minimum temperature in June instead of May. Subsequently, this iteration evaluates the impact of a different slope of the temperature change of the TSN. The total results of this iteration can be seen in Table 4.9 and for each month in Appendix B - Iteration calculations and results.

Table 4.9: Electricity demand [MWh], extracted source energy [MWh], and share of extracted energy [%] for the fourth iteration. In which the heating season has been extended to cover September through June.

	Heating	Cooling	Total
Total electricity demand [MWh]	256.5	68.0	324.5
Extracted source energy [MWh]	1 191.7	792.2	1 983.9
Share of extracted energy [%]	82	92	86

Table 4.9 shows that the extended heating season leads to approximately the same coverage as for the reference case. The extracted source energy for heating has been decreased slightly as the linear variation leads to lower temperatures earlier in the winter. However, the extracted source energy for cooling has increased slightly, resulting in a total difference of 0.6 MWh between this iteration and the reference case.

4.5.6 Fifth iteration - borehole adjusted

As mentioned, the results seen for the previous iterations ideally assume the temperatures for each month. Therefore, to evaluate the impact of the geothermal balancing, the fifth iteration is based on the simulations made in EED 4.3. The results of the simulations are covered in Section 4.6.1 and in further detail in Appendix C - Geothermal storage. Subsequently, the temperatures of the TSN were matched to that of the borehole storage's temperature, and when they occur during the simulation's last year, the 25th. The resulting yearly temperature variation of the TSN can be seen in Appendix B - Iteration calculations and results along with the technical performance of the iteration for each month. The total demands for the iteration can be seen in Table 4.10.

Table 4.10: Electricity demand [MWh], extracted source energy [MWh], and share of extracted energy [%] for the fifth iteration. In which the temperature of the TSN was set to that of the borehole configuration analyzed in EED 4.3.

	Heating	Cooling	Total
Total electricity demand [MWh]	291.6	64.0	359.6
Extracted source energy [MWh]	1 156.6	796.2	1 948.8
Share of extracted energy [%]	80	93	84

Adjusting the TSN temperature to the boreholes is shown by Table 4.10 to decrease the heating coverage and increase the cooling coverage. Furthermore, when using the temperatures of the borehole directly, there would be no need for any potential heating or cooling of the set temperatures for each month.

4.5.7 Summary of iterations

A summary of the resulting extracted source energy and the share of extracted source energy for all iterations and the reference case can be seen in Table 4.11

Table 4.11: Summary of the electricity demand [MWh], extracted source energy [MWh] and share of extracted energy [%] for all the iterations and the reference case.

Iteration	Type	Electricity [MWh]	Extracted source energy [MWh]	Share of extracted energy [%]
Reference case	Heating	255.2	1 193.0	82
	Cooling	68.8	791.5	92
	Total	323.9	1 984.5	86
Iteration 1	Heating	224.5	1 223.7	84
	Cooling	91.7	768.6	89
	Total	316.2	1 992.2	86
Iteration 2	Heating	192.1	1 256.1	87
	Cooling	112.7	747.5	87
	Total	304.9	2 003.6	87
Iteration 3	Heating	226.3	1 221.9	84
	Cooling	93.1	767.1	89
	Total	319.4	1 989.0	86
Iteration 4	Heating	256.5	1 191.7	82
	Cooling	68.0	792.2	92
	Total	324.5	1983.9	86
Iteration 5	Heating	291.6	1 156.6	80
	Cooling	64.0	796.2	93
	Total	359.6	1 948.8	84

The result seen in Table 4.11 is further visualized in Figure 4.1 to highlight the difference in share of extracted energy for each iteration.

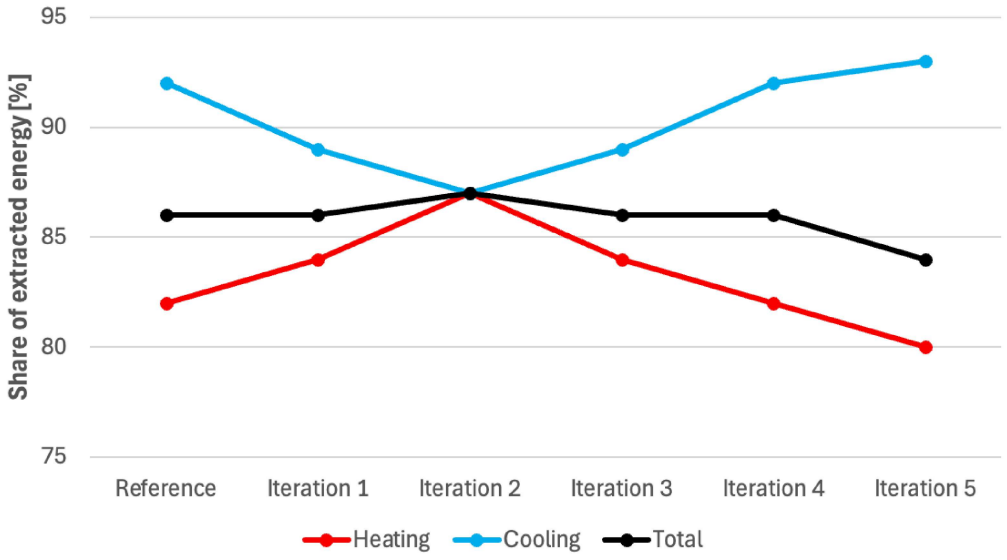

Figure 4.1: Line graph for the difference in heating, cooling, and total share of extracted energy [%] for each iteration.

Figure 4.1 shows that the highest total share of the extracted energy occurs for iteration 2, maximum temperature adjusted to that of Ectogrid in Lund. However, this iteration shows the lowest coverage for the cooling. The fifth iteration has the lowest total coverage or share of extracted energy but as previously mentioned, would not need any further balancing energy. Thus, the fifth iteration is most likely the most accurate share of extracted energy for a real life system of this type. The results seen in Figure 4.1 can also be presented as the SCOP for each iteration. To derive the SCOP, the total heating or cooling demand is divided by the electricity use for either heating or cooling. The resulting SCOP for the iterations can be seen in Table 4.12.

Table 4.12: Heating and cooling SCOP [-] for all iterations and the reference case.

Iteration	$SCOP_H$ [-]	$SCOP_C$ [-]
Reference case	5.7	12.5
Iteration 1	6.4	9.4
Iteration 2	7.5	7.6
Iteration 3	6.4	9.2
Iteration 4	5.6	12.7
Iteration 5	5.0	13.4

As mentioned, Table 4.12 reinforces the results seen in Figure 4.1. In which the SCOP for heating is highest for iteration 2, the iteration which also have the lowest SCOP for cooling.

Based on the electricity usage and the environmental factors seen in Table 3.1, the CO_2 emissions for each iteration was calculated and can be seen in Table 4.13.

Table 4.13: CO_2 emissions in kg CO_2 eq. for all iterations and the reference case.

Iteration	Type	CO_2 emisssions [kg CO_2 eq.]
Reference case	Heating	38 275
	Cooling	10 315
	Total	48 590
Iteration 1	Heating	33 682
	Cooling	13 751
	Total	47 432
Iteration 2	Heating	28 819
	Cooling	16 911
	Total	45 731
Iteration 3	Heating	33 951
	Cooling	13 963
	Total	47 914
Iteration 4	Heating	38 479
	Cooling	10 197
	Total	48 675
Iteration 5	Heating	43 741
	Cooling	9 597
	Total	53 338

The total CO_2 emissions seen in Table 4.13 are highlighted further as a line graph in Figure 4.2.

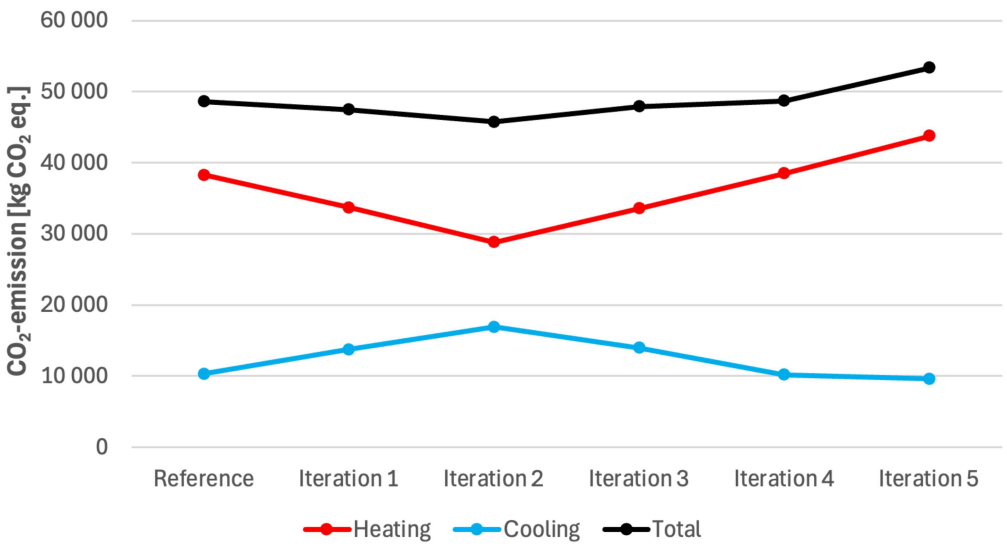

Figure 4.2: Line graph for the difference in heating, cooling, and total avoided CO_2 emissions [kg CO_2 eq.] for each iteration.

Figure 4.2 shows how the emissions for heating or cooling vary greatly between iterations. However, as iterations with increased heating emissions show less cooling emissions, the total emissions fluctuate less between iterations. The highest and lowest CO_2 emissions are for iterations 5 and 2, respectively. However, as stated previously, the fifth iteration is considered the most realistic result.

4.6 Case study - upholding the ideal case

The results shown in Section 4.5 for the reference case and iterations one through four rely on the ideal case. In which the set temperatures of each month in the TSN are assumed to be achieved. The resulting possibilities of achieving the assumed temperatures are highlighted in this section.

4.6.1 Earth Energy Designer version 4.3

To further evaluate the possibilities of geothermal storage in a more detailed approach, the software EED 4.3 was used. The input data and results can be seen in Appendix C - Geothermal storage for all simulations. To evaluate different parameter changes, three cases were evaluated. Firstly, using a separate borehole fluid. Secondly, the reference case TSN connected to the boreholes, and finally, iteration 1's TSN connected to the boreholes. The reason for these cases is to evaluate the effects of the maximum and minimum temperature constraints of the borehole fluid. Additionally, for each case, three different borehole configurations were tested, EED configuration 592 (100 boreholes in 10 rows and 10 columns), 692 (196 boreholes in 14 rows and 14 columns) and 747 (400 boreholes in 20 rows and 20 columns). The distance between rows and columns was 15 m for all borehole configurations, and the sizing of each collector was kept the same for all configurations as well. The simulation period was set as 25 years and the resulting required depth, and the last simulation year's maximum and minimum average fluid temperatures can be seen in Table 4.14.

Table 4.14: Summary of the simulations run in EED v.4.3 showing the temperature constraints [^{o}C], configuration type , resulting depth [m], and the final maximum and minimum mean temperature of the heat carrying fluid [^{o}C].

Case	Constraints [^{o}C]	Borehole config.	Depth [m]	$\overline{T}_{f,fin,min}$ [^{o}C]	$\overline{T}_{f,fin,max}$ [^{o}C]
Separate borehole fluid	-5 / 25	592	221	-5	14.6
		692	115	-5	14.2
		747	54.2	-5	15.1
Reference case	4 / 18	592	506	4	12.6
		692	314	4	10.9
		747	182	4	9.9
Iteration 1	8 / 22	592	No solution	-	-
		692	613	8	11.6
		747	460	8	10.4

As Table 4.14 indicates, an increase in the minimum fluid temperature constraint leads to a greater required borehole depth as the final minimum temperature equals that of the constraint. Implying that in order for the TSN fluid to be connected directly to the

boreholes, either the depth or amount of boreholes need to be increased, resulting in higher investment costs. Furthermore, as one would expect, the simulation shows that an increase in the amount of boreholes lowers the required depth per borehole.

For the EED simulations, the chosen borehole configuration for the fictional district is the separate borehole fluid 592, motivated by the depth of 221 meters. Aligning with the average borehole depth of Sweden (GeoExPro Magazine, 2024). The resulting temperature change for the full simulation of 25 years can be seen in Figure 4.3 for configuration 592.

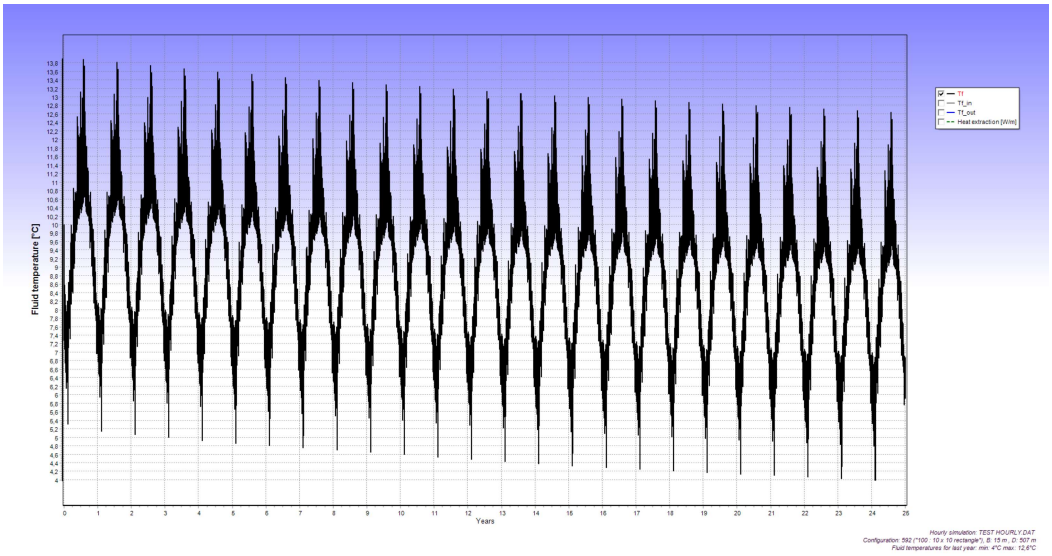

Figure 4.3: Temperature variation for borehole configuration 592 and mean temperature restraints as 4/18^{o}C.

The temperature change for the entire simulation period seen in Figure 4.3 algins with the convergence towards steady state seen in Figure 3.19 for MATLAB. Therefore, the resulting temperatures for the last year of the simulation were used for the fifth iteration's TSN temperatures. The final years temperature's can be seen in Appendix C - Geothermal storage and the borehole adjusted TSN temperatures can be seen in Appendix B - Iteration calculations and results.

The results seen by the geothermal analysis indicate that the current balance between buildings with heat demand, cooling demand, and waste heat sources is possible, although the TSN has a higher heating demand than cooling demand. However, the effects of changing the balance between heating and cooling demand were not concluded with regard to the third thesis question.

4.7 Economic analysis of iterations

The investment cost for all iterations and the reference case is the same and divided up into the investment for boreholes, HP:s and CH:s, electric connection, the DH and DC connection, and the distribution system. The DH and DC connection is set to cover half of the demand of the system, acting as top up balancing and redundancy. The cost of

each investment excluding VAT can be seen in the list below and is explained further in Appendix E - Economic analysis.

- Boreholes, HP:s, and electric connection - 12 939 200 SEK
- DH and DC connection - 2 669 703 SEK
- Distribution - 1 404 500 SEK

The operational cost excluding VAT, split up into the electricity and the circulation, for the iterations can be seen in Table 4.15.

Table 4.15: Operational cost excl. VAT [SEK/year], split up into electricity and circulation for all iterations.

Iteration	Electricity [SEK/year]	Circulation [SEK/year]
Reference case	502 708	98 249
Iteration 1	488 401	97 782
Iteration 2	470 253	97 652
Iteration 3	491 805	97 474
Iteration 4	504 454	98 417
Iteration 5	542 678	96 619

4.8 Result summary

To answer the last thesis question regarding a solution's performance compared to its economic and environmental aspects, a summary of all the base cases and iterations made for the project follows. As the environmental aspects follow as direct result of the technical performance and since only the operational impact is evaluated, no technical performance is shown specifically. Thus, the investment cost and the operational cost along with the CO_2 emissions for all cases and iterations can be seen in Table 4.16.

Table 4.16: Investment [SEK] and operation cost [SEK/year] along with the CO_2 emissions in kg CO_2 eq. for all iterations and the base cases (DH / DC & Geothermal).

Iteration	Type	Investment cost [SEK]	Operational cost [SEK/year]	CO_2 emisssions [kg CO_2 eq.]
DH / DC	DH	4 388 462	2 823 387	69 514
	DC	3 841 194	1 254 714	0
	Total	8 229 656	4 078 101	69 514
Geothermal	-	14 558 400	666 285	61 979
Reference case	-	17 013 403	600 957	48 590
Iteration 1	-	17 013 403	586 183	47 432
Iteration 2	-	17 013 403	567 905	45 731
Iteration 3	-	17 013 403	589 279	47 914
Iteration 4	-	17 013 403	602 871	48 675
Iteration 5	-	17 013 403	639 297	53 338

The CO_2 emissions seen in Table 4.16 can be reduced using the emissions factors seen in Table 3.1 for solar power. A switch to solar power through installed solar panels

instead of bought electricity would result in an emission reduction between 70.7% and 92.8%. However, this would come at the cost of an additional investment cost.

To visualize the comparison between cases for the three aspects of investment, operational, and emissions, the maximum value for each aspect was determined. The value of an aspect for each iteration was then divided by the maximum value for the respective aspect. Resulting in a relative ratio between 0 and 1 for each aspect, which can be seen as a rose diagram for all cases in Figure 4.4 A). In Figure 4.4 B), only the geothermal base case and the TSN iterations are compared to remove the outlying values of the DH and DC base case.

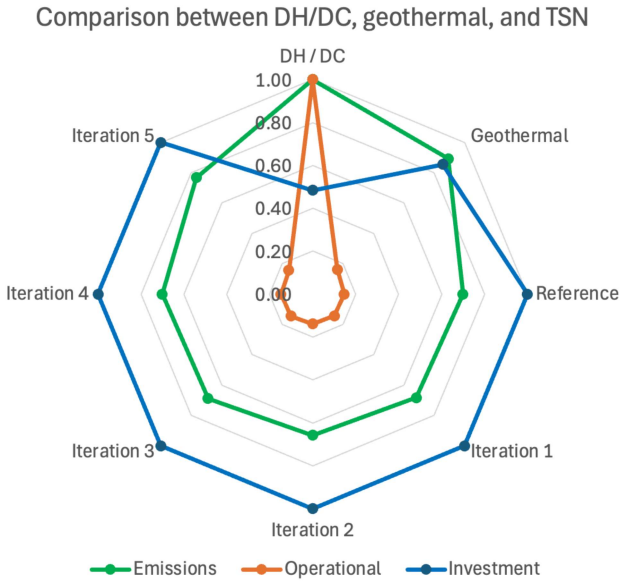

A)

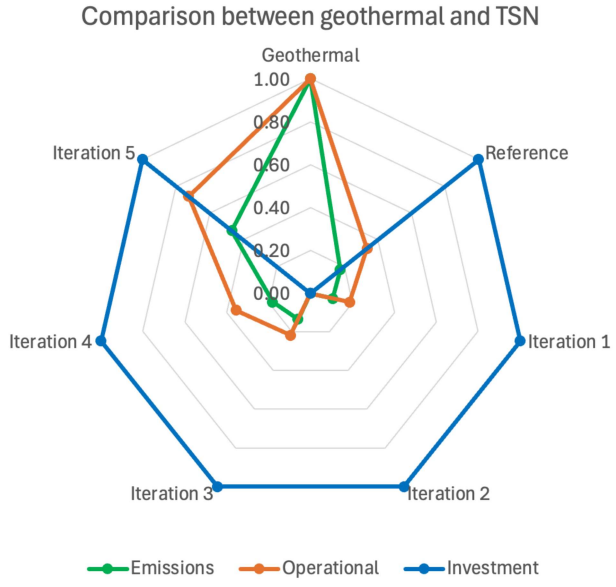

B)

Figure 4.4: Relative ratio between the maximum of each aspect and the value for A) comparison between all cases. B) Comparison without DH and DC.

The results seen in Figure 4.4 A), highlight how the DH and DC base case has a lower investment cost at the draw back of a higher operational cost and emissions. When comparing only the geothermal to the TSN as seen in Figure 4.4 B), it is now the geothermal base case that has a lower investment, but with higher operational costs and emissions as a drawback.

Additionally, a payback time comparison was made between the fifth iteration, as it is seen as most realistic, and the base cases. Calculated by dividing the difference in investment cost by the difference in operational cost. When comparing the fifth iteration to the DH and DC base case, the payback time resulted in 2.6 years. For the geothermal base case, the payback time was instead 91.0 if including the security investment of a DH and DC connection to the TSN. However, if such a connection is omitted, the fifth iteration proves to have lower investment and operational costs, along with lower CO_2 emissions.

5

Discussion

Due to the scale of the conducted project, the discussion is divided into sections of technical aspects, economic aspects, and finally, environmental aspects. Lastly, a general discussion of the practicality, drawbacks, and limitations is made. For all aspects, an addition of a subsection discussing how further studies could solve or take into account different solutions, problems, and factors is made.

5.1 Technical aspects

For the results of the study, as expected one could clearly see that when the temperatures of the TSN were set closer to that of the building's system temperatures, the average COP is increased, which decreases electricity usage and thus the CO_2 emissions. However, to achieve the temperatures set by the TSN, active cooling or heating might need to be used. The fifth iteration of the TSN, where the temperatures were adjusted to those of the boreholes, is most likely the closest to the actual temperatures. This means that for the other iterations the active cooling or heating would need to cover the difference, the energy demand for this would depend on the volume of the TSN and is thus difficult to estimate.

A flaw of the study is the time frame of the chosen building's energy demands. As the simulations and energy measurements do not take place in the same year, the simultaneity of the energy demand might be underestimated, thus underestimating the peak demands. Additionally, the choice of energy measurements and the energy simulations from IDA ICE does not take into account the actual dimension of the technical components needed for the worst case scenarios. This is due to the internal gains being included in the simulations and measurements.

The data used for the waste heat source of a supermarket was chosen in a conservative approach to not overestimate the available waste heat. As the cooling demand of Building SM was conservatively assumed as seasonally constant with daily fluctuations, the actual cooling demand would most likely be higher during the summer period if evaluated and measured further. This extra available waste heat to the system would lead to a more balanced energy demand over the year. However, seasonally increased cooling for Building SM would result in a higher cooling demand overall for the summer period. Thus, the need for boreholes would be less and the investment cost could be lowered further, but the temperatures of the boreholes would vary more rapidly over the year as the heating of the boreholes during the summer would increase.

An aspect that is not taken into account for the buildings is the effect of the control strategy for DHW heating. DHW requires heating above that of the set maximum level of the buildings heating systems. One possibility would be to heat it up through the use of the HP:s, but would imply a lower COP since the required temperature increase is higher than for the heating system. Furthermore, this would mean that the HP would work in intervals between DHW heating and space heating. The control of the interval depends on the DHW usage and the dimension of the accumulator tanks. An example of another option would be to use immersion heaters for any heating above the set maximum temperature of the heating system. However, this would lead to a high energy use for the immersion heaters during the summer period as the heating system's operate at a lower temperature than during the winter period.

To achieve the desired performance of the system, the control strategy of the TSN is of importance. In some cases it might be more beneficial to not allow the TSN fluid to pass through the boreholes and instead be utilized directly. Another case would be if it is more beneficial to heat or cool through an external energy source such as DH and DC instead of the boreholes. The control strategy could be further expanded to include technical systems such as, solar thermal collectors which utilize solar power for heating. Additionally, controlling the system to utilize the fluctuations in the electricity market are other potential measures that will affect the system's performance. All of these aspects would optimize the system to allow for an improved performance and thus potentially lower operational costs and emissions at the drawback of further investment and a costly design process.

By assuming a temperature variation for the TSN as the one visualized in Figure 3.10, the possibility of achieving the proposed temperature for each month must be evaluated. By assuming temperatures for each month results in 12 boundary conditions instead of setting a maximum and minimum temperature of the TSN which would result in only 2 boundary conditions. However, using only two boundary conditions would still result in the need of assuming the temperature of each month as monthly calculations are used for the study. Thus, still indirectly utilizing 12 boundary conditions nonetheless. The possibilities of achieving the assumed temperatures depend on the balancing units used and, if not evaluated, risks having negative effects on the average COP.

As a result of the directly exchangeable energy between buildings in the TSN, the energy demand for a borehole storage is decreased. Thus, the amount of boreholes needed is lowered compared to the geothermal base case, as seen by the results presented in Chapter 4. Furthermore, apart from the lowered investment cost, as only one geothermal storage is needed instead of five separate, the design and constructions process will be simplified. Leading to both technical and economic advantages compared to multiple smaller geothermal storage units. A clear advantage for the TSN compared to an individual geothermal storage for each building.

For the geothermal analysis, a TSN using regular water implies minimum fluid temperature constraints of above 0^{o}C which results in a large need of boreholes or fewer at greater depths than a geothermal storage using a separate borehole fluid with anti freezing properties. When using a separate borehole fluid, the TSN would need the

investment into a separate HP to extract and inject energy into the geothermal storage. Therefore, leading to increased investment and operational costs as the extraction and injection would occur in two phases instead of one. If a separate borehole fluid is used, it could be argued that the same fluid should be used for the entire TSN system. As a drawback for this is however, the increased need and thus investment for the borehole fluid. If regular water is to be used, one could also evaluate the use of an accumulator tank as storage instead of geothermal. However, this would be more reliant on energy balance and external energy sources as the storage possibilities are limited by the volume of the tank.

5.1.1 Further studies

To gain further understanding of the system's performance, further studies should simulate the system on an hourly basis instead of the monthly basis used in this project. An hourly simulation would provide more context on the matching in energy demands, COP fluctuations, and the resulting electricity use. Furthermore, for such a study, the exact control strategy of the system should be implemented. This could help determine the actual temperature variation of the supply loops and when balancing or external sources should be used. Furthermore, a detailed optimization process of the boreholes would provide increased accuracy. Further studies should also analyze the possibilities of using another balancing unit such as an accumulator tank.

5.2 Economic aspects

As seen by the investment cost for a TSN, the investment of a DH and DC connection will most likely be costly and negatively affects the economic incentive. As this extra investment would need to be covered through the lowered operational cost, thus prolonging the time until profits can be seen. For redundancy reasons, the connection is needed as the geothermal storage would not be sufficient long-term if an important energy source moves out of the system. Therefore, the connection is a costly investment for security and redundancy reasons.

For the economic results of the study, it is clear that the traditional solution of using DH and DC has a low investment cost compared to the geothermal and TSN solution. However, the operational cost for the DH and DC are much higher than for the other cases. One possible reason for this could be that the operational cost for the geothermal base case and the TSN is underestimated due to not including potential maintenance and replacement costs. As the DH and DC distribution system is owned by the energy supplier, the maintenance and replacement cost is covered by the supplier. The maintenance and replacement for the geothermal base case and TSN system must be covered by the consumers. These "hidden" costs will most likely be more for the TSN as the geothermal base case only maintains the boreholes. The TSN system on the other hand, need to maintain the distribution system with its pipes and circulation pumps.

A major drawback of a TSN system is that the need for distribution system between buildings is owned by the consumers and not by the an energy supplier as for traditional district heating or cooling. A potential risk of this is when a smaller stakeholder wants to place a distribution system in the ground in between buildings, ground that is most likely owned by someone else, often the municipality. This might result in setbacks and

problems as the smaller stakeholder does not have the experience or the authority of a big stakeholder like a district heating supplier.

The investment cost for the base case utilizing geothermal energy and the TSN will be further affected by a detailed optimization process. The current number of boreholes and the depth of each could potentially be decreased if a more favorable geothermal storage configuration can be apprehended. This would lower the payback time and make both the geothermal base case and the TSN system a more profitable investment.

The economic analysis used in this project is based on values gathered from available information from suppliers. For real life projects, the cost and contracts between energy consumers and suppliers depend on a multitude of different factors. For the district heating and cooling market in Sweden, there is one main supplier for different regions. Thus, the district heating and cooling market has monopolistic tendencies. This could for example, lead to the supplier to give a discount if a potential client considers another energy source in order to keep a client. Furthermore, geothermal cost, especially the investment cost, will also vary from case to case which results in difficulties when estimating costs. This is also the case for the electrical cost, where buildings with high electricity usage can often have a special deals made with the supplier. Subsequently, the economic analysis for studies based real life projects, often risks having a large gap between estimated cost and the actual cost for a finished project.

A discussion regarding the economic model is also needed, a suggested model and a model seen from other examples is the creation of a joint cooperative, as seen in Tamarinden. A solution that allows for equal parts between stakeholders but put strain on the system if a stakeholder wants to leave. If allowed, the energy balance would be shifted and risk imbalance. A different model, as seen by Ectogrid, have the benefit of being owned by E.ON that also produces district heating, the consequences would therefore only impact E.ON. However, a smaller joint cooperative without any back-up production would require large investments in security options, as discussed previously with the DH and DC connection. On the other hand, a benefit of the joint cooperative is the reduced juridical work, as only one contract needed for each stakeholder, between themselves and the joint cooperative. Compared to buying and selling energy directly between waste heat sources and consumers which requires contracts between each stakeholder. Therefore, a discussion regarding buy-out options, contract types, terms, and lengths would prove to greatly affect the possibilities for a successful TSN and business model.

5.2.1 Further studies

As mentioned previously, a simple economic analysis as the one made for this project often leads to a potential gap between estimated and actual costs. Therefore, a more detailed study investigating aspects such as actual deals and agreements between consumers and suppliers would prove valuable. Furthermore, an investigation of the impact of fees, taxes, and tariffs depending on the network type for the electricity, described in Section 2.2, would prove beneficial. For such a study, the use of the net present value would help gain an understanding of the long-term profitability of the system. A method that would allow for the incorporation of price growths and market fluctuations.

Which is an aspect that the simplified analysis done in this study neglects. For the social, juridical or cooperative aspect of the economic model, further research is needed for different businesses models and how each stakeholder is affected depending on the choice.

5.3 Environmental aspects

The environmental impact evaluated in this project is heavily dependent on the emission factors, thus, a bias towards the values given by Göteborg Energi has taken place as it is the main energy supplier of Gothenburg. This limits the comparability to other geographical locations further. However, as seen by the results, the environmental impact can be reduced, from 70.7% to 92.8% by investing in solar panels.

The use of primary energy is a potential solution to improve geographical comparison. Additionally, the use of primary energy numbers would align with certifications such as the Swedish grading tool, Miljöbyggnad. However, primary energy number depends on political decisions as national weighting factors depending on the energy carrier should be used. For example, the current weighting factor for electricity, DH, and DC is set at 1.8, 0.7, and 0.6, respectively (Boverket, 2020). Therefore, the additional electricity use for the HP:s and CH:s in the TSN system is unfavorable in such a grading system.

5.3.1 Further studies

A clear drawback of the study is the use of only one environmental indicator, the CO_2 emissions. A detailed study of the environmental impact through a full life cycle assessment would help further understand the full impact of the system. the assessment could evaluate the impact of both more life cycle stages and the impact of other indicators. Additionally, such a study could benefit from an evaluation using primary energy factors to validate any results further.

5.4 General drawbacks and limitations

As the project uses real life projects, the comparison to other systems, demand, or location will not be directly comparable. Especially, as the values and approaches chosen for this project differ from the geographical location or the buildings chosen. Additionally, a difference might also be seen between different consultant companies. However, this difference is unlikely to result in any major differences as all companies follow the set rules and guidelines in the building sector.

When considering the effects of new technology and investments, one must also consider the rebound effect. An effect showing the theoretically lost improvements due to behavioral changes. An example of this is when an energy supply is made more efficient, usage will increase because of a greater availability and affordability. However, since the solutions covered in this master thesis regard energy supply, the rebound effect will be rather small. This is because energy use for heating and cooling will most likely be the same, but a risk of increased heating or cooling energy use due to cheaper energy is still a possibility. This would result in increased energy use and, thus, also increased emissions. Worsening the performance of the evaluated preliminary system.

Compared to a traditional solution, the added electricity usage of the HP:s and CH:s results in a lower security in case of power outages. If not planned for accordingly, a power outage would leave the building incapable of heating or cooling to the set temperatures. In the heating case, it could lead to problems with DHW and thus risk the growth of legionella if the outage is prolonged. Therefore, a proper management strategy for how to handle such risk is needed. For example, installment of back up boilers for heating of DHW or back up generators for HP electricity to heat up the building to a lower set temperature are potential measures. Furthermore, the addition of the DH and DC connection used for the project provides some redundancy in the event of a power outage. For this to be possible, each building would need to have a full DH and DC connection as the regular connection during normal operation uses the HP.

5.4.1 Further studies

General aspects for further studies would be to evaluate different compositions of the fictional district. In other words, how would the system behave when total energy demands for cooling and heating are varied. For example, how would an increase in residential buildings compare to the fictional district used in this project. Such an evaluation would provide further understanding how energy demand and its yearly variation would affect needed geothermal storage, electricity usage, costs, and emissions.

6

Conclusion

The project has evaluated the potential of TSN:s in comparison to two traditional energy supply solutions in the form of DH and DC, and geothermal heat pump system. The evaluation was conducted by researching both national and international examples of TSN:s. Based on the research and interviews, a case study of a fictional district consisting of real life building projects was formed and then evaluated technically, economically, and environmentally. For the current examples, it was seen that a wide variation of solutions have been used, utilizing a multitude of different waste heat sources, balancing methods, and system temperatures. A common balancing method seen, is the use of geothermal storage and was thus used for the created fictional district. The research also concluded that the strict laws and regulations of sharing electricity in Sweden, do not apply for energy sharing through a TSN. The network does, however, need to comply with the District Heating Act if a transaction is taking place, requiring transparent contract between consumers and producers.

For the case study, a conclusion could also be drawn from the fact that a higher average COP for the iteration provides lower electricity usage and thus lower CO_2 emissions for the operational stage. This resulted in, without taking potential balancing need into account, that the iterations with system temperatures closest to that of the building's system temperature show the lowest emissions. However, variations in TSN temperatures proved to have a low effect on the total coverage, showing little variation between iterations. One could also see that by connecting buildings through a TSN, the directly exchangeable energy reduces the need for geothermally stored energy and thus lowers the investment need for geothermal storage compared to multiple separate geothermal storage units. Furthermore, the values of the fifth iteration are deemed the closest to resembling those of a final project. Therefore, a comparison of the fifth iteration was made to a DH and DC case and a geothermal base case. The fifth iteration resulted in a 107% higher investment cost compared to the DH and DC base case, and 17% higher for the geothermal base case. For operational costs, the TSN resulted in a reduction of 84% and 4%, respectively. Expressing the economic profitability in payback time for investing in a TSN results in 2.6 and 91 years, respectively. However, if the redundancy investment of a DH and DC connection is removed from the TSN, the payback time can be lowered to 1.8 and -8.0 years, respectively. Furthermore, for the CO_2 emissions, a reduction of 23% and 14%, could be seen for the TSN investment.

Regarding the aim of the thesis, it was concluded that an investment in a TSN requires further analysis of the economic incentive, but indicates clear benefits for operational costs and reduction in CO_2 emissions, thus contributing to the environmental goals.

7

References

Abugabbara, M., Gehlin, S., Lindhe, J., Axell, M., Holm, D., Johansson, H., Larsson, M., Mattsson, A., Näslund, U., Puttige, A. R., Berglöf, K., Claesson, J., Hofmeister, M., Janson, U., Jensen, A. W. B., Termén, J., & Javed, S. (2023). How to develop fifth-generation district heating and cooling in sweden? application review and best practices proposed by middle agents. *Energy Reports*, *9*, 4971–4983. https://doi.org/https://doi.org/10.1016/j.egyr.2023.04.048

Boverket. (2020). *Boverkets byggregler*. Boverket. Karlskrona, Sweden. https://www.boverket.se/globalassets/publikationer/dokument/2020/konsoliderad-bbr-2011-6-tom-2020-4.pdf

District Energy Award Secretariat. (2011, February). *Whistler athletes village district energy sharing system: Summary* (Project summary report) (Describes performance of the sewagebased District Energy Sharing System in Whistler Athletes Village). District Energy Award Secretariat. Whistler, BC, Canada. Retrieved July 16, 2025, from https://www.districtenergyaward.org/wp-content/uploads/2013/07/CA_Whistler-Athletes-Village_Summary.pdf

Energimyndigheten. (2024, September). *Fjärrvärme* [Last update, 23 september 2024]. Energimyndigheten. Retrieved July 11, 2025, from https://www.energimyndigheten.se/energiberedskap/om-el-fjarrvarme-och-naturgas/fjarrvarme/

E.ON Sverige AB. (2023, November). *Så fungerar ectogrid* [Page last updated 17 November 2023]. E.ON Sverige. Retrieved July 9, 2025, from https://www.eon.se/foeretag/integrerade-energiloesningar/ectogrid/sa-fungerar-ectogrid

E.ON Sverige AB. (2024a, January). *Ectocloud intelligent control for ectogrid systems* [Page last updated 24 January 2024]. E.ON Sverige. Retrieved July 9, 2025, from https://www.eon.se/foeretag/integrerade-energiloesningar/ectogrid/ectocloud

E.ON Sverige AB. (2024b, September). *E.on ectogrid i milano* [Page last updated 26 September 2024]. E.ON Sverige. Retrieved July 9, 2025, from https://www.eon.se/foeretag/integrerade-energiloesningar/ectogrid/e-on-ectogrid-i-milano

E.ON Sverige AB. (2025, June). *Ectogrid medicon village* [Accessed 9 July 2025; page last updated June 2025]. E.ON Sverige. Retrieved July 9, 2025, from https://www.eon.se/foeretag/integrerade-energiloesningar/ectogrid/ectogrid-medicon-village

ETH Zürich. (2020, February). *Anergy grid campus hönggerberg a dynamic underground storage system* (Brochure) (Informational brochure about the ETH Campus Hönggerberg's low-temperature Anergy Grid system). ETH Zürich. Zürich, Switzerland. Retrieved July 17, 2025, from https://ethz.ch/content/dam/ethz/main/eth-zurich/nachhaltigkeit/01_mainpage/dokumente/200129_Anergienetz_A4_6s_Einzel_EN_RZ.pdf

Gehlin, S. E., Spitler, J. D., & Hellström, G. (2016). Deep boreholes for ground source heat pump systems scandinavian experience and future prospects [Conference paper on Scandinavian GSHP borehole practice]. *Proceedings of the ASHRAE Winter Meeting*. Retrieved January 26, 2026, from https://media.geoenergicentrum.se/2016/02/Gehlin_et_al_2016.pdf

GeoExPro Magazine. (2024, July). *Shallow geothermal in sweden a deep penetration in the geo-energy market* [Discusses the importance of shallow geothermal systems in Swedens geo-energy landscape]. GeoExPro Magazine. Retrieved January 26, 2026, from https://geoexpro.com/shallow-geothermal-in-sweden-a-deep-penetration-in-the-geo-energy-market/

Göteborg Energi. (2025a). *Miljö och klimat elavtal* [Information on electricity origin, environmental choices and fossil-free elhandel 20242025]. Göteborg Energi. Retrieved July 12, 2025, from https://www.goteborgenergi.se/foretag/elavtal/miljo-och-klimat

Göteborg Energi. (2025b, June). *Miljövärden för fjärrkyla 2024 centrala nätet, slutliga värden* (Technical report) (Final environmental values for district cooling delivered in 2024). Göteborg Energi. Göteborg, Sweden. Retrieved July 12, 2025, from https://www.goteborgenergi.se/DxF-157494307/Miljovarden-fjarrkyla-centrala-natet-2024-slutliga.pdf?TS=638866008344761840

Göteborg Energi. (2025c, June). *Miljövärden för fjärrvärme 2024 slutliga värden* (Technical report) (Final environmental values for district heating delivered 2024). Göteborg Energi. Göteborg, Sweden. Retrieved August 29, 2025, from https://www.goteborgenergi.se/DxF-157268959/Miljovarden-Fjarrvarme-standard-2024-slutliga.pdf?TS=638863478875719751

Göteborg Energi. (2026a). *Elnätsavgiften företag* [Information on electricity grid tariffs for business customers (elnätsavgifter)]. Göteborg Energi. Retrieved January 16, 2026, from https://www.goteborgenergi.se/foretag/elnat/elnatsavgiften

Göteborg Energi. (2026b). *Elpriser företag* [Electricity prices for business customers in Gothenburg]. Göteborg Energi. Retrieved January 16, 2026, from https://www.goteborgenergi.se/foretag/elavtal/elpriser

Göteborg Energi. (2026c). *Fjärrkylapriser företag* [Current district cooling prices for business customers (energy, effect, and flow components) according to Göteborg Energis 20252026 price list]. Göteborg Energi. Retrieved January 16, 2026, from https://www.goteborgenergi.se/foretag/fjarrkyla/fjarrkylapriser

Göteborg Energi. (2026d). *Fjärrvärmepriser företag* [Current district heating prices for business customers in Gothenburg]. Göteborg Energi. Retrieved January 16, 2026, from https://www.goteborgenergi.se/foretag/fjarrvarme/fjarrvarmepriser

IEA DHC Executive Committee. (2024, February). *District heating network generation definitions* (Technical brochure) (Short definitions of 1st to 5th generation district heating networks). International Energy Agency Technology Collaboration Programme on District Heating Cooling (IEA DHC). Berlin, Germany. Retrieved July 11, 2025, from https://www.iea-dhc.org/fileadmin/public_documents/2402_IEA_DHC_DH_generations_definitions.pdf

Joint Research Centre. (2025, July). *Photovoltaic panels: New rules for assessment of the carbon footprint* [News release about proposed harmonised rules for PV module carbon footprint assessment]. Joint Research Centre. Retrieved December 4, 2025, from https://joint-research-centre.ec.europa.eu/jrc-news-and-

updates/photovoltaic-panels-new-rules-assessment-carbon-footprint-2025-07-07_en

Kim, H.-W., Dong, L., Choi, A. E. S., Fujii, M., Fujita, T., & Park, H.-S. (2018). Co-benefit potential of industrial and urban symbiosis using waste heat from industrial park in ulsan, korea [Sustainable Resource Management and the Circular Economy]. *Resources, Conservation and Recycling*, *135*, 225–234. https://doi.org/https://doi.org/10.1016/j.resconrec.2017.09.027

NIBE Energy Systems. (2023). Product leaflet: M12997-3 [NIBE product data sheet]. Retrieved October 20, 2025, from https://professional.nibe.eu/document/Product%20leaflet%20(PBD)/M12997-3.pdf

NIBE Energy Systems. (2025). *One-of-a-kind heat pump efficiency at xylem* [Case study on ground-source heat pump installations at Xylem's Emmaboda facility]. NIBE Energy Systems. Retrieved January 24, 2026, from https://www.nibe.eu/en-eu/knowledge-bank/nibe-stories/one-of-a-kind-heat-pump-efficiency-at-xylem

NIBE Energy Systems. (2026). *Nibe f1345 ground source heat pump* [Product information for the NIBE F1345 ground source heat pump, available in multiple power sizes]. NIBE Energy Systems. Retrieved January 16, 2026, from https://www.nibe.eu/en-eu/products/heat-pumps/ground-source-heat-pumps/f1345

nPro Energy. (2025). *Technologies: Cost and price overview* [Guidance on estimating technology costs for district energy planning with the nPro tool]. nPro Energy. Retrieved October 20, 2025, from https://www.npro.energy/main/en/help/technology-costs

Örebro kommun. (2023, May). *Tamarinden klimat och energiambition 2.0: Hur nya bostadsområdet tamarinden ska rustas för att möta framtidens behov* (Teknisk rapport) (Pilotdokument för hållbar stadsutveckling i Tamarinden). Örebro kommun. Örebro, Sweden. Retrieved July 10, 2025, from https://extra.orebro.se/download/18.1363db5a1884c55e04f3ec6/1685359076316/Tamarinden%20-%20Klimat-%20och%20energiambition%202.0.pdf

Örebro kommun. (2025). *Tamarinden pilot för systemförändring med lokalt delad energi*. Örebro kommun. Retrieved July 10, 2025, from https://extra.orebro.se/byggorebro/tamarinden.4.4ffbbf5616ac98ac8f49fb.html

Østergaard, P. A., Werner, S., Dyrelund, A., Lund, H., Arabkoohsar, A., Sorknæs, P., Gudmundsson, O., Thorsen, J. E., & Mathiesen, B. V. (2022). The four generations of district cooling - a categorization of the development in district cooling from origin to future prospect. *Energy*, *253*, 124098. https://doi.org/https://doi.org/10.1016/j.energy.2022.124098

Petersson, B.-Å. (2018). *Tillämpad byggnadsfysik* (6:2). Studentlitteratur.

REScoop.eu (European Federation of Renewable Energy Cooperatives). (2024, March). *Transposition tracker* [Last updated: March 2024]. REScoop.eu. Retrieved July 9, 2025, from https://www.rescoop.eu/policy/transposition-tracker

RISE Research Institutes of Sweden. (2024). *Industriell och urban symbios: Ett kunskapsunderlag om positiva effekter av samverkan mellan samhällets aktörer* (ER 2024:27) (Prepared by RISE on behalf of the Swedish Energy Agency). Swedish Energy Agency (Energimyndigheten). Eskilstuna, Sweden. Retrieved July 11, 2025, from https://energimyndigheten.a-w2m.se/Arkitektkopia/GetTemplateResource/121?eloid=8b5587ddd21c49449a33ed4bae43f130&elp=portal&elt=t&fn=ER+2024_27webb.pdf&id=8b5587ddd21c49449a33ed4bae43f130&lr=False&res=

Schroeder, D. V. (2021). *An introduction to thermal physics* (1st ed.). Oxford University Press.

Swedish Civil Defence and Resilience Agency (Myndigheten för samhällsskydd och beredskap). (2021). *Handbok i kommunal krisberedskap 2. kommunala verksamheter energiförsörjning*. Myndigheten för samhällsskydd och beredskap.

Swedish Energy Agency (Energimyndigheten). (2024). *Rapport 2024:20 "arkitektkopia" (title as per internal reference)* (Rapport 2024:20) (Accessed via Arkitektkopia system; report number 2024:20). Energimyndigheten. Retrieved July 9, 2025, from https://energimyndigheten.a-w2m.se/System/TemplateView.aspx?p=Arkitektkopia&id=294bae20fa14458da8673d849234874b

Swedish Energy Agency (Energimyndigheten), Svenska kraftnät, The Swedish Radiation Safety Authority (Strålsäkerhetsmyndigheten), & The Swedish Energy Markets Inspectorate (Energimarknadsinspektionen). (2024, January). Hot- och riskbild: Gemensam hot- och riskbild för sektor energiförsörjning, 22 januari 2024 [PDFrapport, Energimyndigheten]. https://www.energimyndigheten.se/48f61b/globalassets/trygg-energiforsorjning/civilt-forsvar/hot--och-riskbild-2024-01-22.pdf

Swedish Environmental Protection Agency (Naturvårdsverket). (2025, February). *Swedens climate act and climate policy framework* [Last reviewed: 17 February 2025]. Naturvårdsverket. Retrieved July 8, 2025, from https://www.naturvardsverket.se/en/international/swedish-environmental-work/swedens-climate-act-and-climate-policy-framework/

Swedish National Board of Housing, Building and Planning (Boverket). (2023, May). *Gränsvärde för byggnaders klimatpåverkan och en utökad klimatdeklaration* (Report 2023:20) (ISBN 9789189581371). Boverket. Retrieved July 8, 2025, from https://www.boverket.se/globalassets/publikationer/dokument/2023/slutrapport-gransvarde-for-byggnaders-klimatpaverkan.pdf

Swedish National Board of Housing, Building and Planning (Boverket). (2024, October). *Climate declaration for new buildings* [Reviewed: 16 October 2024]. Boverket. Retrieved July 8, 2025, from https://www.boverket.se/en/start/laws-and-regulations/climate-declaration/

United Nations Framework Convention on Climate Change. (2015). *The paris agreement*. Retrieved July 8, 2025, from https://unfccc.int/process-and-meetings/the-paris-agreement

Warfvinge, C., & Dahlblom, M. (2010). *Projektering av vvsinstallationer* (1st ed.). Studentlitteratur.

A

Appendix A - Carnot efficiency

The Carnot efficiency calculation is based on the available technical data for the chosen HP of F1345 from NIBE. For the calculations, a temperature difference between the refrigerant and the source or brine was assumed as 3 K for the evaporator and 5 K for the condenser. See Equation A.1 for the Carnot COP.

$$COP_{Carnot} = \frac{(T_{outgoing} + 273.15) + \Delta T_{condenser}}{(T_{outgoing} + \Delta T_{condenser}) - (T_{brine} - \Delta T_{evaporator})}[-] \tag{A.1}$$

Based on Equation A.1 and the given COP from the NIBE, the Carnot efficiency, η_C can be seen in Table A.1 and calculated by dividing a given COP by the Carnot COP for the same conditions.

Table A.1: Technical data and calculations for the Carnot efficiency (NIBE Energy Systems, 2023).

From NIBE			Calculations	
T_{brine} [^{o}C]	$T_{outgoing}$ [^{o}C]	COP_{NIBE} [-]	COP_c [-]	η_C [%]
0	35	4.49	7.28	62
0	45	3.67	6.10	60
10	35	5.27	9.49	56
10	45	4.30	7.52	57

The calculations of Table A.1 resulted in an average η_C of 59% which was rounded up to 60% for simplicity and the value used for the project.

B

Appendix B - Iteration calculations and results

Appendix B covers the detailed model for the calculations and each iteration's results.

B.1 Calculation model

For the building system side, an ideal linerarized curve was chosen for the needed heating system temperature based on the outdoor temperature. The heating system is set at 50^{o}C until the breakpoint chosen at the outdoor temperature of -10.1^{o}C and is then linear until the next breakpoint at 15^{o}C outdoor temperature where the heating system is set at 25^{o}C. This curve is visualized in Figure B.1

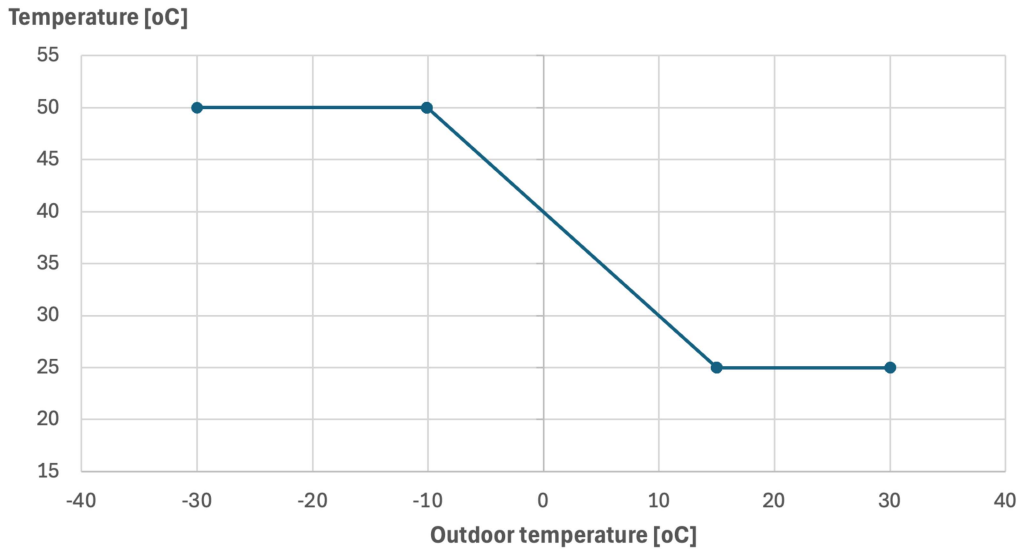

Figure B.1: Assumed and idealized temperature variation of the heating systems in the building used for COP calculations. The x-axis shows the outdoor temperature [^{o}C] and the y-axis shows the heating system temperature [^{o}C].

To calculate the average target heating system temperature for each month, the average outdoor temperature was used for each month, resulting in a temperature on the graph in Figure B.1. The heating system temperatures for each month can be seen in Table B.1.

Table B.1: Heating system temperature [^{o}C] based on the mean outdoor temperature [^{o}C] for each month.

Month	$T_{out,mean}$ [^{o}C]	$T_{heat,sys,lin}$ [^{o}C]
January	0.7	38.6
February	-0.4	39.2
March	2.5	37.5
April	6.4	35.1
May	12.8	31.3
June	14.6	30.2
July	17.7	28.4
August	17.8	28.3
September	13.6	30.8
October	8.8	33.7
November	4.7	36.1
December	2.4	37.5

In combination with the target heating system temperature, and the average temperature of the thermal source network, i.e., the average between the hot and cold supply loop temperature for each month, the COP for heating could be calculated based on Equation B.1, with temperature differences and Carnot efficiency as stated in Appendix A - Carnot efficiency. The average TSN temperature was chosen to account for the temperature difference over the heat pump.

$$COP_{HP} = \eta_C \cdot \frac{(T_{heat,sys,lin} + 273.15) + \Delta T_{condenser}}{(T_{heat,sys,lin} + \Delta T_{condenser}) - (T_{TSN,ave} - \Delta T_{evaporator})} \, [-] \quad \text{(B.1)}$$

For cooling, three different functions could be identified, comfort, refrigeration, and freezer. The temperature set point for comfort cooling was set as 7^{o}C and constant over the year, resulting in Equation B.2 with Carnot efficiency and temperature differences as stated in Appendix A - Carnot efficiency.

$$COP_{CH,comf.} = \eta_C \cdot \frac{(T_{comf.} + 273.15) - \Delta T_{evaporator}}{(T_{TSN,ave} + \Delta T_{condenser}) - (T_{comf.} - \Delta T_{evaporator})} \, [-] \quad \text{(B.2)}$$

The set point for the refrigeration process was set as -5^{o}C, and the COP was calculated by using Equation B.3.

$$COP_{CH,refrig.} = \eta_C \cdot \frac{(T_{refrig.} + 273.15) - \Delta T_{evaporator}}{(T_{TSN,ave} + \Delta T_{condenser}) - (T_{refrig.} - \Delta T_{evaporator})} \, [-] \quad \text{(B.3)}$$

The set point for the freezer process was set as -30^{o}C, and the COP was calculated by using Equation B.4.

$$COP_{CH,freezer} = \eta_C \cdot \frac{(T_{freezer} + 273.15) - \Delta T_{evaporator}}{(T_{TSN,ave} + \Delta T_{condenser}) - (T_{freezer} - \Delta T_{evaporator})} \, [-] \quad \text{(B.4)}$$

Based on the floor plan of the supermarket store, it was estimated as 30% of freezer and 70% of refrigeration and thus the cooling demand of the supermarket was split up accordingly. The final COP for the cooling process was then calculated by using the weighted average for each process cooling demand compared to the total cooling demand of the system.

B.2 Results for iterations

Below is the TSN temperature variation in relation to the reference case and the detailed results for all iterations.

B.2.1 First iteration - increased temperature

For the first iteration, the TSN temperature was increased by 4^{o}C for both supply loops. The yearly variation compared to the reference case can be seen in Figure B.2.

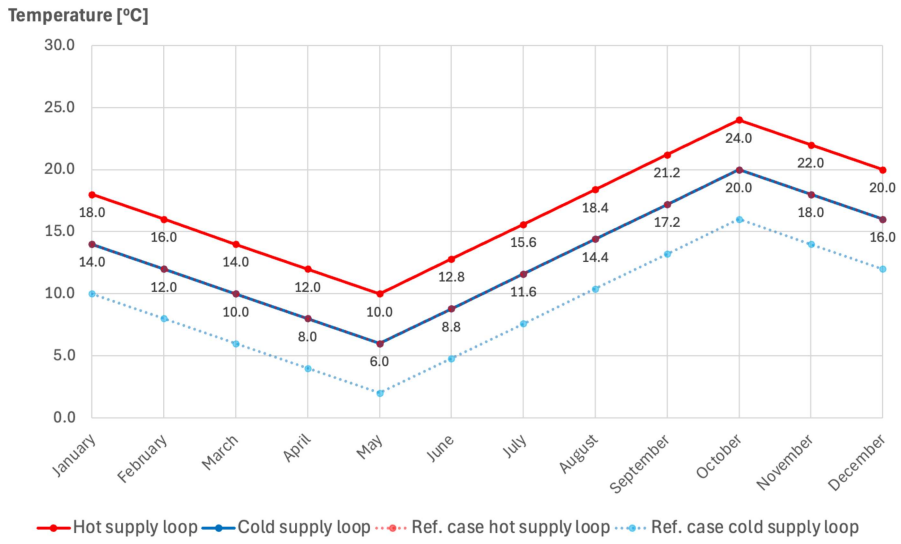

Figure B.2: Temperature variation [^{o}C] of the first iteration's TSN in relation to the reference case.

The results for monthly COP [-] and electricity demand [MWh] for the first iteration can be seen in Table B.2 and are based on the calculation model described in Section B.1.

Table B.2: Resulting COP [-] and electricity demand [MWh] for each month of the first iteration in which the TSN temperature has been raised by 4°C for both loops.

Month	Heating		Cooling	
	COP [-]	Elec. [MWh]	COP [-]	Elec. [MWh]
January	6.2	58.7	8.4	2.8
February	5.7	47.7	9.5	2.3
March	5.7	27.2	10.8	2.9
April	5.7	11.3	12.6	3.1
May	5.9	4.1	15.2	6.1
June	6.7	2.8	11.8	12.4
July	8.1	2.2	9.7	16.3
August	9.2	1.9	8.2	21.5
September	9.4	2.2	7.2	9.8
October	9.5	6.7	6.4	6.9
November	7.8	19.4	6.9	4.3
December	6.9	40.5	7.6	3.2
Total electricity demand [MWh]	-	224.5	-	91.7
Extracted source energy [MWh]	-	1 223.7	-	768.6
Share of extracted energy [%]	-	84	-	89

B.2.2 Second iteration - Ectogrid adjusted

For the second iteration, the maximum TSN temperature was adjusted to the temperature of Ectogrid in Lund. It was increased to 30°C for the heating supply loop, Ectogrid uses 35°C but the maximum of the used HP is 30°C. The temperature between loops was kept at the 4°C. The yearly variation compared to the reference case can be seen in Figure B.3.

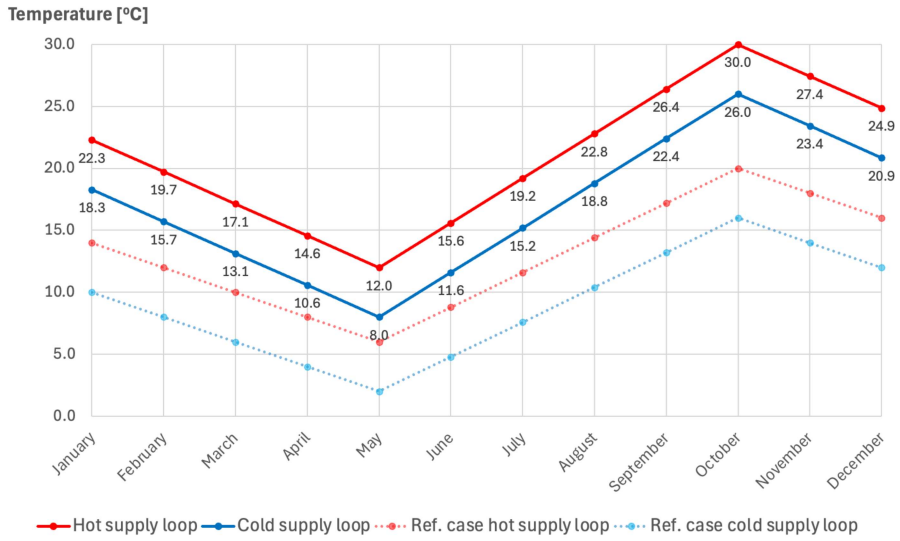

Figure B.3: Temperature variation [°C] of the second iteration's TSN in relation to the reference case.

The results for monthly COP [-] and electricity demand [MWh] for the second iteration can be seen in Table B.3 and are based on the calculation model described in Section B.1.

Table B.3: Resulting COP [-] and electricity demand [MWh] for each month of the second iteration. In which the maximum TSN hot supply temperature has been raised to 30^{o}C and the minimum cold supply set at 8^{o}C with 4^{o}C difference between loops.

Month	Heating		Cooling	
	COP [-]	Elec. [MWh]	COP [-]	Elec. [MWh]
January	7.2	50.5	6.8	3.5
February	6.5	42.4	7.7	2.9
March	6.2	24.6	8.8	3.6
April	6.2	10.4	10.4	3.8
May	6.3	3.8	12.6	7.4
June	7.5	2.5	9.7	15.1
July	9.6	1.8	7.9	20.0
August	11.9	1.5	6.7	26.5
September	12.9	1.6	5.8	12.2
October	13.6	4.6	5.1	8.6
November	10.1	15.1	5.6	5.3
December	8.4	33.3	6.1	4.0
Total electricity demand [MWh]	-	192.1	-	112.7
Extracted source energy [MWh]	-	1 256.1	-	747.5
Share of extracted energy [%]	-	87	-	87

B.2.3 Third iteration - increased temperature difference

For the third iteration, the TSN temperature difference between supply loops was increased to 10^{o}C. The yearly variation compared to the reference case can be seen in Figure B.4.

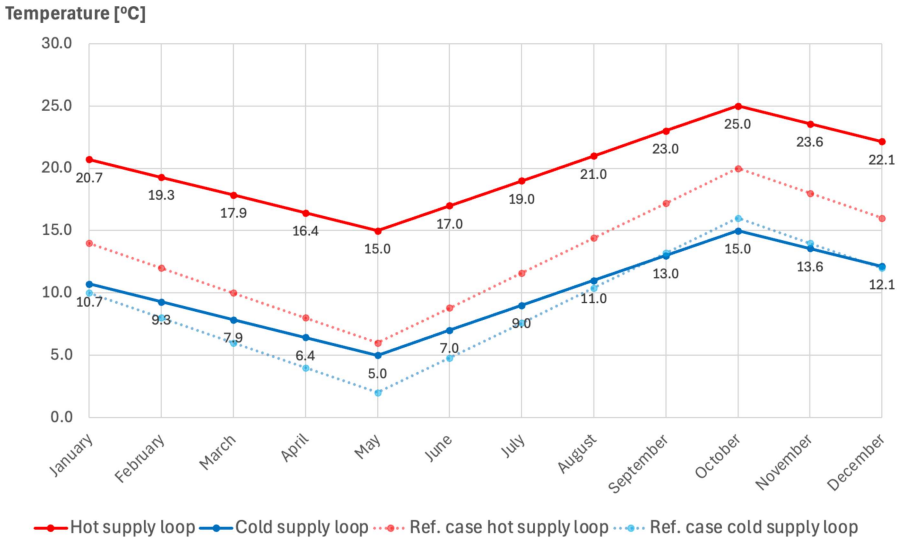

Figure B.4: Temperature variation [^{o}C] of the third iteration's TSN in relation to the reference case.

The results for monthly COP [-] and electricity demand [MWh] for the third iteration can be seen in Table B.4 and is based in the calculation model described in Section B.1.

Table B.4: Resulting COP [-] and electricity demand [MWh] for each month of the third iteration. In which the temperature difference between the loops was increased to 10^{o}C with the hot supply varying between 15 and 25^{o}C.

Month	Heating		Cooling	
	COP [-]	Elec. [MWh]	COP [-]	Elec. [MWh]
January	6.2	59.3	8.6	2.8
February	5.8	47.3	9.3	2.4
March	5.8	26.5	10.2	3.1
April	5.9	10.8	11.3	3.5
May	6.3	3.8	12.6	7.4
June	7.1	2.7	10.8	13.5
July	8.2	2.1	9.5	16.7
August	9.1	1.9	8.4	21.0
September	8.9	2.3	7.6	9.3
October	8.6	7.3	6.9	6.4
November	7.4	20.6	7.4	4.0
December	6.7	41.7	7.9	3.1
Total electricity demand [MWh]	-	226.3	-	93.1
Extracted source energy [MWh]	-	1 221.9	-	767.1
Share of extracted energy [%]	-	84	-	89

B.2.4 Fourth iteration - extended heating season

For the fourth iteration, the heating season was extended to cover September through June. The yearly variation compared to the reference case can be seen in Figure B.5.

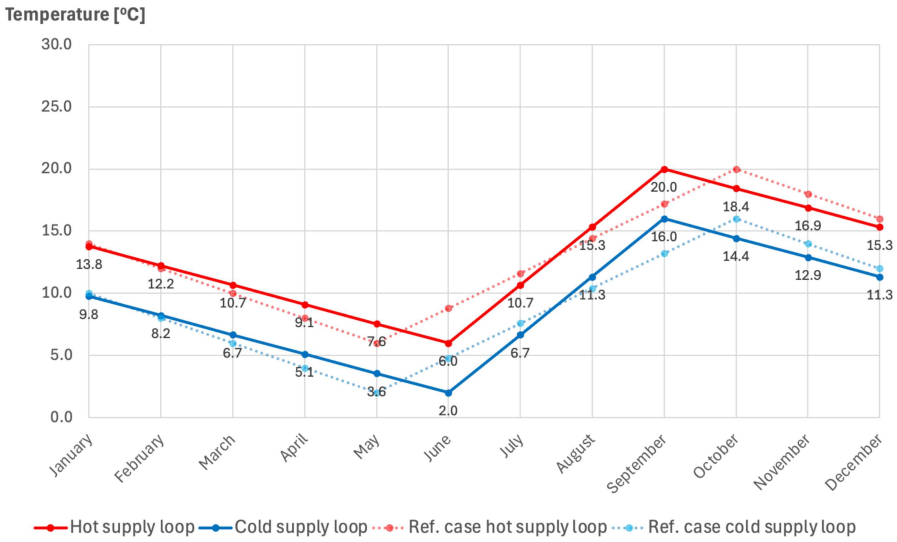

Figure B.5: Temperature variation [^{o}C] of the fourth iteration's TSN in relation to the reference case.

The results for monthly COP [-] and electricity demand [MWh] for the fourth iteration can be seen in Table B.5 and are based on the calculation model described in Section B.1.

Table B.5: Resulting COP [-] and electricity demand [MWh] for each month of the fourth iteration, where the heating season is extended.

Month	Heating		Cooling	
	COP [-]	Elec. [MWh]	COP [-]	Elec. [MWh]
January	5.5	66.8	11.0	2.2
February	5.1	53.2	12.4	1.8
March	5.1	29.9	14.3	2.2
April	5.2	12.2	16.8	2.3
May	5.5	4.4	20.5	4.6
June	5.4	3.5	26.5	5.5
July	6.6	2.7	14.3	11.1
August	8.0	2.2	9.9	17.9
September	8.9	2.3	7.6	9.3
October	7.4	8.5	8.2	5.4
November	6.4	23.6	9.0	3.3
December	5.9	47.3	9.9	2.5
Total electricity demand [MWh]	-	256.5	-	68.0
Extracted source energy [MWh]	-	1 191.7	-	792.2
Share of extracted energy [%]	-	82	-	92

B.2.5 Fifth iteration - borehole adjusted

For the fifth iteration, the TSN temperature variation was adjusted to the last year's temperature variation seen in the results of the borehole simulation in EED 4.3, covered

in Appendix C - Geothermal storage. The yearly variation compared to the reference case can be seen in Figure B.6.

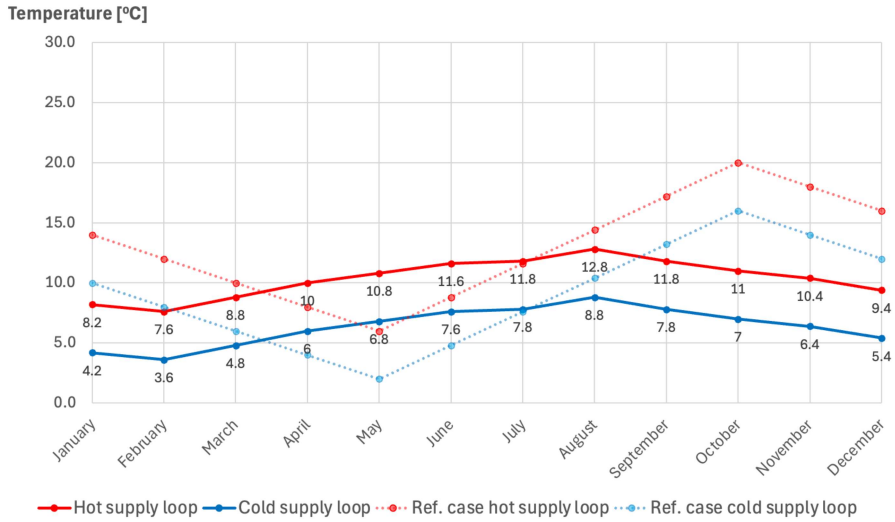

Figure B.6: Temperature variation [^{o}C] of the fifth iteration's TSN in relation to the reference case.

The results for monthly COP [-] and electricity demand [MWh] for the fifth iteration can be seen in Table B.6 and are based on the calculation model described in Section B.1.

Table B.6: Resulting COP [-] and electricity demand [MWh] for each month of the fifth iteration. In which the temperature of the TSN was set to that of the borehole configuration analyzed in EED 4.3.

Month	Heating		Cooling	
	COP [-]	Elec. [MWh]	COP [-]	Elec. [MWh]
January	4.7	77.5	18.8	1.3
February	4.6	59.8	20.4	1.1
March	4.9	31.4	17.4	1.8
April	5.4	11.9	15.2	2.6
May	6.1	4.0	14.1	6.7
June	6.5	2.9	13.1	11.2
July	6.9	2.5	12.9	12.3
August	7.2	2.4	11.8	14.9
September	6.4	3.2	12.9	5.5
October	5.7	11.0	13.8	3.2
November	5.3	28.8	14.6	2.0
December	5.0	56.0	16.3	1.5
Total electricity demand [MWh]	-	291.6	-	64.0
Extracted source energy [MWh]	-	1 156.6	-	796.2
Share of extracted energy [%]	-	80	-	93

C

Appendix C - Geothermal storage

C.1 Derivations and MATLAB

To evaluate the need for geothermal storage, calculations were done by hand and by MATLAB R2023b developed by MathWorks along with the use of the software Earth Energy Designer version 4.3 developed by buildingphysics.com. For the hand calculations, the main assumptions and equations can be seen in Figure C.1.

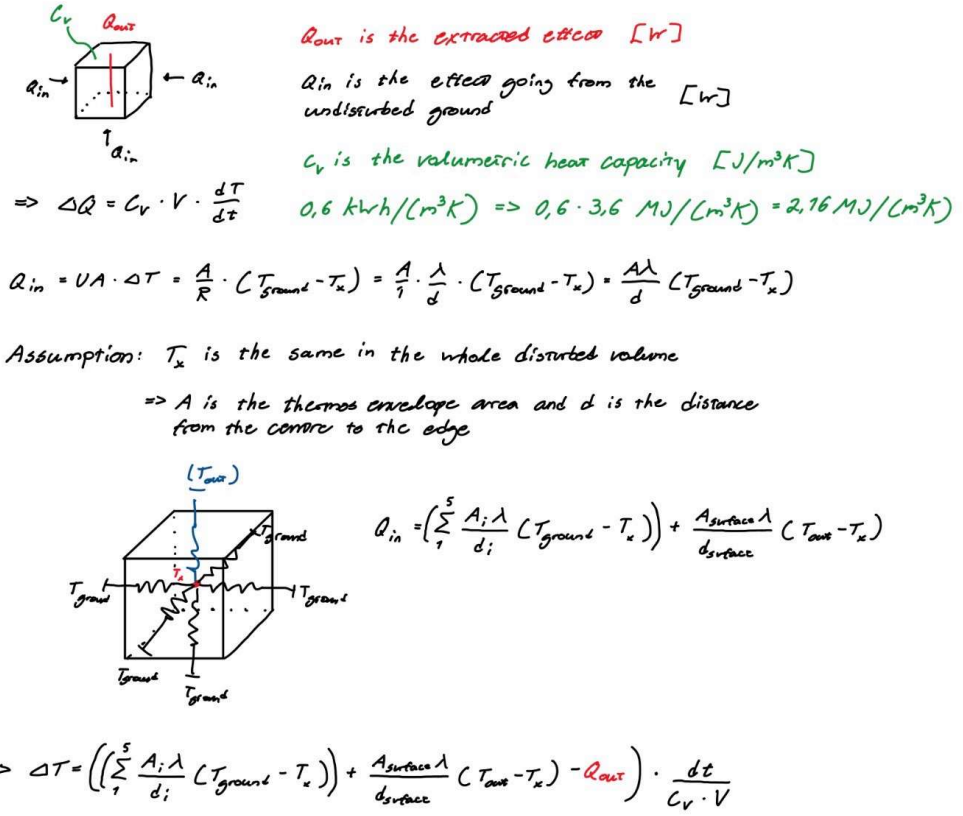

Figure C.1: Sketches, assumptions and equations used for the hand calculations of the temperature change of the ground.

The equations seen in Figure C.1 were transferred to MATLAB to calculate and visualize the temperature change in the ground and the used code can be seen in Appendix D - MATLAB code for geothermal storage.

Table C.1: Variable input data used for the MATLAB code.

Ground properties		
Parameter	Value	Comment
Soil conductivity, λ	3.5 W/(m·K)	Assumed for Gothenburg
Geothermal gradient, q_{geo}	0.06 W/m^2	Assumed for Gothenburg
Volumetric heat capacity, C_V	0.6 kW/$(m^3 \cdot K)$	Geoenergicentrum
Ground temperature, T_{ground}	8^{o}C	Yearly average for Gothenburg
Borehole configuration and properties		
Number of rows	10	Assumed
Number of columns	10	Assumed
Borehole row distance	15 m	Assumed
Borehole column distance	15 m	Assumed
Number of boreholes	100	Assumed
Maximum borehole effect	40 W/m	Geoenergicentrum

The geothermal gradient of 0.06 W/m^2 seen in Table C.1 is assumed based on the course compendium of the course VBF021 - "Building physics, advanced course". However, EED 4.3 uses the value of 0.04 W/m^2 for the geothermal gradient of Gothenburg which is used for the EED simulations and therefore differs between the MATLAB and EED simulations. This value was used to calculate a new ground temperature at half the depth of the boreholes, which acts as a temperature difference for the heat flux into the geothermal storage from the surrounding soil. Using the input data seen in Table C.1, the temperature change of the ground volume resulted in the graph seen in Figure C.2

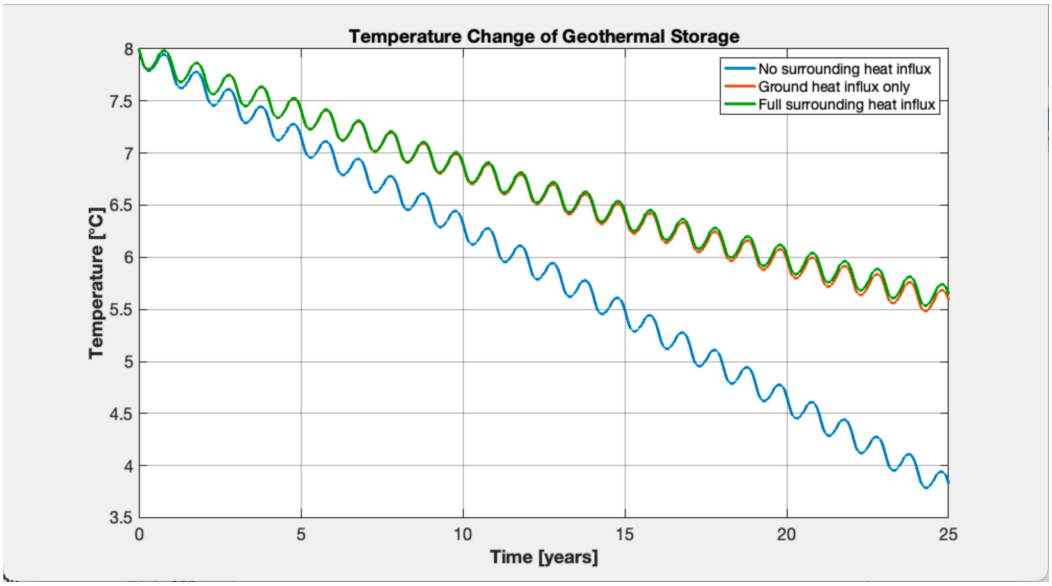

Figure C.2: Estimated temperature change of the ground for 100 boreholes at 261 m of depth with 15 m spacing with geothermal gradient.

Without geothermal gradient the temperature change was estimated as the graph seen in Figure C.3

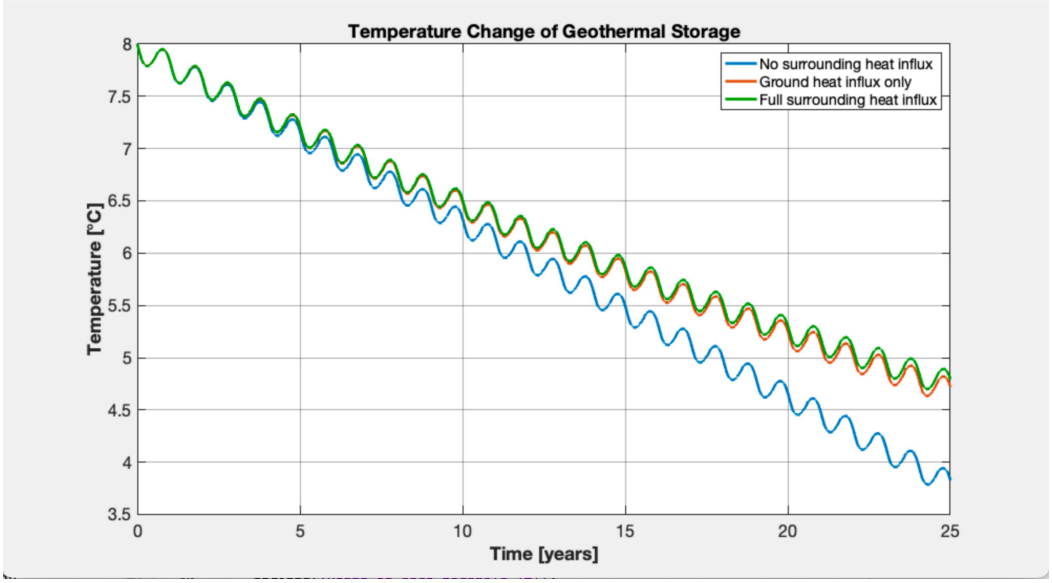

Figure C.3: Estimated temperature change of the ground for 100 boreholes at 261 m of depth with 15 m spacing without geothermal gradient.

The depth of the boreholes used was changed iteratively, while the depth was calculated using the maximum peak effect demand and the maximum possible effect extraction of 40 W/m (Gehlin et al., 2016).

C.2 EED 4.3

For the calculations done in EED, the input data can be seen in Figure C.4, where the only changed parameters for the different iterations are the borehole configuration and the mean temperature constraints of the heat carrier fluid.

```
GROUND

  Ground thermal conductivity                3,5 W/(m·K)
  Ground heat capacity                       2,16 MJ/(m³·K)
  Ground surface temperature                 7,1 °C
  Geothermal heat flux                       0,04 W/m²

BOREHOLE

  Configuration:                             592 ("100 : 10 x 10 rectangle")
  Borehole depth                             220 m
  Borehole spacing                           15 m
  Borehole installation                      Single-U
  Borehole diameter                          110 mm
  U-pipe diameter                            40 mm
  U-pipe thickness                           2,4 mm
  U-pipe thermal conductivity                0,42 W/(m·K)
  U-pipe shank spacing                       65 mm
  Filling thermal conductivity               0,6 W/(m·K)
  Contact resistance pipe/filling            0 (m·K)/W

THERMAL RESISTANCES

  Borehole thermal resistances are calculated.
  Number of multipoles                       10
  Internal heat transfer between upward and downward channel(s) is considered.

HEAT CARRIER FLUID

  Thermal conductivity                       0,48 W/(m·K)
  Specific heat capacity                     3795 J/(Kg·K)
  Density                                    1052 Kg/m³
  Viscosity                                  0,0052 Kg/(m·s)
  Freezing point                             -14 °C
  Flow rate per borehole                     2 l/s

BASE LOAD

  Number of simulation years                 25
  First month of operation                   JAN

               C A L C U L A T E D    V A L U E S
               ==================================
                     * Hourly calculation *

  Total borehole length                      2,202E4 m


THERMAL RESISTANCES

  Borehole therm. res. internal              0,45 (m·K)/W

  Reynolds number                            1,464E4
  Thermal resistance fluid/pipe              0,003887 (m·K)/W
  Thermal resistance pipe material           0,04844 (m·K)/W
  Contact resistance pipe/filling                  0 (m·K)/W

  Borehole therm. res. fluid/ground          0,1086 (m·K)/W

  Effective borehole thermal res.            0,1092 (m·K)/W
```

Figure C.4: Input data used for the EED calculations. The only parameter changed between iteration are the borehole configuration and temperature constraints.

Three different types of borehole configurations were used for the simulations in EED, called 592, 692, and 747 in the software. 592 consists of 100 boreholes with 10 rows and 10 columns. 692 consists of 196 boreholes with 14 rows and 14 columns. 747 consists of 400 boreholes with 20 rows and 20 columns.

As a basis, the reference case was run with the heat carrier fluid seen as a separate fluid from the TSN with mean temperature constraints at minimum -5^oC and maximum at 25^oC, which is within the temperature interval of NIBE's heat pump F1345, the result for the 592 borehole configuration can be seen in Figure C.5.

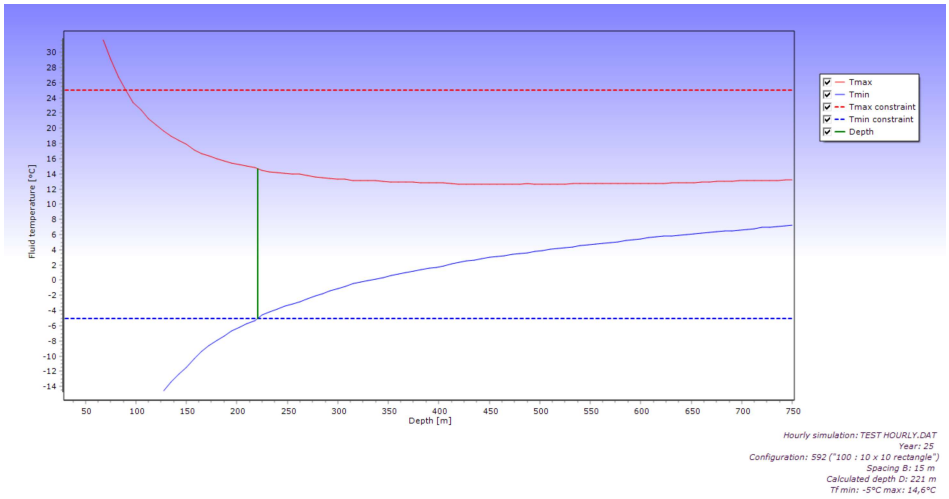

A)

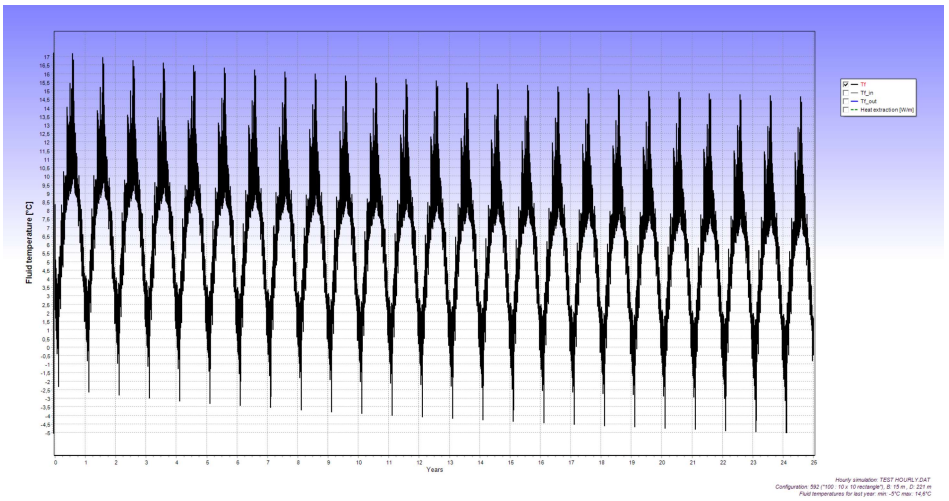

B)

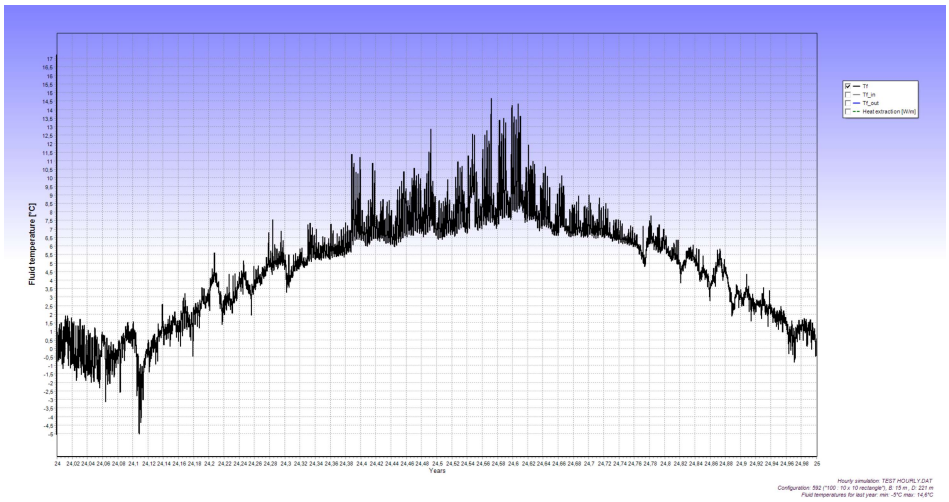

C)

Figure C.5: Results for borehole configuration 592 and mean temperature restraints as -5/25^{o}C. A) Required borehole depth. B) Fluid temperature variation over the full simulation length. C) Fluid temperature variation for the last year.

The result for the 692 borehole configuration can be seen in Figure C.6.

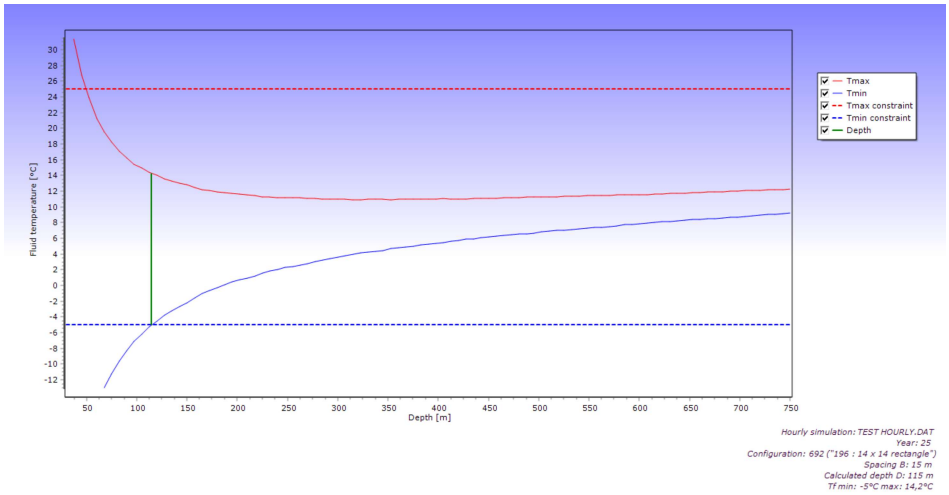

A)

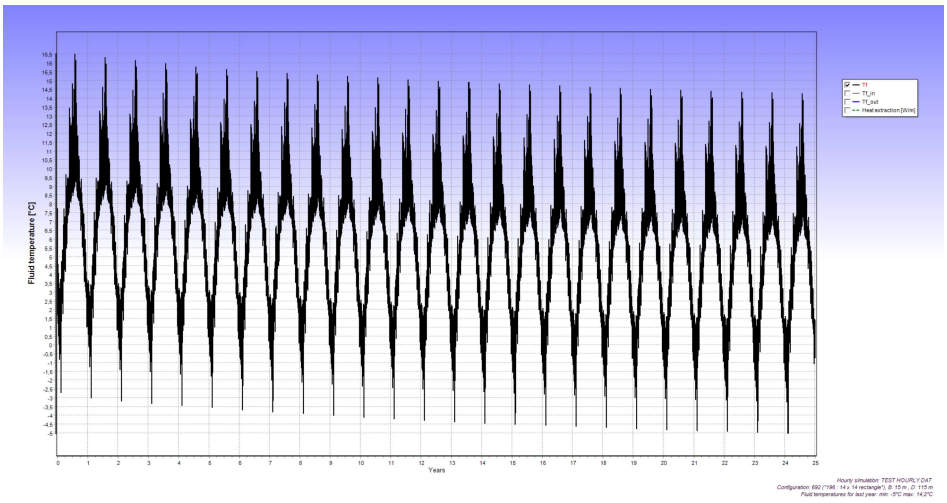

B)

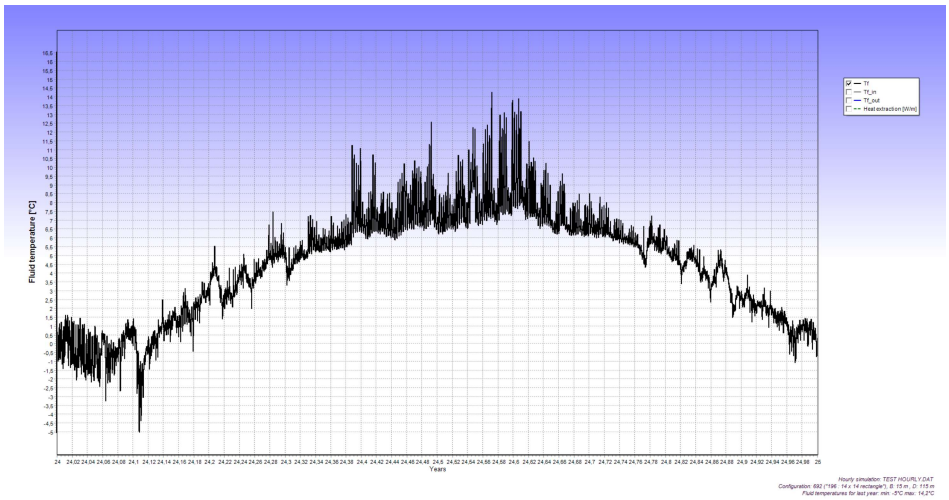

C)

Figure C.6: Results for borehole configuration 692 and mean temperature restraints as -5/25^{o}C. A) Required borehole depth. B) Fluid temperature variation over the full simulation length. C) Fluid temperature variation for the last year.

The result of the 747 borehole configuration can be seen in Figure C.7.

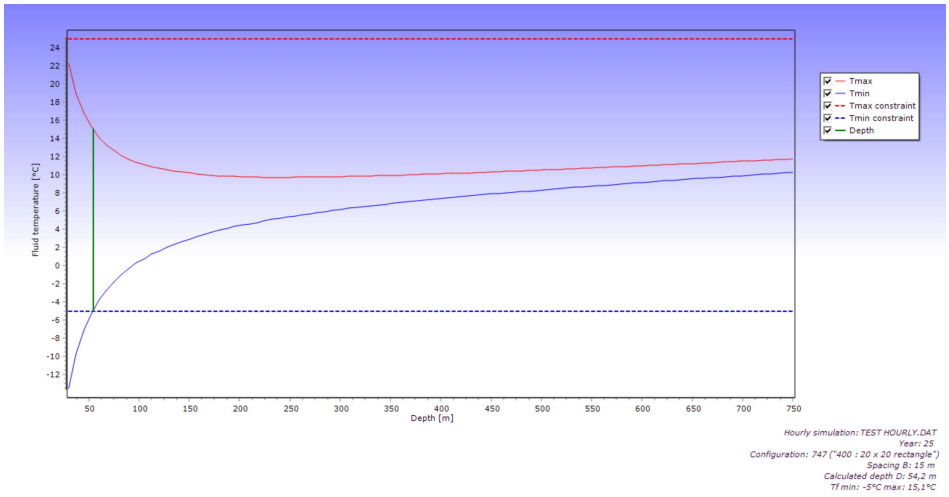

A)

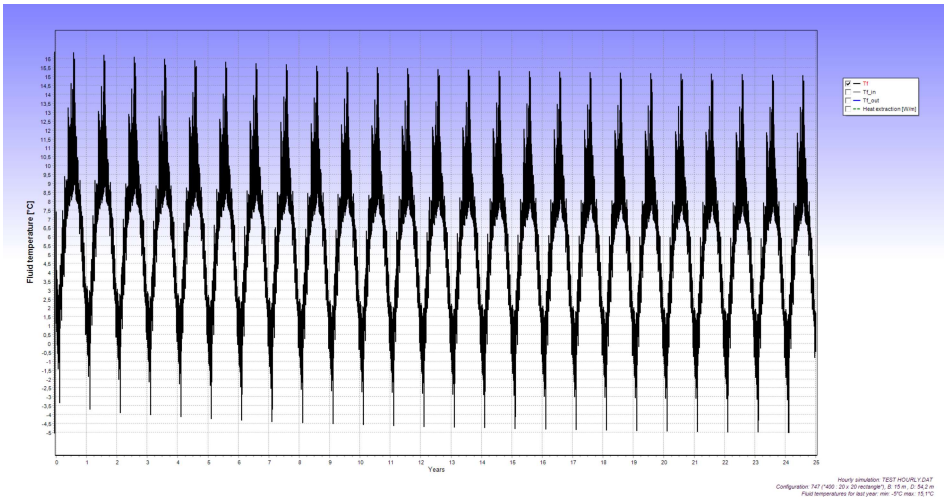

B)

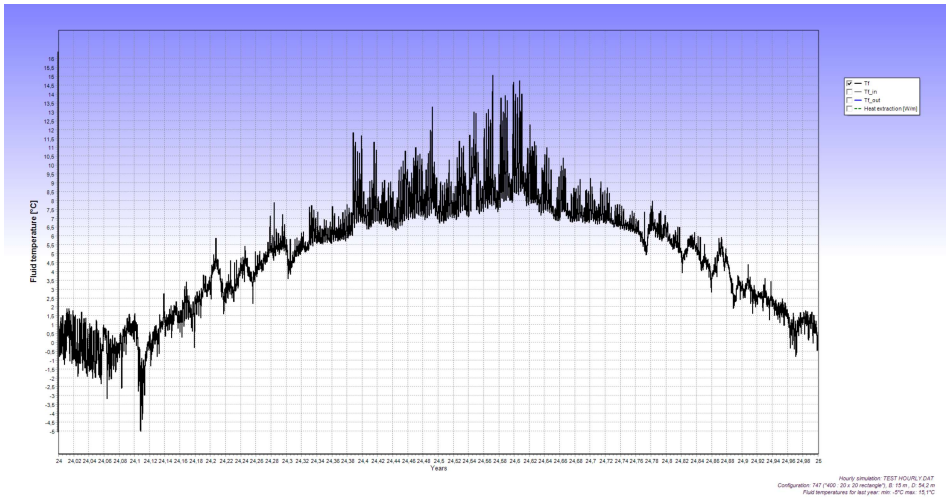

C)

Figure C.7: Results for borehole configuration 747 and mean temperature restraints as -5/25^{o}C. A) Required borehole depth. B) Fluid temperature variation over the full simulation length. C) Fluid temperature variation for the last year.

Furthermore, to evaluate the possibility to have the TSN fluid be used as the borehole heat transfer fluid, the mean temperature constraints of the borehole fluid were set to the reference case's maximum and minimum mean fluid temperature. The result of this for the 592 borehole configuration can be seen in Figure C.8.

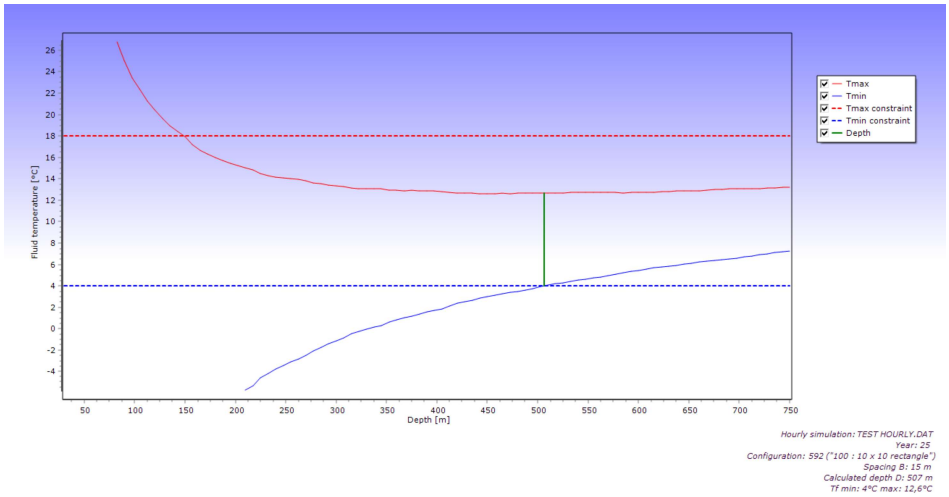

A)

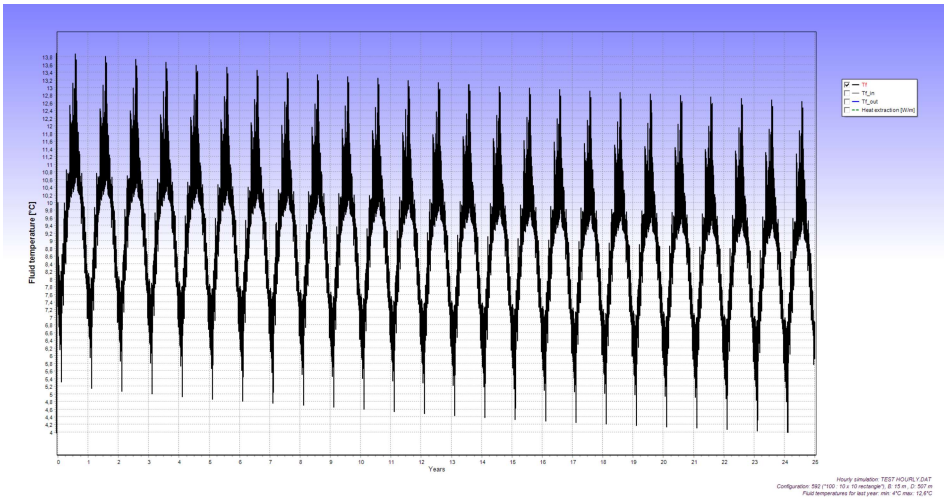

B)

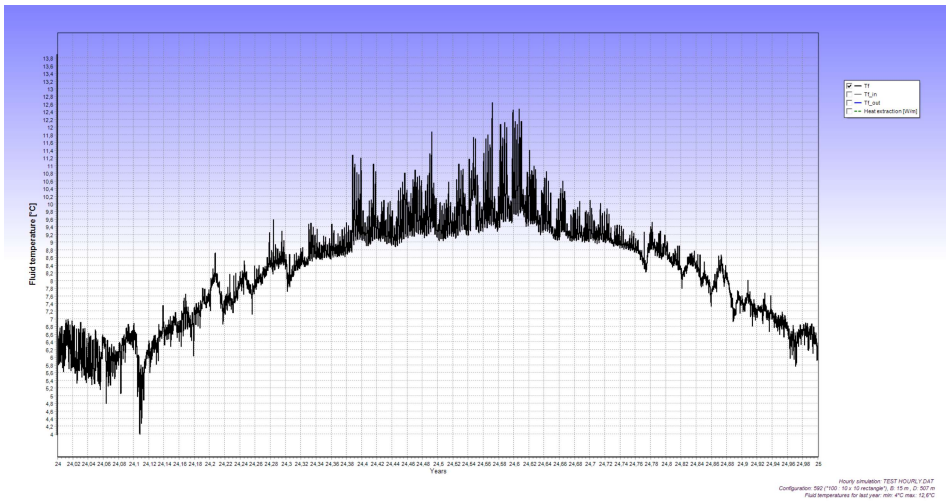

C)

Figure C.8: Results for borehole configuration 592 and mean temperature restraints as 4/18^{o}C. A) Required borehole depth. B) Fluid temperature variation over the full simulation length. C) Fluid temperature variation for the last year.

The result of the 692 borehole configuration can be seen in Figure C.9.

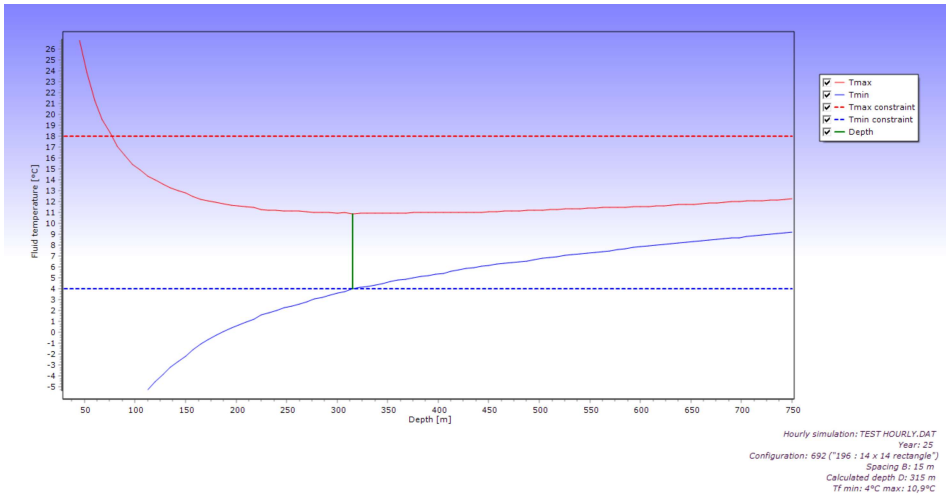

A)

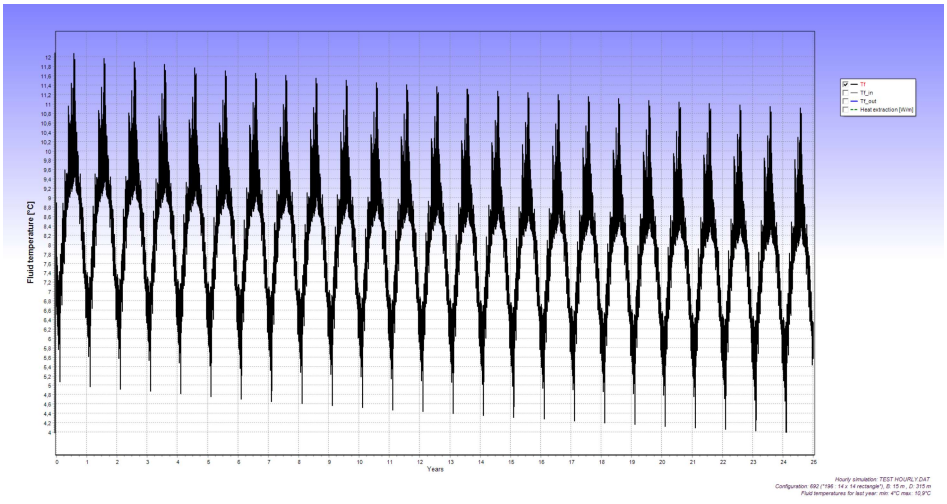

B)

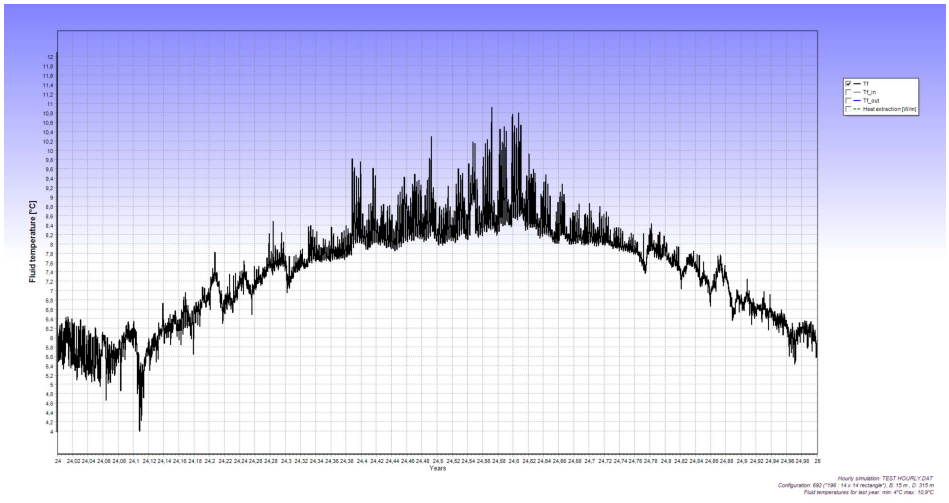

C)

Figure C.9: Results for borehole configuration 692 and mean temperature restraints as 4/18^{o}C. A) Required borehole depth. B) Fluid temperature variation over the full simulation length. C) Fluid temperature variation for the last year.

The result of the 747 borehole configuration can be seen in Figure C.10.

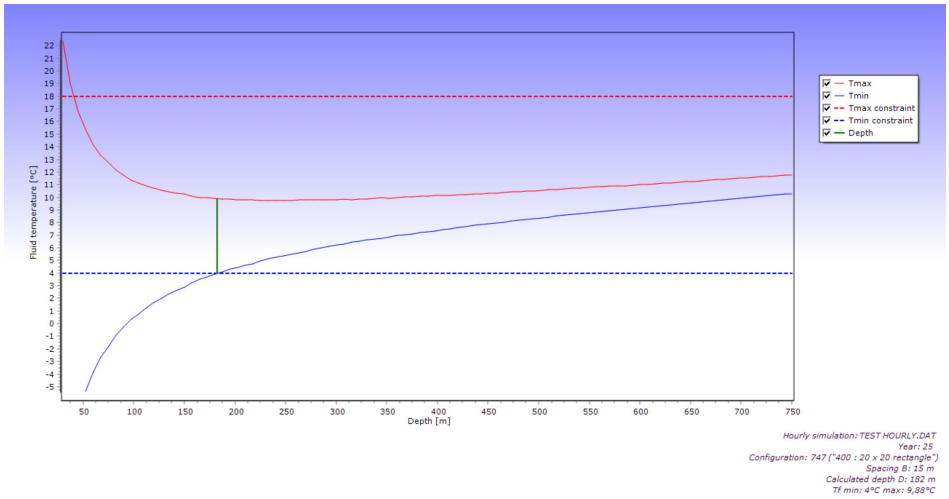

A)

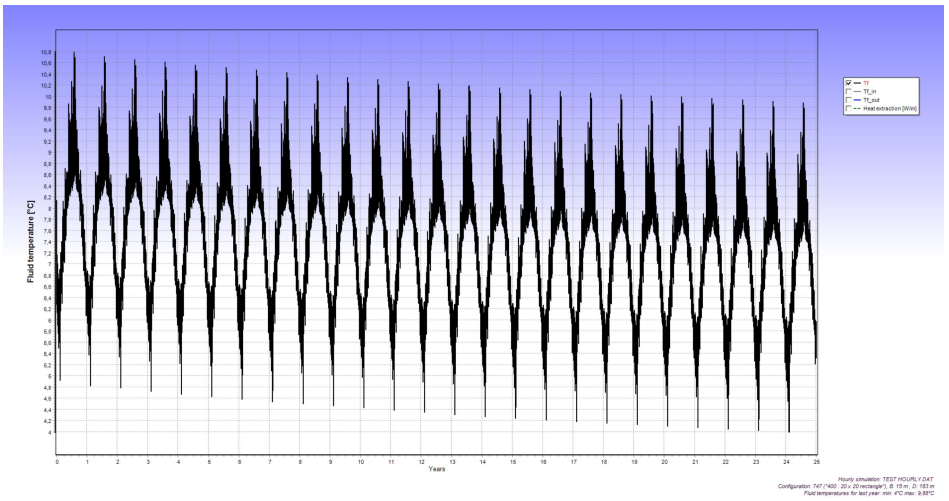

B)

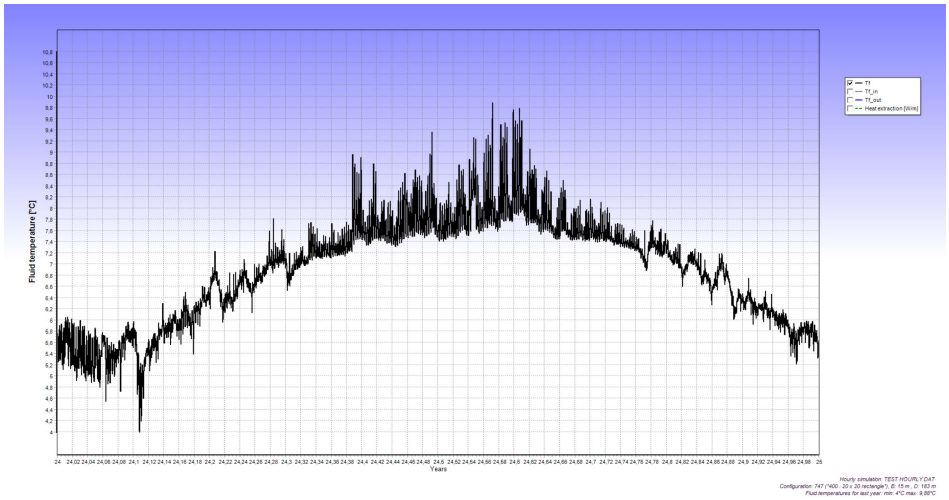

C)

Figure C.10: Results for borehole configuration 747 and mean temperature restraints as 4/18^{o}C. A) Required borehole depth. B) Fluid temperature variation over the full simulation length. C) Fluid temperature variation for the last year.

Additionally, simulations were performed for the first iteration of the TSN to evaluate what a further temperature difference would result in, and this can be seen in Figure C.11 for the 592 borehole configuration.

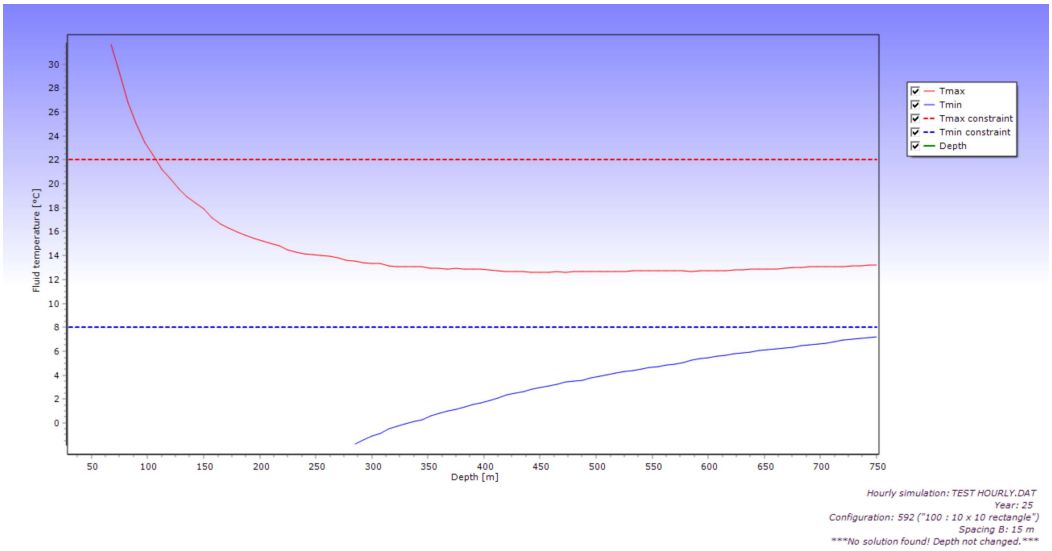

Figure C.11: Required borehole depth for borehole configuration 592 and mean temperature restraints as 8/22^{o}C.

Figure C.11 shows how there is no solution for the chosen parameters. The result of the 692 borehole configuration can instead be seen in Figure C.12

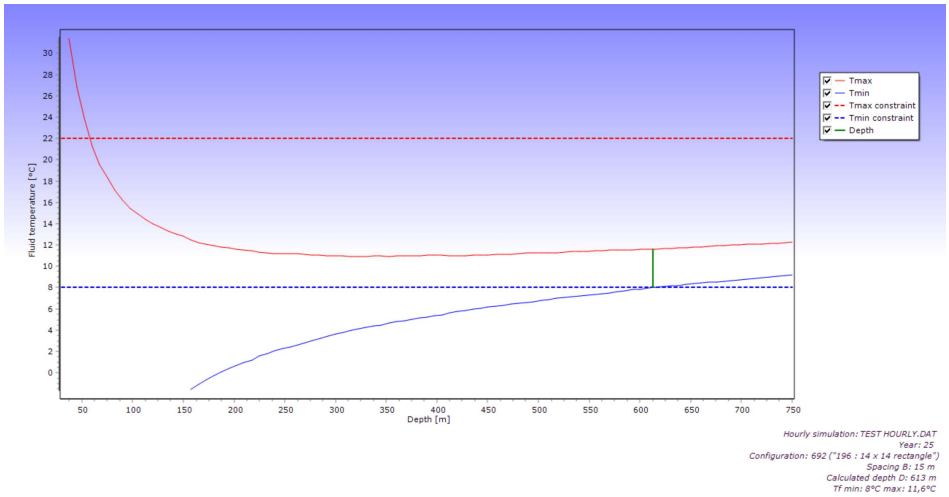

A)

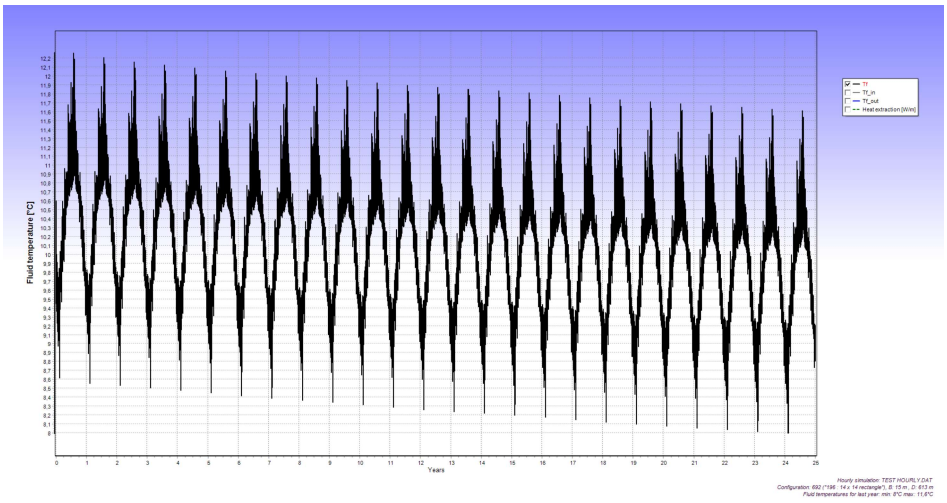

B)

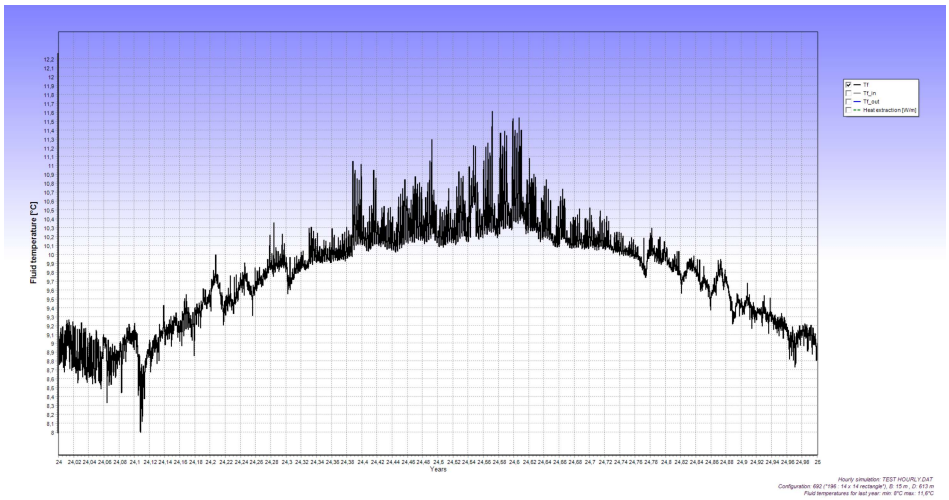

C)

Figure C.12: Results for borehole configuration 692 and mean temperature restraints as 8/22^{o}C. A) Required borehole depth. B) Fluid temperature variation over the full simulation length. C) Fluid temperature variation for the last year.

The result of the 747 borehole configuration can be seen in Figure C.13

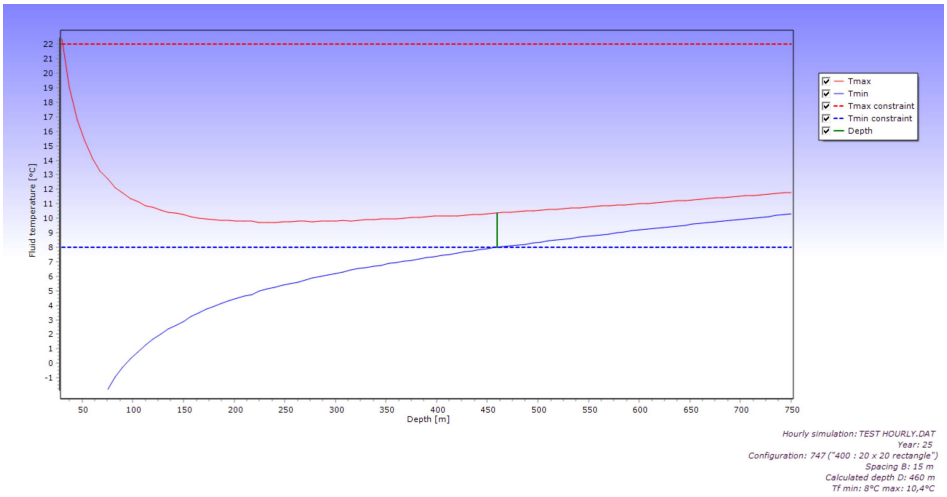

A)

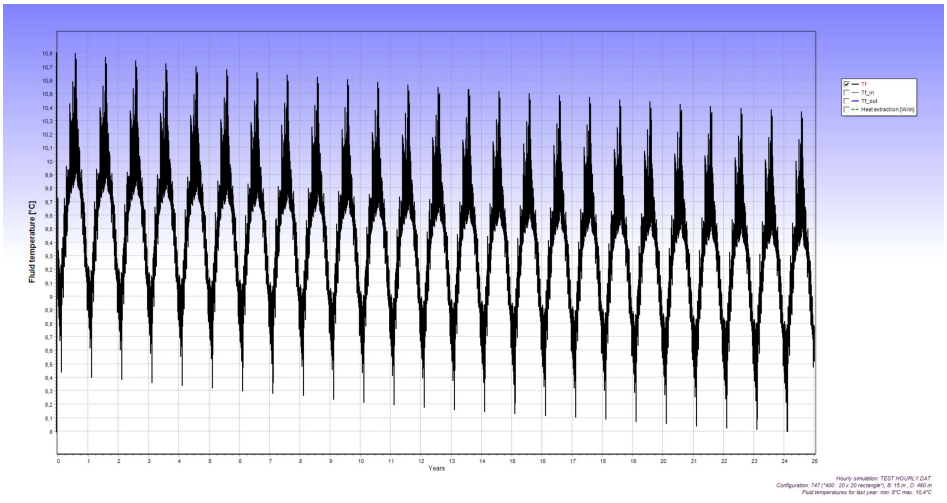

B)

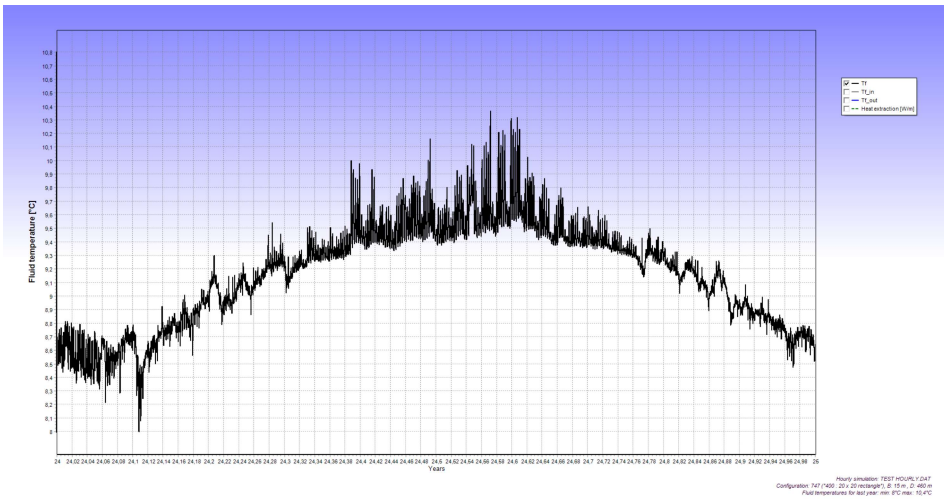

C)

Figure C.13: Results for borehole configuration 747 and mean temperature restraints as 8/22^{o}C. A) Required borehole depth. B) Fluid temperature variation over the full simulation length. C) Fluid temperature variation for the last year.

D

Appendix D - MATLAB code for geothermal storage

Following is the created MATLAB code for the estimation of the temperature change in a ground volume of geothermal storage.

```
set(groot,'defaultTextInterpreter','none')
set(groot,'defaultLegendInterpreter','none')
set(groot,'defaultAxesTickLabelInterpreter','none')

clear
clc
% This code estimates an assumed temperature of the centre of the
% boreholes.
% The code is created autumn 2025 by Anton Gustafsson for the Master thesis,
% "Optimizing Urban Energy Flows - Theoretical Insights into Energy
% Sharing Between Buildings"

% Input data
load RefData.txt % [Time [h] Net demand [W]]
load WeatherFileGBG.txt % Weather file [Dry-bulb temp [oC]]

%%%%%%%%%%% CHOSEN PARAMETERS %%%%%%%%%%

% Simulation Period
Years=25; % Chosen amount of years to simulate

% Borehole configuration
nRows=10; % [-] Assumed
nColumns=10; % [-] Assumed

RowDistance=15; % [m] Assumed
ColumnDistance=15; % [m]Assumed

MaxHeatExtraction=40; % [W/m] Given from Geoenergicentrum

O=0; % Overwrite borehole depth, 1 for yes, 0 for no
B=150; % Wanted value to overwrite borehole depth

% Ground properties
LambdaGround=3.5; % [W/mK] Ground conductivity
qgeo=0.06; % [W/m^2] geothermal heat flux for Gothenburg
Tave=8; % [degC] Gothenburg yearly average
CVolume=0.6; % [kWh/(m^3*K)] % Volumetric heat capacity from
geoenergicentrum

%%%%%%%%%%% END OF CHOSEN PARAMETERS %%%%%%%%%%

MaxDemand=max(RefData(:,2));
NeededTotalDepth=MaxDemand/MaxHeatExtraction; % [m]

disp('Amount of boreholes [-]')
```

```
Amount of boreholes [-]
```

```
Boreholes=nRows*nColumns % [-]
```

```
Boreholes =
   100
```

```
disp('Depth of each borehole [m]')
```

```
Depth of each borehole [m]
```

```
format short g
if O==1
    BoreholeDepth=B % [m]
else
    BoreholeDepth=NeededTotalDepth/Boreholes % [m]
end
```

```
BoreholeDepth =
       261.06
```

```


% Simpliifed geometry of geo storage
A=[nRows*RowDistance*BoreholeDepth % [m^2] Left
    nColumns*ColumnDistance*BoreholeDepth % [m^2] Front
    nRows*RowDistance*BoreholeDepth % [m^2] Right
    nColumns*ColumnDistance*BoreholeDepth % [m^2] Back
    nRows*nColumns*RowDistance*ColumnDistance % [m^2] Bottom
    nRows*nColumns*RowDistance*ColumnDistance]; % [m^2] Top

d=[(nRows*RowDistance)/2 % [m] Distance from storage center to left
    (nColumns*ColumnDistance)/2 % [m] Distance from storage center to front
    (nRows*RowDistance)/2 % [m] Distance from storage center to right
    (nColumns*ColumnDistance)/2 % [m] Distance from storage center to back
    (BoreholeDepth/2) % [m] Distance from storage center to bottom
    (BoreholeDepth/2)]; % [m] Distance from storage center to top

Volume=A(6,1)*BoreholeDepth; % [m^3] Storage volume

% Conductances
K=zeros(6,1);
for i=1:6
    K(i,1)=(A(i,1)*LambdaGround/d(i,1));
end

Kground=sum(K)-K(6,1); % Sum of ground to ground conductances

% Temperature change
SimHours=Years*8760; % [h] Simlation in hours
OutTemp=repmat(WeatherFileGBG,Years); % Creation of weather file input

SimInData=repmat(RefData,Years,1); % Creation of input data
SimOutData=zeros(SimHours,4); % Output matrix
```

```
Tground=Tave+qgeo*(d(6,1)/LambdaGround); % Undisturbed ground temperature
at half the depth, simplification

% With heat influx and outdoor temp influx
for i=1:SimHours
    SimOutData(i,1)=SimOutData(i,1)+i;
    SimOutData(i,2)=SimOutData(i,2)+SimInData(i,2);
    if i==1
        SimOutData(i,3)=-(SimInData(i,2)/1000)*(1/(CVolume*Volume));
    else
        deltaT=Tground-SimOutData((i-1),4);
        SimOutData(i,3)=(((Kground*deltaT)/1000)+
((K(6,1)*(OutTemp((i-1),1)-SimOutData((i-1),4)))/1000)-(SimOutData((i-1),2)/
1000))*(1/(CVolume*Volume));
    end
    if i==1
        SimOutData(i,4)=8+SimOutData(i,3);
    else
        SimOutData(i,4)=SimOutData((i-1),4)+SimOutData(i,3);
    end

end

% With heat influx only from ground
GroundInflux=zeros(SimHours,4);
for i=1:SimHours
    GroundInflux(i,1)=GroundInflux(i,1)+i;
    GroundInflux(i,2)=GroundInflux(i,2)+SimInData(i,2);
    if i==1
        GroundInflux(i,3)=-(SimInData(i,2)/1000)*(1/(CVolume*Volume));
    else
        deltaT=Tground-GroundInflux((i-1),4);
        GroundInflux(i,3)=(((Kground*deltaT)/1000)-(GroundInflux((i-1),2)/
1000))*(1/(CVolume*Volume));
    end
    if i==1
        GroundInflux(i,4)=8+GroundInflux(i,3);
    else
        GroundInflux(i,4)=GroundInflux((i-1),4)+GroundInflux(i,3);
    end

end

% Without influx

NoInflux=zeros(SimHours,4);
for i=1:SimHours
    NoInflux(i,1)=NoInflux(i,1)+i;
    NoInflux(i,2)=NoInflux(i,2)+SimInData(i,2);
    if i==1
```

```
        NoInflux(i,3)=-(SimInData(i,2)/1000)*(1/(CVolume*Volume));
    else
        deltaT=0;
        NoInflux(i,3)=(((Kground*deltaT)/1000)-(NoInflux((i-1),2)/1000))*(1/
(CVolume*Volume));
    end
    if i==1
        NoInflux(i,4)=8+NoInflux(i,3);
    else
        NoInflux(i,4)=NoInflux((i-1),4)+NoInflux(i,3);
    end

end

% Plot
PlotData = [NoInflux(:,4) GroundInflux(:,4) SimOutData(:,4)];
hours = 1:length(PlotData);
tYears = hours / 8760;

figure('Position', [200 350 1000 550]);

colors = [0.0000 0.4470 0.7410;  % blue
          0.8500 0.3250 0.0980;  % orange
          0.0000 0.6000 0.0000]; % green

ax = gca;
set(ax, 'ColorOrder', colors, 'NextPlot', 'replacechildren');

plot(tYears, PlotData, 'LineWidth', 2.5);
hold on;

% styling
xlabel('Time [years]', 'FontSize', 15, 'FontWeight', 'bold')
ylabel('Temperature [degC]', 'FontSize', 15, 'FontWeight', 'bold')
title('Temperature Change of Geothermal Storage', 'FontSize', 17,
'FontWeight', 'bold')
grid on
set(gca, 'GridAlpha', 0.35, 'LineWidth', 1.2, 'FontSize', 16)
xlim([0 max(tYears)])
legend({'No surrounding heat influx', 'Ground heat influx only', 'Full
surrounding heat influx'}, ...
       'FontSize', 14, 'Location', 'northeast')
box on
```

E

Appendix E - Economic analysis

The appendix covers the calculations for district heating, district cooling, and electricity costs excluding VAT along with the economic analysis for the case study.

E.1 District heating costs

The pricing model and prices of Göteborg Energi were used for the evaluation. The district heating price is split up into three parts, the connection investment, operational effect cost, and operational energy cost. The connection investment differs from building to building and based on experience from GICON was assumed to be split up into an max effect and a equipment cost. The max effect cost was set as 2000 SEK/kW and the equipment at 275 000 SEK.

The operational effect cost for Göteborg Energi depends on the average of the three highest daily effect averages over the past twelve months. Table E.1 displays the cost depending on the maximum three day average effect for 2026.

Table E.1: Fixed and operational effect cost depending on the maximum three day average effect demand for 2026 (Göteborg Energi, 2026d).

$\overline{Q}_{3day}$ [kW]	Fixed price [SEK/year]	Operational price [SEK/kW,year]
0-100	10 870	1 408
100-250	16 070	1 356
250-500	29 320	1 303
500-1 000	58 820	1 244
1 000-2 500	117 820	1 185
>2 500	270 320	1 124

The cost of the energy usage can be seen in Table E.2.

Table E.2: Energy price for the different months of the year for 2026 (Göteborg Energi, 2026d).

Month [-]	Energy price [SEK/kWh,year]
January	531
February	531
March	497
April	333
May	249
June	85
July	46
August	57
September	148
October	360
November	422
December	531

Furthermore, the price of district heating could be reduced if the return temperature from the building is lowered but this is not taken into account for this study. Based on the effect, and energy prices, the operational cost for each building in the case study can be seen in Table E.3.

Table E.3: District heating cost for the buildings of the case study.

Building [-]	Total cost [SEK/year]	Total op. cost [SEK/MWh]
A	1 032 308	3 387
B	226 568	2 021
C	233 137	1 163
D	1 331 374	1 591
Total	**2 823 387**	**1 941**

E.2 District cooling costs

As for the district heating, the pricing model and pricing of Göteborg Energi were used. The district cooling cost is split up into the connection investment, operational effect cost, operational energy cost, and operational flow cost. The connection investment was assumed as for the DH. Effect size cost of 2 000 SEK/kW and an equipment cost for the substation of 275 000 SEK. The operational effect cost for Göteborg Energi is based on the maximum effect of the last 12 months and can be seen in Table E.4

Table E.4: Fixed and operational effect cost depending on the maximum three day average effect demand for 2026 (Göteborg Energi, 2026c).

$\overline{Q}_{3day}$ [kW]	Fixed price [SEK/year]	Operational price [SEK/kW,year]
0-100	22 740	953
100-250	38 940	791
250-500	77 190	638
500-1 000	114 190	564
>1 000	139 190	539

The cost of the energy usage can be seen in Table E.5.

Table E.5: Energy price for the different months of the year for 2026 (Göteborg Energi, 2026c).

Month [-]	Energy price [SEK/kWh,year]
January	136
February	136
March	230
April	305
May	323
June	323
July	323
August	323
September	323
October	291
November	234
December	136

The flow cost was assumed as zero for this study as the flow demand of each building is not known. Based on the effect, and energy prices, the operational cost for each building in the case study can be seen in Table E.6.

Table E.6: District cooling cost for the buildings of the case study.

Building [-]	Total cost [SEK/year]	Total op. cost [SEK/MWh]
A	734 574	2 079
B	-	-
C	-	-
D	411 109	1 468
SM	109 032	480
Total	**1 254 714**	**1 459**

E.3 Electricity costs

The price of electricity for the study was also based on the pricing model and prices of Göteborg Energi. The electricity price can be split up into three parts, the electricity supply price, the network tariff, and the energy tax. The monthly average electricity supply price for the year of 2025 can be seen in Table E.7.

Table E.7: Average monthly electricity supply price for sector 3 in 2025 (Göteborg Energi, 2026b).

Month [-]	Electricity price [SEK/MWh]
January	634.4
February	770.5
March	507.9
April	376.3
May	429.3
June	227.8
July	370.1
August	485.7
September	523.3
October	628.2
November	696.4
December	516.8

For the prices seen in Table E.7, it was assumed that Göteborg Energi adds 20% to the prices of the market as a markup.

The network tariff for Göteborg Energi is split up into three parts, a fixed cost per year, a transfer cost, and a effect cost. The effect cost is based on the maximum average hourly effect for each month and the values of a connection over 63A can be seen in Table E.8. However, only the 2026 values are available.

Table E.8: Network tariff cost for Göteborg Energi 2026 (Göteborg Energi, 2026a).

Connection type	Fixed [SEK/month]	Transfer [SEK/MWh]	Effect [SEK/kW]
Over 63A	800	105	66.3

Additionally, as the market electricity price is only available for 2025, the energy tax was set as the 2025 value at 439.0 SEK/MWh. The energy tax for 2026 has been lowered from 2025, and thus, the 2025 value can be seen as conservative.

Lastly, for the additional electricity demand of the installed HP:s and CH:s, there is a need for an increased electric transfer capacity. Therefore, the maximum electric effect demand for each building was converted to current for a three-phase system through Equation E.1.

$$I = \frac{W_{max}}{\sqrt{3} \cdot U \cdot PF}[A] \tag{E.1}$$

In Equation E.1, W_{max} [W] is the maximum electric effect demand, U [V] is the voltage of the system set at 400 V, and PF [-] is the power factor set at 0.9.

The resulting additional current demand is then seen as installed in 250A connections, thus the electric current demand for each building or iteration is divided by 250 and rounded up to the nearest integer if reasonable. For each connection, an assumed investment cost of 100 000 SEK was assumed based on experience from GICON. The conversion to current from the maximum hourly electric effect demand of a HP can be seen in Table E.9.

Table E.9: Maximum electric effect [kW], resulting current [A], and the number of 250A cables needed for each building.

Building [-]	Max elec. effect [kW]	I [A]	Nr. of cables [-]
A	116	187	1
B	21	33	0
C	19	30	0
D	125	201	1
SM	6	10	0

As the demand additional current demand is much lower for Buildings B, C, and SM, an extra cable is not used as it is not considered necessary.

E.4 Borehole costs

The investment cost for the installment of boreholes was assumed based on experience from GICON as 10 000 SEK per borehole and 300 SEK per meter of depth for each borehole. Furthermore, the investment in a heat pump is necessary, and the cost of the used NIBE F1345 can be seen in Table E.10.

Table E.10: Cost for NIBE F1345 with and without VAT (NIBE Energy Systems, 2026).

Effect	Cost incl. VAT [SEK]	Cost excl. VAT [SEK]
24	195 575	156 460
30	220 025	176 020
40	248 500	198 800
60	302 675	242 140

The prices excluding VAT are used for the analysis and the operational cost was assumed as the price of electricity described previously in Section E.3.

E.5 Thermal source network costs

For the investment needed for the thermal source network, it was assumed that the geothermal storage would use the same pricing as the boreholes. Furthermore, the investment in heat pumps can be seen in Table E.10. The investment cost for the distribution pipes was calculated per meter of trench and based on the values from nPro.

Table E.11 shows the values for different uninsulated pipe dimensions in an urban environment.

Table E.11: Cost per meter for different pipe dimensions of uninsulated pipes in an urban environment (nPro Energy, 2025).

Diameter [mm]	Pipe cost [€/m]	Installation cost [€/m]	Total cost [€/m]
80	16	270	286
100	26	300	326
150	58	370	428
200	100	430	530
300	240	570	810

As the temperature difference is low for most iterations, and thus flows are high, an average dimension of 200 mm was chosen. For an assumed trench length of 300 m, the total investment cost for TSN distribution was estimated at 1 404 500 SEK.

The operational costs of the system can be seen as the electricity need for the pump circulating the distribution fluid at 1 kWh/m^2 of building area, in addition to the electricity for the heat pumps. The added electricity was then multiplied by the average electricity price per kWh for each iteration. A potential additional cost for both operation and investment is the connection and energy cost of district heating and cooling used for balancing the system.

E.6 Cost summary

A summarized view of the different costs for each system can be seen in Table E.12.

Table E.12: Identified investment and operational costs for the base cases and the TSN.

Type	DH and DC	Geothermal	TSN
Investment costs	Connection	Drilling per borehole + drilling per meter + HP and CH + elec. connection	DH and DC connection + drilling per borehole + drilling per meter + HP and CH + elec. connection + distribution system
Operational costs	Energy price	Electricity	Electricity and circulation + energy for DH and DC

F

Appendix F - Geothermal base case

To evaluate the performance and key performance indicators for the geothermal base case, EED 4.3 was used. The main input data was kept the same as in Appendix C - Geothermal storage with the temperature constraint set as -5^{o}C and 30^{o}C, aligning with the available temperature interval for the chosen HP, NIBE's F1345. To obtain the needed amount of boreholes, the depth of the boreholes was aimed at approximately 200 to 300 meters (GeoExPro Magazine, 2024). Worth noting is that a full optimization of the needed amount, depth, flow, and so on is out of the scope of the study. The results for each base case can be seen in Table F.1.

Table F.1: Summary of the base case simulations run in EED v.4.3 showing the temperature constraints [^{o}C], configuration type with amount of boreholes in parenthesis, resulting depth [m], and the final maximum and minimum mean temperature of the heat carrying fluid [^{o}C].

Building	Constraints [^{o}C]	Borehole config.	Depth [m]	$\overline{T}_{f,fin,min}$ [^{o}C]	$\overline{T}_{f,fin,max}$ [^{o}C]
A	-5 / 30	423 (36)	209	-4.6	30.0
B	-5 / 30	282 (9)	212	-5.0	5.3
C	-5 / 30	282 (9)	232	-5.0	3.7
D	-5 / 30	512 (64)	210	-5.0	9.7
SM	-5 / 30	233 (4)	176	26.8	30

Furthermore, Figure F.1 shows the simulation results for Building A.

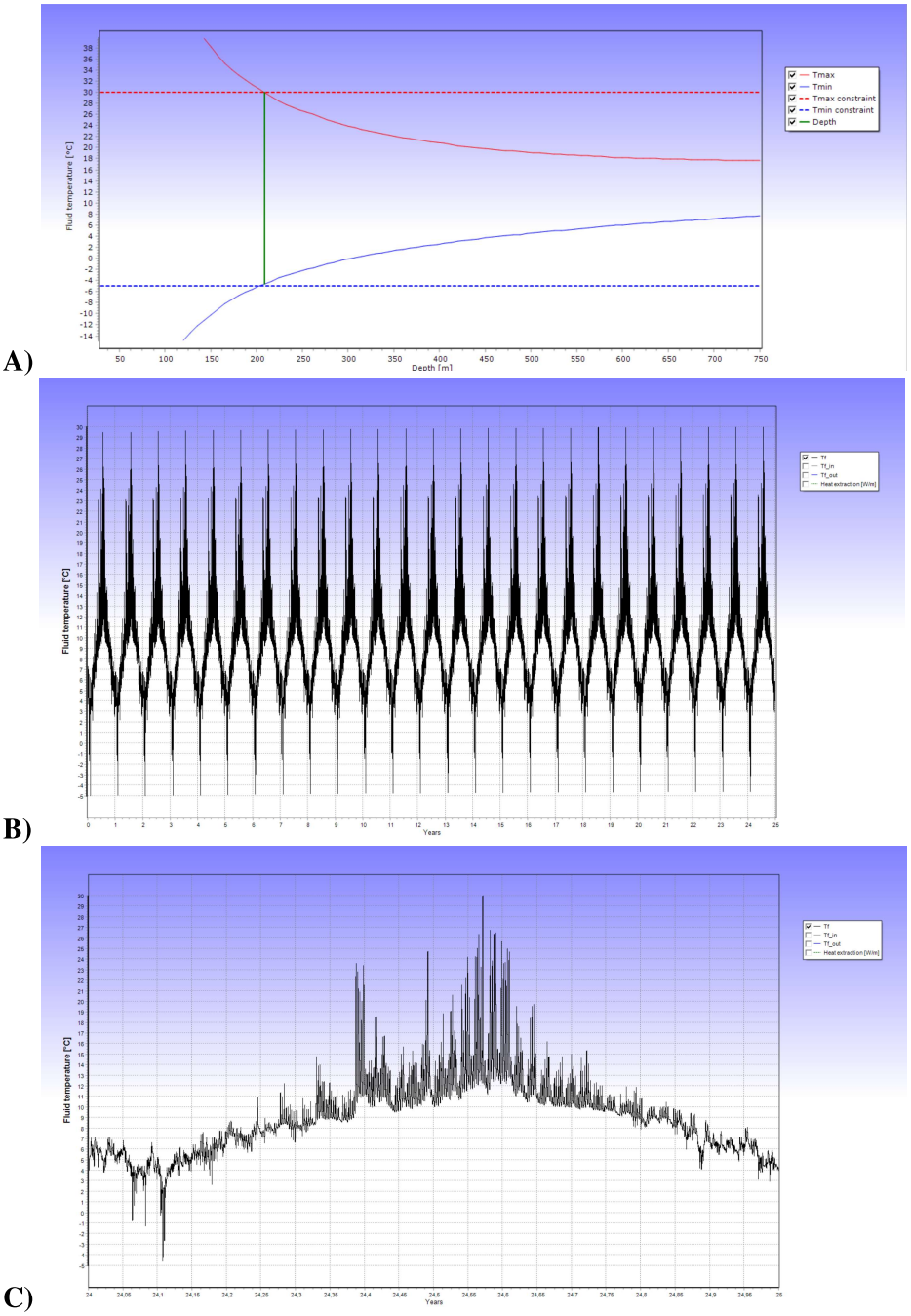

Figure F.1: Results for Building A showing, A) required borehole depth. B) Fluid temperature variation over the full simulation length. C) Fluid temperature variation for the last year.

Figure F.2 shows the results for Building B.

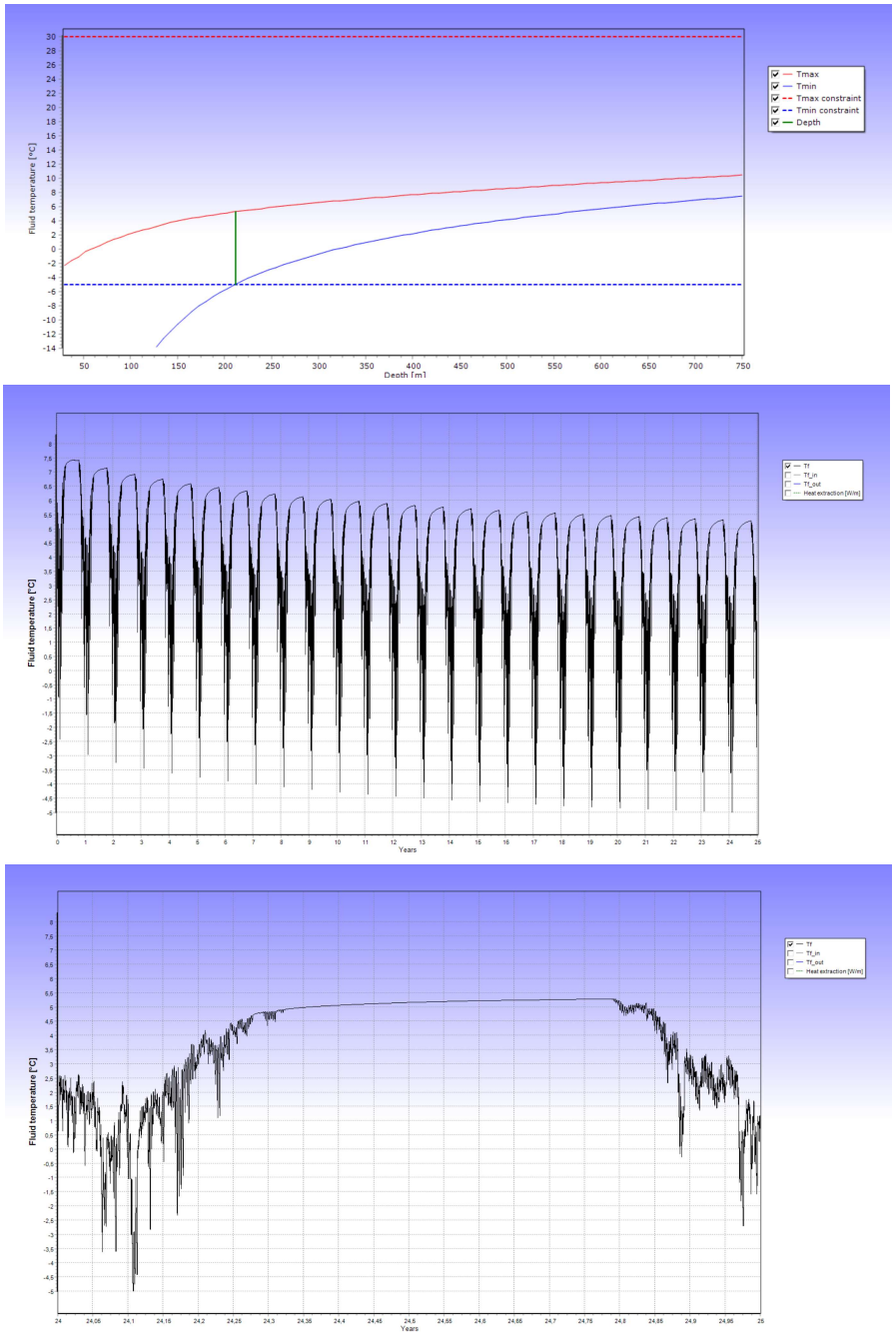

Figure F.2: Results for Building B showing, A) required borehole depth. B) Fluid temperature variation over the full simulation length. C) Fluid temperature variation for the last year.

Figure F.3 shows the results for Building C.

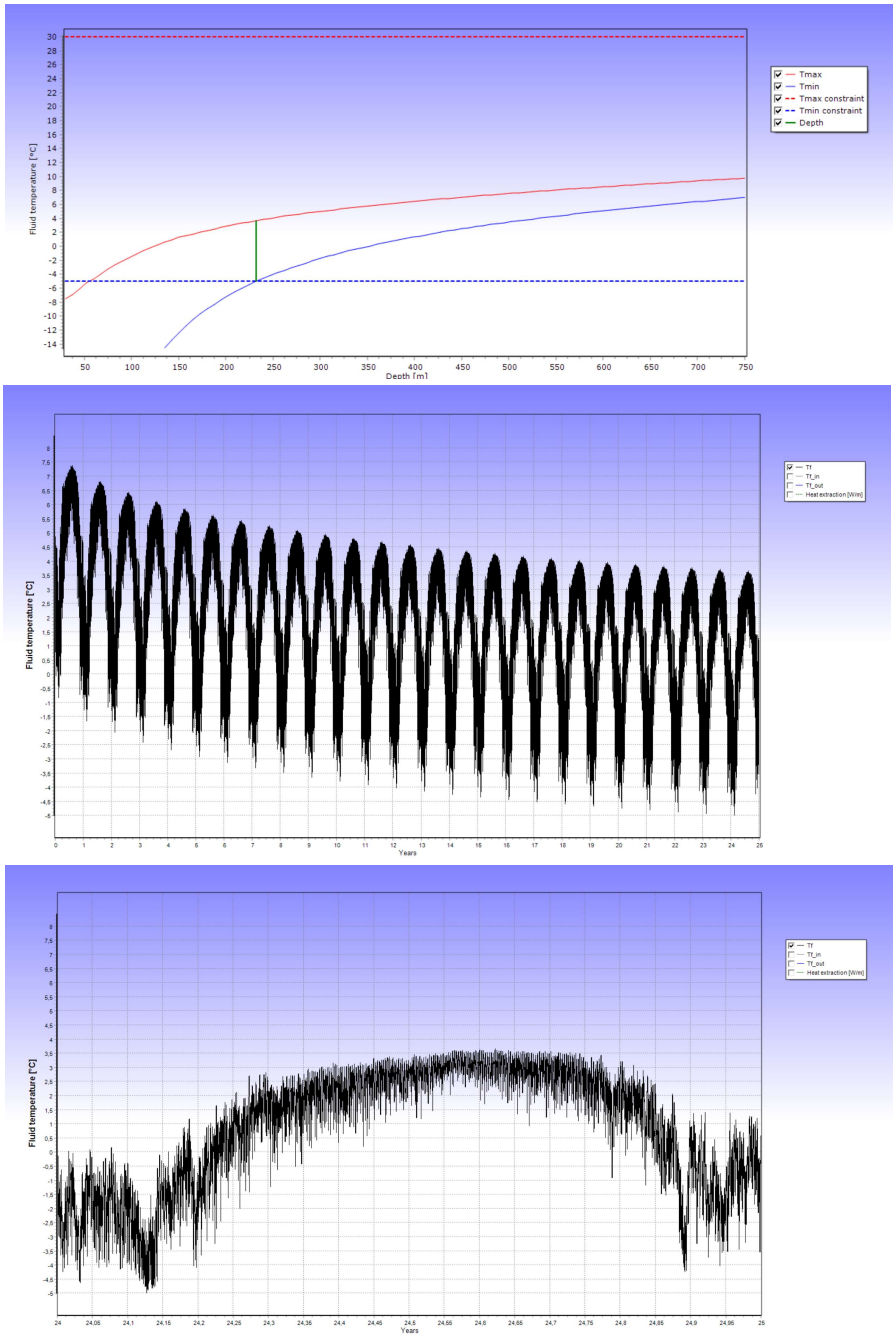

Figure F.3: Results for Building C showing, A) required borehole depth. B) Fluid temperature variation over the full simulation length. C) Fluid temperature variation for the last year.

Figure F.4 shows the results for Building D.

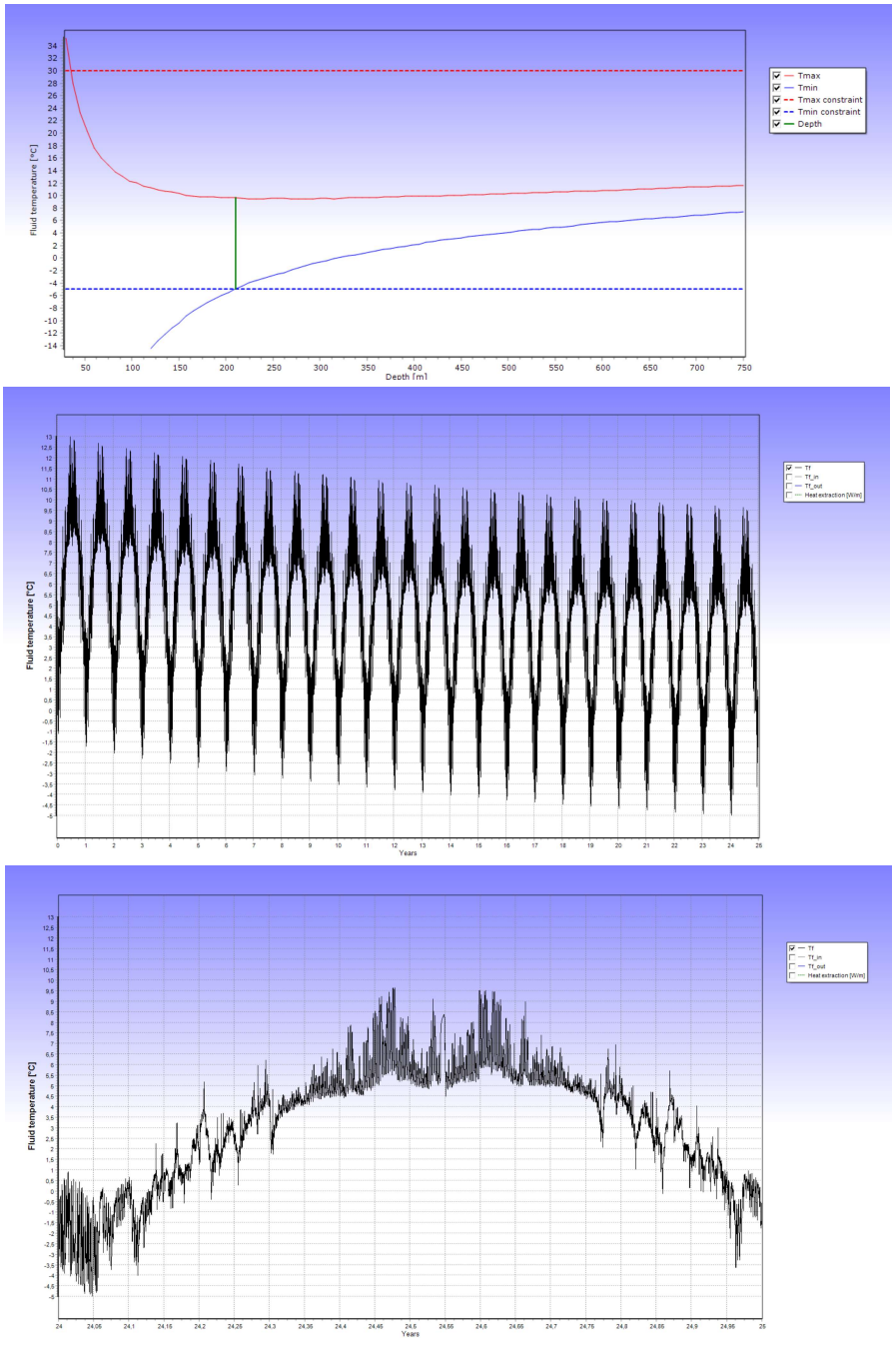

Figure F.4: Results for Building D showing, A) required borehole depth. B) Fluid temperature variation over the full simulation length. C) Fluid temperature variation for the last year.

Lastly, Figure F.5 shows the results for Building SM.

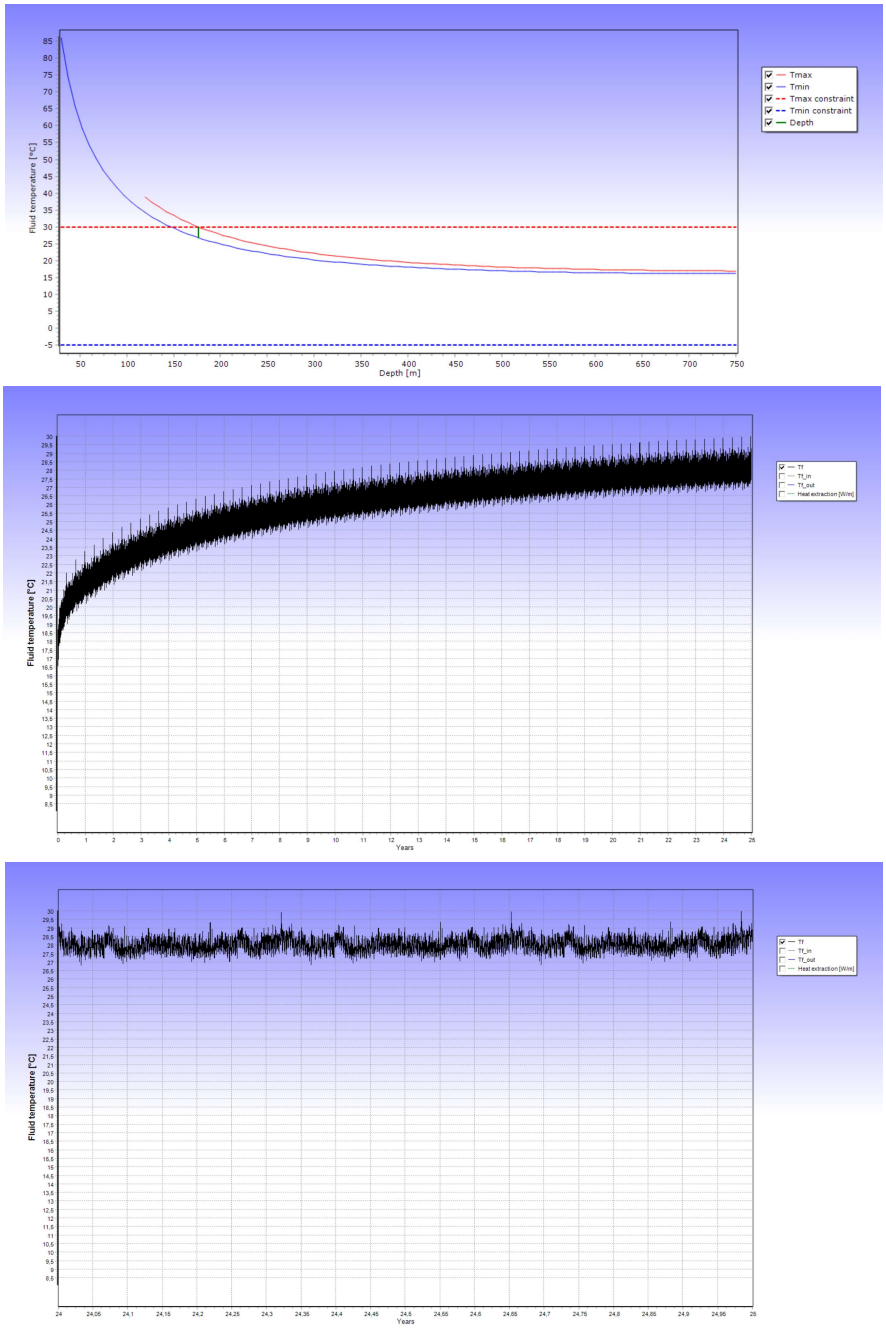

Figure F.5: Results for Building SM showing, A) required borehole depth. B) Fluid temperature variation over the full simulation length. C) Fluid temperature variation for the last year.

Based on the results from EED 4.3, the COP for each month and the resulting electricity demand could be calculated according to Appendix A - Carnot efficiency and Appendix B - Iteration calculations and results. The resulting investment, and operational cost excluding VAT could therefore be calculated for each based on Appendix E - Economic analysis. The results of this can be seen in Table F.2.

Table F.2: Summary of the base case simulations run in EED v.4.3 showing the HP investment [SEK], number of boreholes [-], resulting depth [m], borehole investment [SEK] and the operational cost for the electricity [SEK/year].

Building	HP [-]	HP inv. [SEK]	Number of boreholes [-]	Depth [m]	Borehole invest. [SEK]
A	9 x 60 kW	2 179 260	36	209	2 617 200
B	2 x 60 kW	484 280	9	212	662 400
C	2 x 40 kW	397 600	9	232	716 400
D	9 x 60 kW	2 179 260	64	210	4 672 000
SM	1 x 40 kW	198 800	4	176	251 200

With the additional electric connection for the needed electric capacity increase, the total investment cost excluding VAT can be seen in Table F.3.

Table F.3: Summary of the base case simulations run in EED v.4.3 showing the HP investment [SEK], number of boreholes [-], resulting depth [m], borehole investment [SEK] and the operational cost for the electricity [SEK/year].

Building	Elec. connection [SEK]	Total investment [SEK]	Operational cost [SEK/year]
A	100 000	4 896 460	163 631
B	0	1 146 680	47 375
C	0	1 114 000	78 350
D	100 000	6 951 260	316 919
SM	0	450 000	60 611

The environmental impact in CO_2 emissions for each building can be seen in Table F.4.

Table F.4: CO_2 emissions [kg CO_2-eq.] for each building of the geothermal base case.

Building	CO_2-emissions [kg CO_2 eq.]
A	13 971
B	3 770
C	7 097
D	31 204
SM	5 937
Total	61 979

DEPARTMENT OF ARCHITECTURE AND
CIVIL ENGINEERING
CHALMERS UNIVERSITY OF TECHNOLOGY
Gothenburg, Sweden 2026
www.chalmers.se

CHALMERS
UNIVERSITY OF TECHNOLOGY